AN ABSTRACT OF THE THESIS OF

Priti B. Singh for the degree of Master of Science in Toxicology presented on February 17, 2014

Title: Flavin- Containing Monooxygenase: Metabolism and Toxicity of Anti-Tuberculosis Drug Ethionamide in Lung

Abstract approved:

David E. Williams

Multiple drug resistance (MDR) Tuberculosis (TB), leads to increased use of “second-line” drugs; one of the most effective is ethionamide (ETA). ETA is a prodrug metabolized by a mycobacterial flavin-containing monooxygenase (EtaA) as well human flavin-containing monooxygenases (FMOs). Of the five functional FMOs of humans, FMOs 1, 2, and 3 are the most important in metabolism of xenobiotics. FMO2 is a major isoform in the lung expressed in most mammals. In humans a polymorphism encoding inactive FMO2 is the common allele, while the wild type allele encoding active FMO2.1 has been documented only in individuals of African and Hispanic origin, at an incidence of up to 50% and 7%, respectively. Human FMO2.1 is more efficient than EtaA in the first S-oxygenation of ETA to ETA S-oxide (ETASO). ETASO is a sulfenic acid and capable of redox-cycling with glutathione (GSH) producing oxidative stress and toxicity. We hypothesized that the FMO2 polymorphism will result in differences in the concentration and spectrum of ETA prodrug and metabolites. TB-infected individuals expressing active FMO2.1 will have reduced ETA efficacy in inhibition and killing of *M. tuberculosis* and enhanced oxidative stress, pulmonary toxicity and cell death in the host. To test this hypothesis, *Fmo1/2/4* knockout mice modeling the

*FMO2*2* genotype were utilized to study ETA metabolism and toxicity compared to wild type mice in order to model humans expressing the *FMO2*1* allele.

All mice were capable of metabolizing ETA to ETASO. Wild type mice had significantly higher plasma and epithelial lining fluid (ELF) levels of ETASO than ETA. In contrast, *Fmo 1/2/4* knockout mice had higher plasma and ELF levels of ETA than ETASO. ETASO, a sulfenic acid, was significantly higher in wild type mice than knockout mice in both plasma and ELF. Investigation of the effects of higher levels of ETASO in wild type mice was warranted. Long-term ETA dosing was utilized to examine oxidative stress and toxicity. Compare to *Fmo 1/2/4* knockout mice, wild type male and female mice showed more differentially expressed genes in lung related to oxidative stress and antioxidant defense pathways. Altered *Fmo1, 2* and *4* expression was also found in lung and liver of long-term ETA-treated wild type mice in comparison to vehicle controls. To examine ETA therapeutic efficacy in the presence and absence of FMO, wild type and knockout mice were infected with *M. avium* and dosed with 50 mg/kg of ETA for 28-days and compared with vehicle-dosed mice for bactericidal effects. An ETA dose of 50 mg/kg did not significantly reduce the mycobacterium infection, leaving the fundamentally question of the role of FMO2 polymorphism on ETA efficacy unresolved. Though interestingly, significant higher bacterial load was observed in the ETA treated wildtype compared to ETA treated knockout mice which suggest that the presence of FMO in wildtype is making these mice more susceptible to bacterial infection when ETA is dosed.

Collectively these studies suggest that humans expressing active FMO2.1 may be at higher risk of ETA toxicity than individuals with inactive FMO2.2 that are undergoing long-term ETA treatment for MDR-TB. This work

highlights the potential of the FMO2 human genetic on TB drug selection to maximize treatment efficacy and minimize toxicity. Another study of *M. tuberculosis* infected mice with 125 mg/kg dose of ETA is required to understand ETA therapeutic efficacy in the presence and absence of FMOs.

Flavin- Containing Monooxygenase: Metabolism and Toxicity of Anti-Tuberculosis Drug Ethionamide in Lung

By

Priti B. Singh

A THESIS

Submitted to

Oregon State University

in partial fulfillment of

the requirements for the

degree of

Master of Science

Presented February 17, 2014

Commencement June 2014

Master of Science thesis of Priti B. Singh

presented on February 17, 2014

APPROVED:

Major Professor, representing Toxicology

Head of the Department of Environmental and Molecular Toxicology

---

Dean of the Graduate School

I understand that my thesis will become part of the permanent collection of Oregon State University libraries. My signature below authorizes release of my thesis to any reader upon request.

Priti B. Singh, Author

ACKNOWLEDGEMENTS

I would like to express my sincere appreciation to my mentor, Dr. David Williams, for the opportunity and privilege of conducting my master's research and training under his advisement. He is one of the leading researchers in the field of Flavin Containing Monooxygenases; hence I felt very fortunate and privileged to work on this project under his mentorship. I would like to thank Dave for his constant guidance, encouragement and expertise which provided an ideal environment for me to grow as a researcher.

My deep appreciation goes out to Dr. Sharon Krueger for her direction, immense support, and supervision. Her enthusiasm, expertise and patience in research has in turn inspired me to be a better researcher myself. I learnt a great deal from working so closely with her and I shall be always indebted to her for that precious gift. I could not have done this without knowing that I could approach her for any help and suggestions whenever I needed to.

I would like to thank Dr. Luiz Bermudez for his scientific contributions and guidance that encouraged me to think critically. Dr. Arup Indra, Dr. Elisa Monaco, Dr. Tod Harper, Dr. Pushpinder Kaur, Tammie McQuistan and Beth Siddens, generously provided indispensable technical training and advice. Animal studies would not have been possible without the assistance of David Sampson, Elyssa Ridinger and Rachel Azevedo.

I would like to express my deepest gratitude to my husband Ashutosh Singh for always inspiring me to be greater than I believe I could be. He has undoubtedly been the best support and guidance I could ever have.

To my parents, thanks for your everlasting support, love and blessings, I hope to continue to make you proud of me. Thanks to my father-in-law for his continuous encouragement towards my higher education. Special recognition also goes to all my friends here, who have been by my side during some of the toughest as well as the most joyous moments of my life. Lastly, a special thanks to my son Shaurya for lighting up my everyday with his beautiful smile that inspires me in everything that I do.

CONTRIBUTION OF AUTHORS

Chapter 2: David Williams (DW) and Sharon Krueger (SK) provided assistance in experimental design, data interpretation and manuscript editing. Priti Singh (PS) carried out the study and prepared the manuscript. Tammie McQuistan provided assistantship in sample collection and HPLC analysis. David Sampson helped in sample collection and genotyping. Ian Phillips (IR) and Elizabeth Shephard (ES) have developed the mouse model used in the study.

Chapter 3: DW provided assistance in experimental design, data interpretation and manuscript editing. SK provided assistance in experimental design, sample collection, data interpretation and manuscript editing. PS carried out the study and prepared the manuscript. Amy palmer provided assistantship with sample collection. IR and ES have developed the mouse model used in the study.

TABLE OF CONTENTS

TABLE OF CONTENTS (Continued)

Page

LIST OF FIGURES

Figure Page

LIST OF FIGURES (Continued)

Figure Page

LIST OF TABLES

LIST OF APPENDICES

LIST OF APPENDIX FIGURES

LIST OF APPENDIX TABLES

Table page

Chapter 1 General introduction

1.1 Tuberculosis

Tuberculosis (TB), an infectious disease caused by *Mycobacterium tuberculosis* bacteria, is second only to HIV/AIDS as the greatest killer worldwide due to a single infectious agent. This airborne disease typically affects the lungs, but can also affect other organs. The earliest unambiguous detection of *M. tuberculosis* involves evidence of the disease in the remains of bison dated to approximately 17,000 years ago (Rothschild et al. 2001). In 1993, the World Health Organization (WHO) declared TB a global health emergency with about one-third of the world's population having latent TB. In 2012, 8.6 million people fell ill with TB and 1.3 million died (Eurosurveillance editorial 2013). In 2012, the largest number of new TB cases occurred in Asia, accounting for 60% of new cases globally, however sub-Saharan Africa carried the greatest proportion of new cases per population with over 255 cases per 100,000 people (Eurosurveillance editorial 2013). A total of 9,945 TB cases (a rate of 3.2 cases per 100,000 persons) was reported in the United States in 2012 (Centers for Disease and Prevention 2013). TB is preventable and curable; a standard treatment against fully susceptible TB is a combination of isoniazid (INH), rifampicin (RIF), ethambutol (EMB) and pyrazinamide (PZA) given over two months, followed by INH and RIF for four more months (Bastian and Colebunders 1999; Sahbazian and Weis 2005). This cocktail of medications is well tolerated in most individuals. In 2006, the Stop TB Partnership launched the *Global Plan to Stop TB 2006–2015* (http://www.stoptb.org/global/plan/) a roadmap for scaling up TB prevention and treatment, for research, development, and for financing. The plan's goals included halving TB deaths compared to 1990 levels by 2015 – still a target today (Babior 1999; Raviglione 2006; Stop 2006). If no improvements in TB

control are made from 2010 onwards, about 10 million people will die from TB by 2015.

1.1.1 Multiple drug resistance-TB (MDR-TB)

MDR-TB is defined as TB that is resistant to the first line drugs, most commonly, INH and RIF. MDR-TB is a major public health problem that threatens progress made in TB care and control worldwide. Drug resistance arises due to improper use of antibiotics in treatment of patients with drug-susceptible TB. Worldwide, about 450,000 people developed MDR-TB in 2012, while 630,000 cases with MDR-TB were reported in 2011 (Eurosurveillance editorial 2013). Up to 10% of MDR-TB is extensively drug resistant (XDR)-TB (Eurosurveillance editorial 2013). About 170,000 MDR-TB deaths are estimated to have occurred in 2012 (Eurosurveillance editorial 2013). Treatment of MDR-TB requires prolonged (up to two years) and expensive chemotherapy using second-line drugs of heightened toxicity and at greater cost (typically, US$ 2000-5000 per patient). If resistance to the second line drugs also develops then the disease becomes virtually untreatable. Sub-Saharan Africa is especially burdened with drug-resistant TB. The recent report from KwaZulu Natal Province in South Africa of an outbreak of XDR-TB, where rapid progression to death was observed in 98% of patients, demonstrates the vulnerability of sub-Saharan Africa to outbreaks of untreatable disease (Gandhi et al. 2006). One of the aims of *the Global Plan to Stop TB 2006-2015*, is to have at least 75% of MDR-TB patients completing their treatment successfully by 2015 (Babior 1999; Raviglione 2006; Stop 2006). Common second-line MDR-TB drugs are capreomycin, kanamycin, amikacin, ethionamide (ETA), fluoroquinolones, and cycloserine.

1.2 Ethionamide

ETA is a second-line anti-TB drug, first used for TB treatment in the early 1950's. Because of the increasing incidences of MDR-TB, ETA has become an important second line drug. ETA is used as replacement for INH and RIF due to structural similarities. The average daily dose for ETA is 250 mg/day orally but if well tolerated, can be increased up to 1 g/day (Thee et al. 2011). ETA can exhibit adverse drug reactions like nausea, vomiting, gastrointestinal disorder and hepatotoxicity (Bastian and Colebunders 1999; Henderson et al. 2008).

Pharmacokinetics (PK) of ETA are well-studied and complete. Zhu et al. (2002) had showed that pharmacokinetics (PK) parameters of ETA were independent of age, weight, height, gender, and creatinine clearance. ETA PK parameters differed between TB patients and healthy volunteers, possibly due to differences in the completeness of absorption. TB patients appeared to have lower volumes of distribution (3.22 L/Kg) and clearance values (1.88 L/h/Kg) compared to healthy volunteers (Table 1.1) (Zhu et al. 2002).

Table 1.1 Pharmacokinetics parameters of ETA in humans

Half life (h)	AUC (mg.h/L)	C_{max} (μg/mL)	Volume of distribution (L/Kg)	PK methodology
1.94	7.67	2.16	93.5 (sugar coated tablets)	Mean PK for 250 mg oral dose using film-coated tablets in healthy adults (FDA label)

ETA is a prodrug that must undergo metabolic activation to exert its cytotoxic effects. Mycobacterial flavin-containing monooxygenase (EtaA or EthA) and human flavin containing monooxygenases (FMO) can activate ETA (DeBarber et al. 2000; Qian and Ortiz de Montellano 2006; Vannelli et al. 2002). When the EtaA gene is mutated, ETA resistance occurs (Dover et al. 2007). Like INH, ETA is thought to exert a toxic effect on mycolic acid constituents of the cell wall of the bacillus (Banerjee et al. 1994; Quemard et al. 1992; Vilcheze et al. 2008). The activated metabolite of both INH and ETA targets the enoyl-acyl carrier protein reductase, (inhA) which is involved in the production of mycolic acid (Dover et al. 2007). A single mutation in the inhA gene confers resistance to both INH and ETA affecting mycolic acid synthesis (Banerjee et al. 1994; Quemard et al. 1992). Unlike ETA, INH is activated through katG, a catalase-peroxidase (Baulard et al. 2000). When katG is mutated, mycobacteria become resistant to INH but not ETA (Baulard et al. 2000). The proposed ETA and INH mechanism of action proposed by Vilcheze et al. (2005), is that the activated ETA form reacts with NAD^+ to form an ETA-NAD adduct, this adduct inhibits the target InhA resulting in mycolic acid bisynthesis inhibition and cell lysis. They have also shown that mutation in type II NADH dehydogenase (NdhII) causes resistance to INH and ETA.

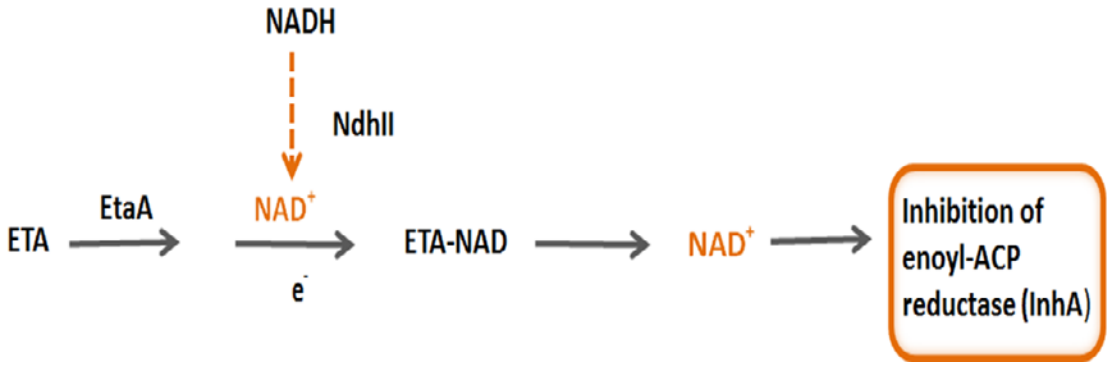

Figure 1.1 ETA mechanism of action (Vilcheze et al. 2005)

1.3 Flavin-Containing Monooxygenase

Mammalian FMOs are a protein family that consists of a group of related drug metabolizing enzymes. FMO catalysis requires flavin adenine dinucleotide (FAD) as a prosthetic group, and nicotinamide adenine dinucleotide phosphate (NADPH) as a cofactor and molecular oxygen (Cashman 1995; Phillips and Shephard 2008; Ziegler 1993). Like cytochrome P450 (CYPs), FMOs are localized to the endoplasmic reticulum and exhibit broad substrate specificity. Substrates for FMO are structurally diverse compounds that contain a soft nucleophile and commonly oxygenate xenobiotics containing nitrogen and sulfur heteroatoms (Cashman 1995; Cashman 2003; Henderson et al. 2004; Krueger and Williams 2005; Poulsen et al. 1979; Poulsen et al. 1986; Ziegler 2002). In general, FMOs detoxify various xenobiotics and make them more excretable; though in some cases the metabolites generated are more harmful than the parent compound.

The number of reported *FMO* genes in humans is 11, which include 5 functional and 6 pseudo genes, while in mice 9 families have been documented that may all be expressed (Hernandez et al. 2004; Hines et al. 2002). For the five forms of functional human *FMO* (i.e., *FMO1* to *FMO5*), sequence identity ranges between 52% and 60%, with the exception of *FMO3* and *FMO6*, which share 71% identity (Cashman 1995; Cashman 2003; Phillips and Shephard 2008). *FMO* genes are located on the long arm of chromosome 1 (McCombie et al. 1996; Shephard et al. 1993). *FMO* pseudo genes are located in another region of chromosome 1 as a cluster (Hernandez et al. 2004). FMO proteins are 532-558 amino acids in length with highly conserved FAD- and NADPH- binding domains (Atta-Asafo-Adjei et al. 1993; Lawton and Philpot 1993). Small base changes that may affect enzyme function are alleles and they introduce considerable variability into the FMO enzymes (Cashman 2004; Cashman and Zhang 2002). *FMO* expression is developmentally

regulated, tissue-specific and species-dependent (Hines et al. 1994; Ziegler 2002). Table 1.2 presents a comparative view of *FMO1, 2* and *3* expression levels in lung and liver of human and mouse of both sexes. *FMO1* has the broadest substrate specificity and, in humans, is located primarily in fetal liver as well as adult kidney, and intestine, however in mouse; *Fmo1* expression is present in both lung and liver (Table 1.2). *FMO3* specificity is moderate and is the primary constituent of the liver in human; though in mouse only female mouse express it in the liver (Table 1.2). *FMO2* is primarily located in the lungs and has the strictest binding specificity (mostly by size exclusion) (Cashman 1995; Krueger et al. 2005). FMOs 1, 2, and 3 are the most important in the metabolism of xenobiotics.

1.3.1 Interindividual differences of FMO2

Unlike nonhuman primates and other mammals, FMO2 is not a prominent functionally active enzyme in human lung (Yueh et al. 1997). Approximately 26% of African-, 7% of Puerto Rican-, and 2% of Mexican-American individuals tested possess one normal allele encoding a full-length enzymatically active functional protein (Dolphin et al. 1998; Krueger et al. 2002a; Krueger et al. 2004; Whetstine et al. 2000). All Caucasians and Asians genotyped to date are homologous for a genetic polymorphism, the *FMO2*2* allele, in which a C→T transition at bp 1414 replaces a glutamine at amino acid residue 472 with a stop codon (Dolphin et al. 1998; Whetstine et al. 2000). This change produces a non-functional truncated FMO2.2 protein (Dolphin et al. 1998; Krueger et al. 2002a). FMO2.2 does not incorporate FAD and is not detected on western blots of human pulmonary microsomes, presumably due to degradation and incorrect folding. Recently, a high percentage of Sub-Saharan Africans (50%) with *FMO2*1* was documented and intriguingly this corresponds to the region of highest TB incidence

Table 1.2 Relative *FMO1/2/3* distributions in adult humans and mice.

			Lung			Liver		
Species	Sex	Genotype	FMO1	FMO2	FMO3	FMO1	FMO 3	Best Models
								Humans:
Human	M & F	*hFMO2*1*		++++++++		+	+++++	
Mouse	M	Wildtype(wt)	++	++++++	±	+++		*hFMO2.1 & hFMO3 null*
	F	Wildtype	+++	++++++	±	++++	+++++	*hFMO2.1 & hFMO3 wt*
Mouse	M	*mFmo1/2/4 null*			±			*hFMO2.2 & hFMO3 null*
	F	*mFmo1/2/4 null*			±		+++++	*hFMO2.2 & hFMO3 wt*

Human expression: (Zhang and Cashman 2006)' Mouse expression: (Janmohamed et al. 2004; Siddens et al. 2008)

(Veeramah et al. 2008). So, FMO polymorphisms may have the potential to induce varying therapeutic and adverse health effects or benefits from the drugs.

1.4 ETA metabolism

The prodrug ETA can be activated by mycobacterial flavin-containing monooxygenase EtaA as well as FMO1, FMO2.1, and FMO3 present in humans and other mammals (Francois et al. 2009; Henderson et al. 2004; Henderson et al. 2008; Johnston et al. 1967; Qian and Ortiz de Montellano 2006; Vannelli et al. 2002). Both EtaA and FMO can catalyze ETA oxygenation in two steps, first to the ethionamide sulfoxide (ETASO) a sulfenic acid and second to the sulfinic acid (Fig. 1.2A). The third product detectable, 2-ethyl-4-amidopyridine (ETA -amide) (ETAA) is thought to be a spontaneous breakdown product of the sulfinic acid (DeBarber et al. 2000; Fraaije et al. 2004; Vannelli et al. 2002). Catalytic activity of mammalian FMO is higher than EtaA in the first step oxygenation whereas EtaA is faster at the second oxygenation (Henderson et al. 2008). Minimum inhibitory concentration (MIC) for ETASO are shown lowers than ETA suggesting greater activity against *M. tuberculosis* than ETA itself (Prema et al. 1976). Hanoulle et al. (2006) has shown that ETASO was present outside the bacterial cell and accumulated overtime by following ETA activation directly within living mycobacterial cell by high resolution magic angle spinning-NMR (HRMAS-NMR). This suggest that ETASO is not the final bactericidal metabolite, it itself needs further activation to a final cytotoxic species (Baulard et al. 2000). Because of the absence of toxicity of the amide derivative against mycobacteria, it has been proposed that a sulphinic acid intermediate is the putative active compound (DeBarber et al. 2000) (Fig.1.2 B).

(A)

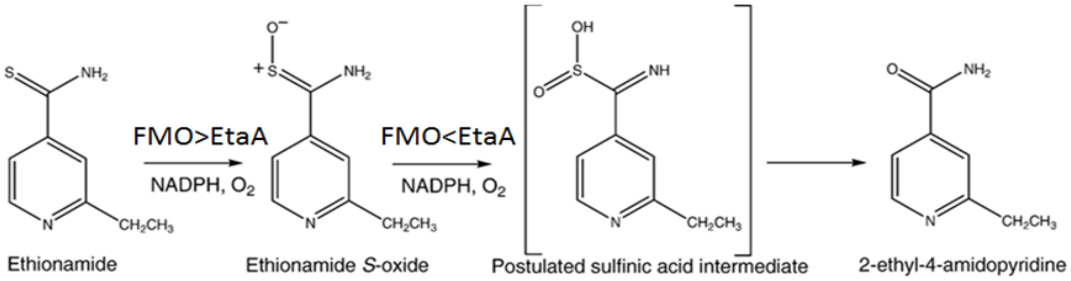

(B)

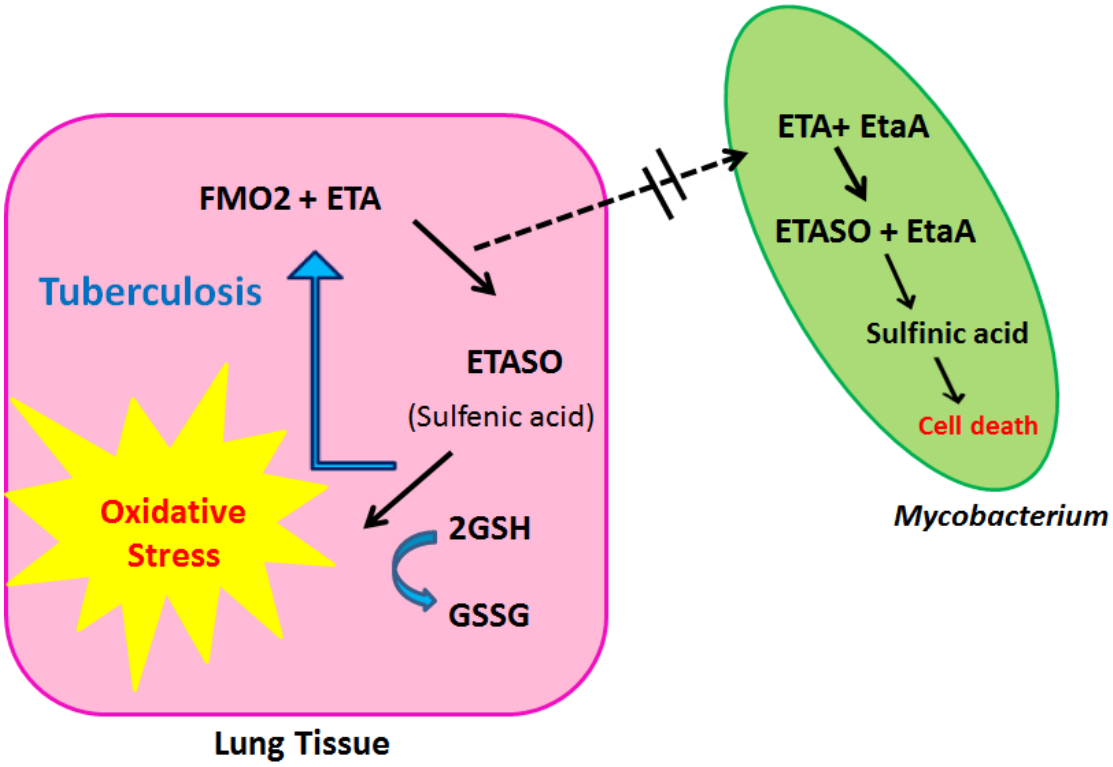

Figure 1.2 Proposed scheme of ETA metabolism and toxicity.
(A) Proposed scheme of ETA metabolism by FMOs and EtaA, (B) Cartoon depicting proposed scheme of ETA metabolism in the lung of TB patients with active *Mycobacterium* infection and expressing the active FMO2.1 protein.

Both human and mouse FMOs catalyze ETA sulfoxygenation but with different catalytic efficiencies (Henderson et al. 2008). The specificity constants ranged from 0.17 to 0.86 with hFMO and 0.21 to 2.62 with mFmos (Table 1.3).

Table 1.3 Kinetic values for mouse and human FMOs and ETA.

Protein	K_m (µM)	K_{cat} (min^{-1})	Specific Constant *(Kcat/Km)*
hFMO1	105	89.9	0.86
hFMO2	261	48.3	0.19
hFMO3	336	58.4	0.17
mFmo1	104	271	2.62
mFmo2	2131	567	0.21
mFmo3	114	60.6	0.53

(Henderson et al.2008)

The sulfenic acid ETASO is capable of redox cycling with glutathione (GSH) and reducing the GSH/GSSG ratio (Henderson et al. 2004) leading to oxidative stress and cell injury *in vitro*. FMO has been demonstrated to produce liver toxicity exactly in this fashion *in vivo* when metabolizing thiocarbamides (Krieter et al. 1984; Neal and Halpert 1982). Sub-Saharan Africa has both the largest number of individuals with active FMO2.1, and co-incidentally the highest rates of TB, with increasing number of MDR-TB every year (Eurosurveillance editorial 2013). We predict there is an FMO2 genotype-specific difference in therapeutic efficacy and/or toxicity of ETA that has not previously been reported that will be most prevalent in Sub-Saharan Africa due to the co-prevalence of elevated *FMO2*1* polymorphism and disease. Our central hypothesis is that individuals producing active FMO2.1 will have enhanced oxidative stress and toxicity with long-term ETA treatment and will

experience reduced therapeutic efficacy in inhibition and killing of mycobacteria. Our laboratory has estimated that FMO2.1, when expressed in pulmonary tissue, is present at about 9 pmol/mg microsomal protein (Krueger et al. 2002a), while total CYP estimates in lung are 1-10 pmol/mg (Hukkanen et al. 2002; Wheeler and Guenthner 1990). Human FMO2.1 produces H_2O_2 in the presence of substrate, which could directly kill *M. tuberculosis* (Siddens et al. 2014). FMO2.1 expression in lung could impact *M. tuberculosis* survival in a number of ways. It could metabolize ETA to the sulfenic acid (ETASO) such that more drug is excreted or is unable to be taken into the infected cells so that less drug reaches its target. This could result in reduced therapeutic efficacy and perhaps enhanced oxidative stress in lung. Alternatively if ETASO produced by mammalian cells was efficiently taken up by mycobacteria it could enhance bactericidal efficacy, due to the slower rate that mycobacteria EtaA perform in the first oxidative step. Up-take of activated ETASO would reduce the metabolic work-load on mycobacteria in comparison to uptake of prodrug ETA. In addition to expression of FMO enhancement of oxidative stress, infection (TB) and inflammation often leads to significant alteration in drug metabolizing enzymes, including CYPs and FMO (Iber et al. 1999; Morgan 2009; Rahman and MacNee 2000; Rahman et al. 2009; Schmith and Foss 2008; Zhang et al. 2009). This phenomenon could have a major impact on adverse drug reactions in TB patients.

1.5 *Fmo* Knockout mouse model

Engineered *Fmo* knockout mouse lines are required to study many of the problems associated with quantifying the contribution of an FMO to drug metabolism *in vivo*. To date only one *Fmo* knockout mice line has been produced and used to study the consequences of a lack of an FMO activity (Hernandez et al. 2006; Hernandez et al. 2009). In order to investigate the

effects of FMO2 on the metabolism of ETA, we utilized an *Fmo1/2/4* knockout mouse model. *Fmo 1/2/4* knockout mice were developed by deleting exons 2-9 of *Fmo2, 1-7* of *Fmo4* and the entire *Fmo1* gene by chromosomal engineering (Hernandez et al. 2006). Mice used in our studies were backcrossed to C57BL/6 mice for 8-9 generations. Expression and activities of human FMOs are not directly comparable to those found in mice (Table 1.2, 1.3) (Henderson et al. 2008; Janmohamed et al. 2004). *Fmo1/2/4* knockout mice reflect the situation with respect to the profile *of FMOs present in human* lung expressing inactive *FMO2.2.* This knockout mice also models adult human liver very well by deleting *Fmo1.*Though animal models can never truly represents the situation in human, by direct comparison of *FMOs* expression levels between human and mouse, wild type female mouse is most near to humans expressing *FMO2.1* while knockout females best model for human expressing *FMO2.2* (Table 1.2). In terms of enzymatic kinetics, mouse Fmo1 specific constant towards ETA is much higher than human (Table 1.3) and wildtype mice express Fmo1 in lung whereas to humans do not (Table 1.2). It is estimated that in Sub-Saharan Africa, some 200 million people possess the *FMO2*1* allele (Veeramah et al. 2008), and thus are likely to express functional FMO2 protein. So far, it is not yet clear whether possession of either the ancestral or nonfunctional allele would be beneficial or would confer an increased risk of adverse drug reactions. In case of ETA drug treatment, we think there might be an increased risk of toxicity with reduced efficacy in long-term MDR-TB treatment.

1.6 Dissertation specific aims and hypothesis

Specific Aim 1: To determine the ETA metabolism differences in wild type versus *Fmo1/2/4* knockout mice and to study *Fmo1-5* gene expression with long-term ETA treatment (Chapter 2).

My working hypothesis is that there will be an FMO genotypic impact on ETA metabolism. Wild type mice will have faster ETA metabolism and higher levels of the major metabolite ETASO, a sulfenic acid, whereas knockout mice will have higher levels of the ETA parent prodrug.

Specific Aim 2: To determine the effect of long-term ETA treatment on wild type and *Fmo1/2/4* knockout mice on oxidative stress (Chapter 3).
My working hypothesis is that higher production of sulfenic acid via ETA metabolism in wild type mice will deplete glutathione levels resulting in oxidative stress. I predict that long-term ETA treatment will cause oxidative stress and toxicity in wild type mice.

Specific Aim 3: To determine therapeutic efficacy of ETA in *Mycobacterium avium* infected wild type and *Fmo1/2/4* knockout mice (Appendix- A1).

My working hypothesis is that due to the presence of active Fmo2, the therapeutic efficacy of ETA in *Mycobacterium avium infected mice* will be lower in wild type mice than it will be in *Fmo1/2/4* knockout mice which do not have an active Fmo2.

Specific Aim 4: To test ETA toxicity in a bronchial epithelial cell line (BEAS-2B) stably transfected with human FMO2.1 and 2.2 (Appendix-A2).

My working hypothesis is that BEAS-2B cells with active FMO2.1 will show elevated ETA toxicity and oxidative stress compared to BEAS-2B cells with inactive FMO2.2. I predict that ETA metabolism by FMO2.1 will produce sulfenic acid, which is very reactive and causes toxicity by glutathione

depletion. Cells with inactive FMO2.2 will not be able to matabolize ETA and will not show any toxicity.

Chapter 2 Altered Plasma and Epithelial Lining Fluid Levels of the Prodrug Ethionamide and its Major Metabolite, Ethionamide S-Oxide, in Flavin Containing Monooxygenase 1, 2 and 4 Deficient Mice: Impact of Genotype

Priti B. Singh[1,2] , Tammie J. McQuistan[2], David A. Sampson[1], Sharon K. Krueger[2], Ian R. Phillips[3], Elizabeth A. Shephard [4], and David E. Williams[1, 2]

[1]Department of Molecular and Environmental Toxicology, Oregon State University, Corvallis OR, USA, [2]The Linus Pauling Institute, Oregon State University, Corvallis, OR, USA, [3]School of Biological and Chemical Sciences, Queen Mary, University of London, London United Kingdom, [4] Department of Structural and Molecular Biology, University College London, London, United Kingdom

2.1 Abstract

Ethionamide (ETA), an important second-line antituberculosis drug, is a prodrug and needs to be activated by the mycobacterial flavin containing monooxygenase enzyme EtaA to exert antimicrobial activity. ETA is also a substrate for human flavin-containing monooxygenase (FMO). FMO2 is a major FMO isoform in the lung. However, most humans do not express active FMO2.1 in lung and produce only inactive FMO2.2. Activation of ETA by both EtaA and FMO produces ethionamide S-oxide (ETASO). We hypothesize that this FMO2 genotype in humans could affect ETA metabolism, bactericidal efficacy and toxicity. *Fmo 1*/*2*/*4* knockout mice were utilized to study ETA metabolism and compared to wild type mice. ETA and metabolites were analyzed in plasma and epithelial lining fluid (ELF) of mice at 0.5, 1, 2 and 3 hour post-gavage. We demonstrated a clear difference in ETA metabolism between wild type and knockout mice. Wild type mice had significantly higher levels of ETASO than ETA in both plasma and ELF. In contrast, knockout mice had significantly more ETA than ETASO in both plasma and ELF. The metabolite ETASO, a sulfenic acid, can undergo redox cycling in the presence of glutathione. This conjugation with glutathione was significantly higher in wild type mice than knockout mice in both plasma and ELF samples. The higher levels of ETASO in wild type mice may deplete glutathione pools and induce oxidative stress and toxicity. We also examined the effect of long term ETA treatment on *FMO* mRNA expression levels. Altered *Fmo 1, 2* and *4* expressions were found in lung and liver of long term ETA-treated wild type mice in comparison to vehicle controls. *Fmo3* and *5* are seen to be down-regulated in knockout mice in both long term ETA-treated and vehicle-treated mice. *Fmo 1, 2* and *4* expression changes in wild type mice suggest probable association of ETA metabolism mediated oxidative stress and toxicity consequences, though further studies are needed for validation.

Key words: Ethionamide, Tuberculosis, Flavin-containing monooxygenase

2.2 Introduction

Ethionamide (ETA) is one of the most widely used drugs for the treatment of multidrug-resistance tuberculosis (MDR-TB). It is a prodrug which is activated by a flavin monooxygenase enzyme (EtaA) present in many mycobacterium, including *Mycobacterium tuberculosis* to ethionamide S-oxide (ETASO) (Baulard et al. 2000; DeBarber et al. 2000). ETA is also a substrate for human flavin-containing monooxygenase (FMOs), a phase I drug metabolizing enzyme which oxygenate a wide range of xenobiotics. Humans express five functional FMO genes (FMO1 to FMO5) in a developmental-, sex-, and tissue-specific manner (Cashman 1995; Hernandez et al. 2004; Krueger and Williams 2005; Ziegler 2002).Our focus here is FMO2 which is primarily located in lung and is the predominant drug metabolizing FMO isoform in this organ (Baulard et al. 2000; DeBarber et al. 2000; Furnes et al. 2003; Phillips and Shephard 2008; Qian and Ortiz de Montellano 2006; Quemard et al. 1992). Opposite to nonhuman primates and other mammals, FMO2 is not a prominent functionally active enzyme in human lung (Yueh et al. 1997). In African Americans, 26% of the population and 5% of Hispanics, have at least one copy of the active allele (*FMO2*1*) encoding for the full length protein (Dolphin et al. 1998; Furnes et al. 2003; Krueger et al. 2009; Whetstine et al. 2000). A premature stop codon (1414T) in FMO2 (*FMO2*2*) removes the last 64 amino acids on the C-terminus, truncating the protein and rendering FMO2.2 inactive (Dolphin et al. 1998; Furnes et al. 2003). In people of Asian and Caucasian decent *FMO2*2* is the only known allele. *FMO2*1* is most prevalent in Sub-Saharan Africans (50%) (Veeramah et al. 2008), coincidentally same region also corresponds to high incidences of TB with

increasing number of MDR-TB every year (Eurosurveillance editorial 2013) is of great importance.

FMO isoforms are expressed in a tissue-specific manner and at certain developmental stages (Cashman 1995; Krueger and Williams 2005; Whetstine et al. 2000). Genetic variation is the primary factor in *FMO* expression, although *FMO2* and *FMO4* elevated expression has been observed associated with conditions generating oxidative stress and toxicity (Eom et al. 2013; Park et al. 2009; Rahman et al. 2009). Hepatic *Fmo1, Fmo3* and *Fmo5* mRNAs were also found to be down-regulated in lipopolysaccharide (LPS) models of inflammation (Zhang et al. 2009). *FMO4* and *5* expressions were also induced with antibiotic rifampin treatment of primary human hepatocytes (Rae et al. 2001). ETASO, an FMO-oxygenation product of ETA, is a sulfenic acid which can react with glutathione (GSH) inducing oxidative stress through a futile redox cycle (Guo et al. 1992; Henderson et al. 2004; Kim and Ziegler 2000; Smith and Crespi 2002). FMO has been demonstrated to produce liver toxicity in this fashion when metabolizing thiocarbamides (Krieter et al. 1984; Neal and Halpert 1982).

We hypothesized that FMO2 genotype have the potential to induce varying therapeutic and adverse health effects or benefits of ETA. In order to investigate the effect of FMO2 polymorphism on ETA therapeutic efficacy and toxicity, we utilized *Fmo 1/2/4* null mouse model developed using a Cre/loxP system to effectively remove the genes from mouse embryonic stem cells (Hernandez et al. 2006). We used a single dose study to assess ETA metabolism in both the C57BL/6 wild type and *Fmo1/2/4* knockout mouse. We detected prodrug ETA and metabolite ETASO in both plasma and epithelial lining fluid (ELF) at 0.5, 1, 2 and 4 hour post-gavage and compared levels observed strain-dependent differences in metabolism. We then conducted a

long-term (4-week) ETA dosing study to assess resulting *Fmo1, 2, 3, 4* and *5* mRNA expressions in lung and liver tissue of wild type and knockout mice.

This study investigates the effect of FMO expression on ETA metabolism in mice as well as regulation with long term ETA dosing in both wild type and Knockout mice. This provides a model for the human, ethnic-dependent genetic polymorphism in FMO2 expression and its potential role in the therapeutic efficacy and toxicity of ETA in long term TB treatment.

2.3 Material and Methods

Chemicals

High performance liquid chromatography (HPLC) grade reagents were purchased from Sigma-Aldrich (St. Louis, MO). The vehicle for gavage suspension (Vet syrup®) was from FlavoRx (Washington, D.C.). ETASO was custom synthesized by Tjaden BioSciences (Burlington, IA). ETAA was a gift from Paul R. Ortiz de Montellano (University of California, San Francisco, CA) (Vannelli et al. 2002) .

Animals

Male and female C57BL/6J mice were purchased from Jackson Laboratory (Sacramento, CA). These mice were 11 weeks of age and allowed one week of acclimation at the mouse facilities at Oregon State University (OSU) (Corvallis, OR) before study initiation. *Fmo1*$^{-/-}$, *Fmo2*$^{-/-}$, *Fmo4*$^{-/-}$ eight generation back-cross knockout mice, on a C57BL/6 background (Hernandez et el., 2006) were shipped from University College (London, UK) to Harlan Laboratories (Hillcrest, UK) where they were rederived prior to shipment to

OSU, where a breeding colony was established. The *Fmo* genotype was confirmed for all knockout mice on arrival at OSU (data not shown). A breeding colony was established and maintained at LPSC. Mice were provided pellet diet (Purina 5053) and water *ad libitum*. Mice were kept on a 12 hour light cycle under a controlled temperature between 22-23^{0}C. Mice were housed in microisolator a cage with up to 5 mice per cage. Studies were approved by the Oregon State University Institutional Animal Care and Use Committee.

Single ethionamide dosing and blood collection

ETA was ground into fine powder and suspended in Vet syrup (at 12.5 µg /µl) with 10 min of sonication and 30 sec of vortexing. A single dose of 125 mg ETA/kg body weight was administered orally by gavage. Gavage volume used was 10 µl/g body weights. The drug suspension was vortexed before each gavage to ensure a uniform dose was achieved. At designated intervals (0.5, 1.0, 2.0, and 3.0 hour post-gavage) blood and bronchoalveolar lavage fluid were collected. Mice were *ip* injected with 50 µl of heparin (1000 U/ml) to anti-coagulate for 5 min before isoflurane administration (3-5%). Once mice were deeply anesthetized and reflexes were absent necropsy was performed. Blood was collected from the posterior vena cava, mixed with 33 IU of sodium heparin to prevent clotting and was stored on ice until all samples were collected for the day. Plasma was prepared by centrifugation of whole blood at 2,000 x *g* for 10 min and was stored at -80°C for analysis of ETA. A small aliquot of plasma was frozen separately for urea assay.

Bronchoalveolar Lavage Fluid (BALF) Collections

After blood collection a cannula from which needle was removed (Terumo, Somerset, NJ) was inserted in the nicked trachea. The chest cavity was opened quickly to expose the heart and provide room for lung expansion. 1 ml syringe was attached to the catheter and provided a 1 ml puff of air to the lung 3 times, detaching the syringe and allowing the lung to collapse after each puff. Whole body perfusion was performed with cold 1X phosphate buffer saline (PBS) containing 5 U/ml heparin. Perfusion was performed until organs were blanched of blood and fluid exiting the heart was free of color. Three puffs of air were provided to the lungs as already described, and then a 3 ml of syringe loaded with 1.5 ml of PBS, was attached to the catheter and gently instilled in the lungs. After pausing for 10 sec suction was applied to recover the BALF. The process was repeated 2 more times with 1 ml of PBS for each flush. All lavage fluid aliquots were pooled in one tube and spun for 2 min at 5000 *X g*. BALF supernatant was aliquoted to cryovials and snap frozen in liquid N_2. A small amount of the supernatant was frozen separately for the urea assay.

Sample extraction

ETA and ETASO were measured in plasma and BAL fluid by the extraction method described in Palmer et al. (2012). Briefly, 0.01 mM of thiobenazamide (TBZA) was spiked in all samples as an internal standard and extracted with three aliquots of methanol (MeOH) with vortexing between each addition. The mixture was incubated at room temperature for 10 min, and then centrifuged for 10 min at 4°C at 17,000 x *g*. Supernatant was transferred into1.7-ml microcentrifuge tubes and evaporated to dryness under a stream of compressed nitrogen gas. Residues were resuspended in 100 µl of solvent

(H2O-acetonitrile, 75:25). Samples were centrifuged for 3 min at room temperature at 16,300 x *g*, to pellet any debris. Clear supernatant was transferred into.2.5-mL Waters (Milford, PA) HPLC vials with 150-µl glass inserts, for analysis. HPLC analysis was performed on a Waters 2695 separations module equipped with a 2996 photo diode array detector and a Waters C_{18} Atlantis® 5 µm, 3.9 x 150 mm column. The flow rate was 0.8 ml /min. Solvents for the mobile phase consisted of 80% H_20 and 20% MeOH at a temperature of 35°C running isocratically for 20 minutes. Quantitation of ETA and ETASO was performed with standards measured at 267 nm. A broad spectra range was also collected from 210 nm to 400 nm to verify the identity of each analyte by absorption profiles. One hundred-250 µl of plasma and 500-700 µl of BALF were taken for quantitation. The sensitivity of this assay for ETA was 0.25 µg /ml and 0.32 µg /ml for ETASO (Palmer et al. 2012).

Quantification of ELF volume and ETA concentration in ELF

The amount of ELF recovered was calculated by the urea dilution method (Rennard et al. 1986). Urea nitrogen was measured in plasma and BAL supernatant by using a quantitative colorimetric assay (Pointe Scientific, Canton, MI) with a range of 0.05 to 150 mg/dL. The volume of ELF in BAL fluid was derived from the relationship $V_{ELF} = V_{BAL}$ X $urea_{BAL}$ / $urea_{plasma,}$ where V_{ELF} is volume of ELF sampled by the BAL, V_{BAL} is volume of aspirated BAL fluid, $urea_{BAL}$ is concentration of urea in BAL fluid, and $urea_{plasma}$ is concentration of urea in plasma. The concentration of ETA in the ELF (ETA_{ELF}) was derived from the relationship ETA_{ELF} = ETA_{BAL} X V_{BAL}/V_{ELF}, where ETA_{BAL} is the measured concentration of ETA in BAL (Conte et al. 2001).

Long-term ETA dosing, tissue harvest and RNA extraction

ETA dose of 125 mg/kg was given to both wildtype and knockout mice for up to 28 days; whereas vehicle-treated mice received vet syrup. The ETA sample for gavage was prepared the same way as described above. ETA dosing was done each day in late afternoon. Mice were given a one day break from ETA dosing after 6 days of continuous dosing. Mouse weights were measured every day and dosing adjusted accordingly. Animals were monitored twice daily for signs of morbidity, pain or distress. Lung and liver tissue were harvested at the end of the treatment and kept in RNA-later (Quiagen, Valencia, CA) at 4^0C. After 24 hours, RNA later was removed and tissues were frozen at -80^0C. Total cellular RNA was extracted from lung and liver of wildtype and knockout mice by using RNeasy Mini Kit (Qiagen, Valencia, CA) according to manufacturer's protocol. RNA was quantified with a nano-drop^{TM}1000 Spectrophotometer (Thermo Scientific, Wilmington, DE) Total RNA (500 ng) was used for cDNA synthesis using Superscript III First Strand Synthesis kit (Invitrogen, Grand Island, NY). The expression of *FMOs* 1-5 was evaluated by iQ5 Multicolor Real Time PCR Detection System (Bio-Rad, Hercules, CA) in duplicate with RT2 SYBR Green Fluor PCR Master mix (Qiagen, Valencia, CA), with primers and PCR conditions as given in Table A2.1. Glyceraldehyde-3-phosphate dehydrogenase (GAPDH) gene expression was used as an internal control. The gene-specific primer pairs were synthesized (Invitrogen, Grand Island, NY) and used to produce DNA amplicons for real-time PCR calibration curves, and for amplification reactions with test samples. Gene-specific standards were constructed to quantitate each gene target. Lung and liver cDNA from all mice were pooled and PCR products generated (Bio-Rad- iCycler, Hercules, CA) by using the conditions, 95^0C for 5 min, followed by 35 cycle of 95^0C for 30s and 72^0C for 30s using

Table 2.1 – Primers used for quantitative PCR of mouse FMO and housekeeping genes

Gene	Primer Sequence (5' to 3')	Amplicon size (bp)	Annealing temperature	Gene Accession no.	PCR efficiency	Reference
Fmo1	5'-TGTCTCTGGACAGTGGGAAGT 5'-CATTCCAACTACAAGGACTCG	217	60	NM_010231.2	91.10%	Janmohamed et al., 2004
Fmo2	5'-CATCCTGGTGGTTGGAATAG 5'-GTAGCCATCTTCAGAGATTCG	130	60	NM_018881.3	93.10%	IDT
Fmo3	5'-CAGCATTTACCAATCGGTCTTC	227	60	NM_008030.1	95%	Zhang et al., 2009
Fmo4	5'-TGACTTCCCATTTGCCAGTAG 5'-AGCCATGAGAAATTCTGGGACTA 5'-CTTGGCTGTGCAGGATCTGT	277	60	NM_144878.1	89.40%	Zhang et al., 2009
Fmo5	5'-GACTACCCCATCCCAGATCAT 5'-ACCTGCTGTTTCCCTTCACA	200	60	NM_001161765.1	101%	Zhang et al., 2009
Gapdh	5'-TCT CCC TCA CAA TTT CCA TCC CAG 5'-GGG TGC AGC GAA CTT TAT TGA TGG	100	64	M32599	101.90%	Xu and Miller 2004

IDT- https://www.idtdna.com/primerquest/Home/Index

Biolase DNA polymerase (Bioline, London, UK) with 50 µl of reaction mixture. PCR products were electrophoresed on 2% agarose gels and then purified with a Zymoclean^{TM} Gel DNA Recovery kit (Zymo Research Corp. Orange, CA) followed by quantitation with nano-drop spectrophotometer and diluted to cover a 10^6-fold range for the calibration curve. Normalized data were expressed as a ratio of the *Fmo/Gapdh* in pg. Real-time PCR reactions contained 2.0 ml cDNA template (or appropriately diluted DNA standard), 0.4 mM forward primer, 0.4 mM reverse primer for *Fmos* and 0.3 mM forward primer, 0.3 mM of reverse primer for *Gapdh*, 10 ml 2X SYBR1 green master mix (Quiagen, Valencia, CA) and water to make final volume 20 µl. The quantitative PCR reactions were run at 95°C for 10 min, followed by 40 cycles at 95°C for 15s and at 60°C for 1 min followed by melting curve analysis. Duplicate no-template controls were included on the same plate for each gene analyzed. At the end of the PCR cycling steps, product melting curves were inspected and confirmed to have a single amplification peak. PCR products were also run on 2% agarose gel and visualized by GelRed staining to confirm one band of appropriate size.

Sequences for mouse *Fmo1, Fmo2, Fmo3, Fmo4* and *Fmo5* were aligned to identify gene-specific sequences for primer synthesis. Comparison of all the *Fmo* primers with *Fmo6, Fmo9, Fmo12* and *Fmo13* genes showed no alignment, ensuring that the amplified polymerase chain reaction (PCR) products by the primer pairs were from a single template.

Statistical analysis

Statistical analyses were performed by using Graph Pad Prism 4 (GraphPad Software, La Jolla, CA). ETA and ETASO, plasma and ELF level analysis in wild type and knockout mice were compared by using a two-way

analysis of variance (ANOVA) test. The comparisons of interest were genotype (wildtype vs knockout) and time post gavage. For *Fmo 1, 2 and 4*, mRNA levels in ETA-treated mouse groups (wildtype and knockout) were compared with the corresponding controls via a Student's t-test analysis assuming equal variances. If the overall test differences were below $p \leq 0.05$ then they were considered significant. For *Fmo3 and Fmo5* mRNA difference analysis between wildtype and knockout mice, ETA- and vehicle-treated samples of wildtype and knockout mice were combined together to make a larger sample group and then *Fmo3* and *5* expression level in knockout mice was compared with wild type by a Student's *t*-test assuming equal variances.

2.4 Results

Plasma levels of ETA and ETASO- wild type versus Fmo1/2/4 knockout mouse

Sixty-four male mice were taken for the ETA metabolism study. Mice did not show any adverse effect after ETA dosing. Four time points of 0.5, 1, 2 and 3 hours were analyzed for prodrug and metabolite. Each mouse was gavaged with a single dose of 125 mg ETA/kg body weight and then euthanized at the correct time post-ingestion. Both wild type and knockout mouse metabolized ETA. ETA, ETASO and ETAA were quantified in plasma and ELF samples but ETAA was excluded from the final analysis due to very low levels of detection in both wild type and knockout mice. Differences between wild type and knockout mice were observed in metabolic profiles. (representative HPLC tracings are shown in Fig. 2.1 A and B). Pharmacokinetic measurements from wild type and knockout mice are summarized in Table 2.2. The mean concentration maxima (C_{max} ± SD) found in wild type mice for ETA and ETASO were 3.86 ± 1.79 and 7.18 ± 2.2 µg /ml, respectively 1 hour post-gavage. The mean concentration maxima (C_{max} ± SD)

found in Knockout mice for ETA and ETASO were 10.98 ± 4.96 and 5.65 ± 2.35 µg /ml. Two–way ANOVA analysis showed a significant genotypic difference between wild type and knockout mice ($p<0.0001$) (Fig.2.3 A) for plasma ETA levels at all-time points ($p<0.005$) (Fig. 2.3 A). Plasma ETASO levels also showed a significant ($p<0.013$) genotypic difference between wild type and knockout mice (Fig. 2.3 B) at each time point ($p< 0.0001$) (Fig 2.3B) by two-way ANOVA analysis. A significant effect of FMO genotype was observed with respect to the concentration of ETA and ETASO in plasma samples.

ELF levels of ETA and ETASO- wild type versus Fmo1/2/4 knockout mice

We detected ETA and ETASO in ELF of wild type and knockout mice at all four time points. Differences between wild type and knockout mice were observed in metabolic profiles (representative HPLC tracings are shown in Fig. 2.2 A and B). Pharmacokinetic measurements from wild type and knockout mice are summarized in Table 2.3. The mean concentration maxima (C_{max} ± SD) found in wild type mice for ETA and ETASO were 2.07 ± 2.42 and 4.95 ± 2.4 µg /ml, respectively at 2 hour and 1 hour post-gavage. The mean concentration maxima (C_{max} ± SD) found in knockout for ETA and ETASO were 11.1 ± 5.78 and 1.35 ± 0.73 µg /ml, respectively at 2 hour and 3 hour post-gavage. Two–way ANOVA analysis showed a significant ($p<0.0001$) difference with respect to genotype on ELF ETA levels at each time point ($p >0.0068$) (Fig. 2.4 A) between wild type and knockout mice. ELF ETASO level also showed a significance difference due to genotype ($p>0.0001$) at each time point ($p<0.045$) (Fig 2.4 B) between wild type and knockout mice by two-way ANOVA analysis. A significant effect of FMO genotype was observed for the concentration of ETA and ETASO in ELF sample.

ETA and ETASO levels- plasma versus ELF in wild type and Fmo1/2/4 knockout mouse

The maximal ELF/plasma ratios (mean ± SD) observed for ETA concentrations were 0.8 ± 0.47 at 2 hour in wild type mice (Table 2.4). Half an hour and 3 hour time points were not considered as, out of five mice, ELF ETA was detected in only one and two mice at 0.5 and 1 hour, respectively. For Knockout mice, maximal ELF/plasma ratios (mean ± SD) observed for ETA concentrations were 1.63 ±1.07 at 2 hour (Table 2.4). Maximal ELF/plasma ratio (mean ± SD) for ETASO concentrations for wild type mice were 0.99 ± 0.64 at 0.5 hour and for knockout mice were 0.50 ± 0.20, 3 hour post-gavage (Table 2.4).

Table 2.2 Plasma pharmacokinetics parameter of ETA and ETASO

	WT		KO	
Pharmacokinetics parameter	ETA	ETASO	ETA	ETASO
C_{max} (µg/ml)	3.86 ±1.79	7.18±2.2	10.98±4.96	5.65±2.35
t_{max} (hour)	1	1	1	1

Table 2.3 ELF pharmacokinetics parameter of ETA and ETASO

	WT		KO	
Pharmacokinetics parameter	ETA	ETASO	ETA	ETASO
C_{max} (µg/ml)	2.07±2.42	4.95±2.4	11.1±5.78	1.35±0.73
t_{max} (hour)	2	1	2	3

Table 2.4 ELF/plasma ratios of ETA and ETASO

	WT		KO	
	ELF/plasma (µg/mL)		ELF/plasma (µg/mL)	
Time point (hour)	ETA	ETASO	ETA	ETASO
0.5		0.99 ± 0.64	1.04 ± 0.22	0.43±0.20
1	0.54 ± 0.38	0.79 ± 0.45	0.95 ± 0.67	0.19±0.08
2	0.8 ± 0.47	0.32 ± 0.1	1.63 ±1.07	0.37±0.22
3		0.74 ± 0.3	0.99 ± 0.34	0.50±0.20

Abbreviation: WT-Wild type, KO- Knockout

(A)

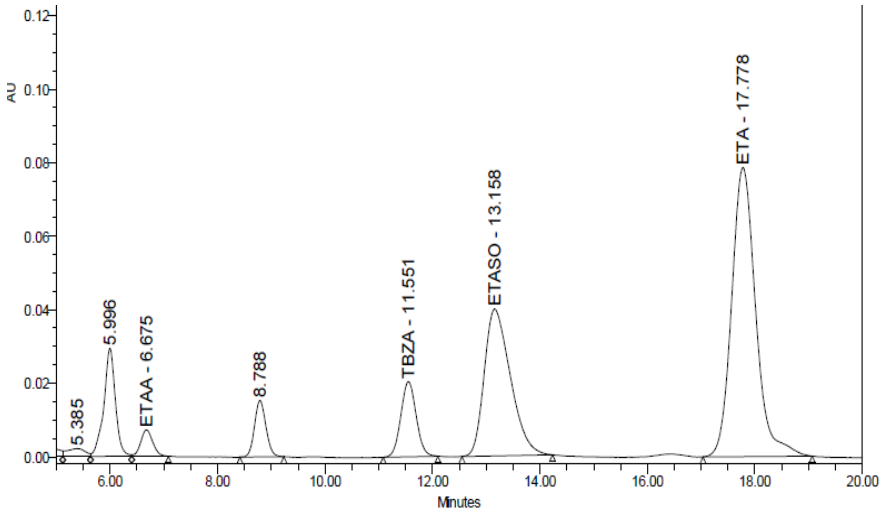

(B)

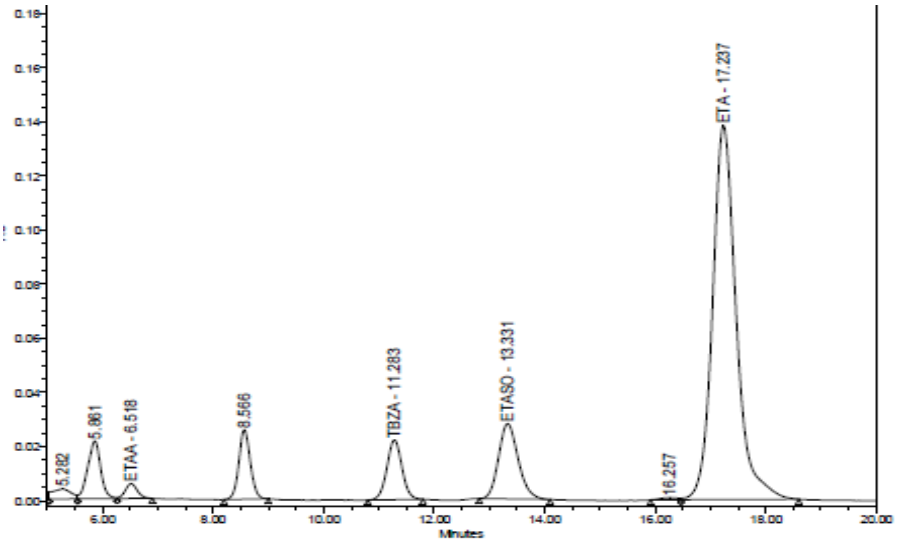

Figure 2.1 Representative examples of plasma HPLC tracings.
Wild type (A) and knockout (B) mice plasma samples showing TBZA, ETA and ETASO peaks by HPLC analysis. All tracings shown are from 1 hour post-gavage.

(A)

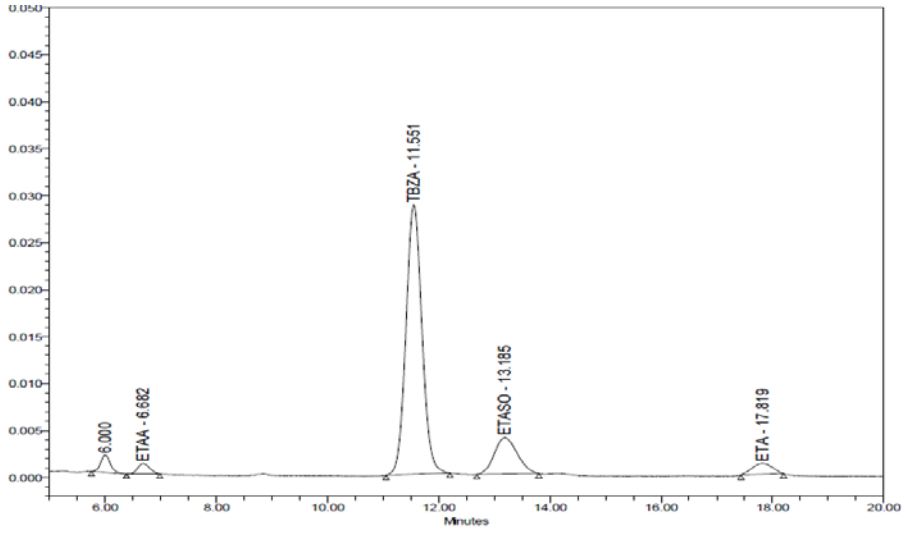

(B)

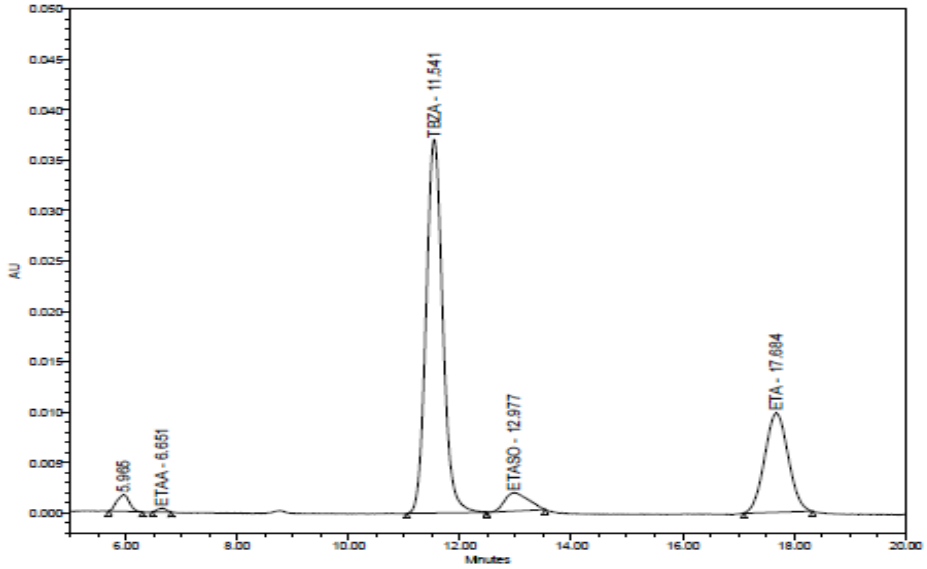

Figure 2.2 Representative examples of ELF HPLC tracings.
Wild type (A) and knockout (B) mice ELF samples showing TBZA, ETA and ETASO peaks by HPLC analysis. All tracings shown are from 1 hour post-gavage

(A)

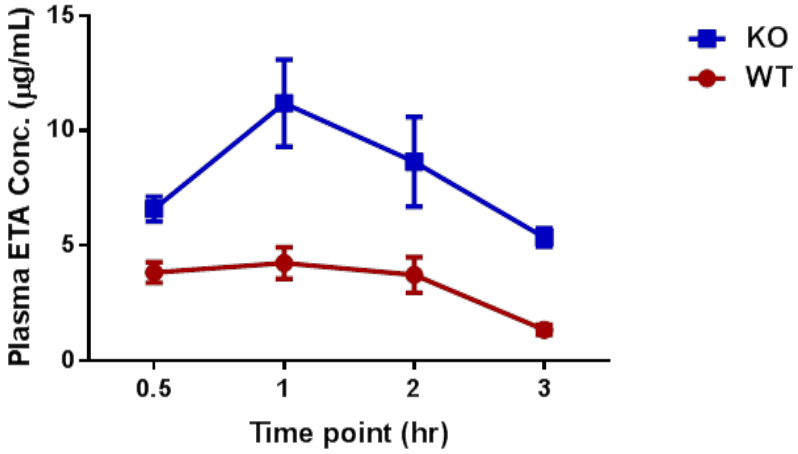

(B)

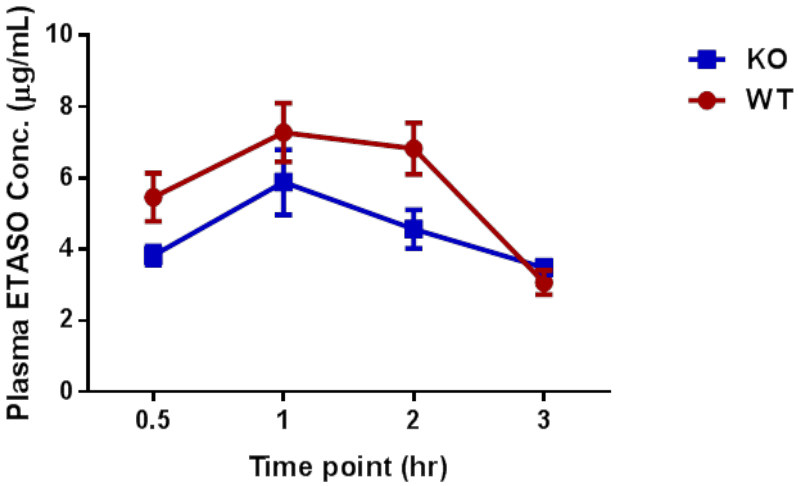

Figure 2.3 Time course for ETA metabolism in plasma.
Metabolic graphs depicting A) the mean of plasma ETA of wild type and knockout mice and B) the mean of plasma ETASO of wild type and knockout mice. The charts are based on time versus plasma concentration (µg/ml), error bars are standard error

(A)

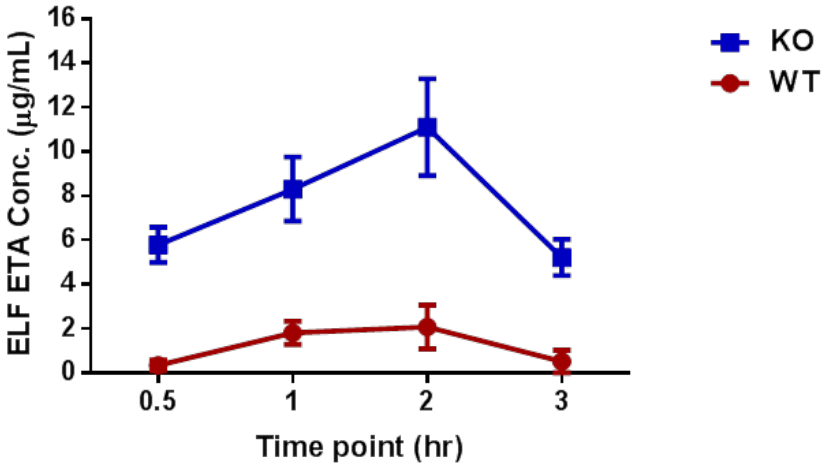

(B)

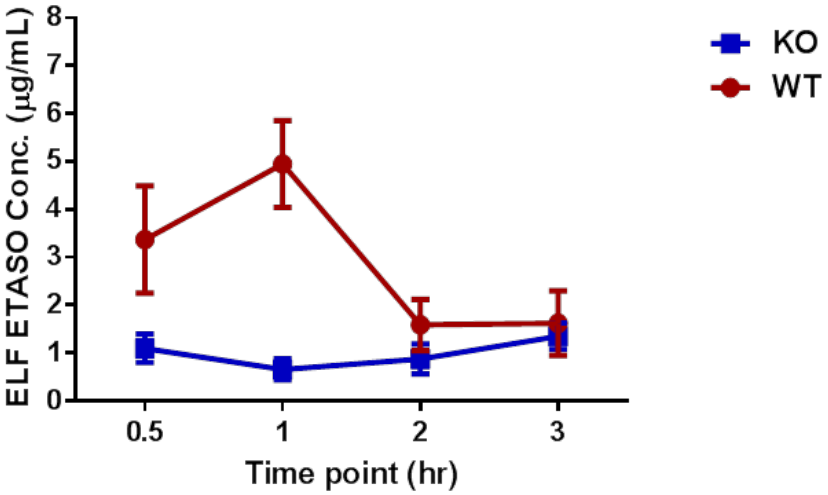

Figure 2.4 Time course for ETA metabolism in ELF.
Metabolic graphs depicting A) the mean of ELF ETA of wild type and knockout mice and B) the mean of ELF ETASO of wild type and knockout mice. The charts are based on time versus ELF concentration (µg/ml), error bars are standard error

Long term ETA treatment effect on expression of Fmo 1, 2 and 4 mRNA in wild type mice

Expression levels of *Fmo1, Fmo2, and Fmo4* were quantitated in lung and liver tissue of wildtype and knockout mice. Levels of *FMO* expressed in each mouse were normalized by GAPDH. Real-time reverse transcription-PCR analysis revealed differential expression of pulmonary and *hepatic Fmo1, Fmo2 and Fmo4 mRNA* in 28- day ETA-treated wild type mice compared to controls. In wildtype male mice *Fmo1, 2* and *Fmo4* mRNA levels were up-regulated with ETA treatment in liver (Fig 2.5 A, B & C). *Fmo1* and *4* mRNA levels in liver were significantly (p=0.036, 0.04 respectively,) increased with ETA treatment (Fig 2.5 A & C), while *Fmo2* up-regulation did not reach to significance (p=0.06) (Fig 2.5 B). *Fmo1* and *4* expression in male lung also showed little elevation (Fig 2.5 A & C) in compare to control treated mice but not significant. *Fmo1, 2* and *4* expression in wild type female lung tissue was seen elevated (Fig 2.6 A, B & C) but not significant with p values 0.07, 0.09, 0.2 respectively.

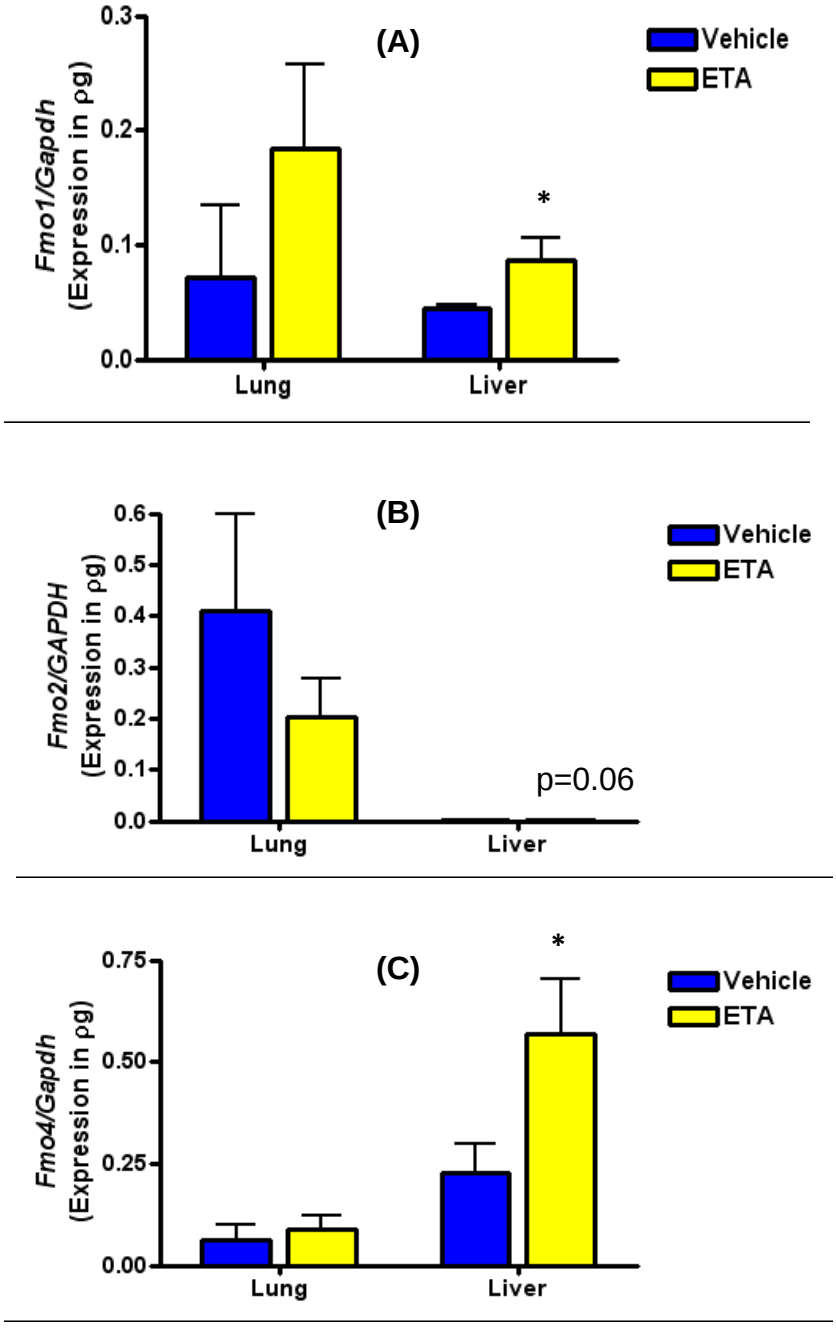

Figure 2.5 ETA treatments effect on *Fmo1, 2* and *4* expressions in wild type male mice.

Fmo1 (A), *Fmo2* (B) and *Fmo4* (C) mRNA levels are shown in lung and liver of wild type male mice after 28- days of ETA treatment in comparison with the corresponding control mice groups. Graphs show mean ± SEM (n= 4 to 5). Liver from ETA-treated male showed significant elevation in *Fmo1* and *Fmo4* mRNA (* $p<0.05$) versus vehicle controls.

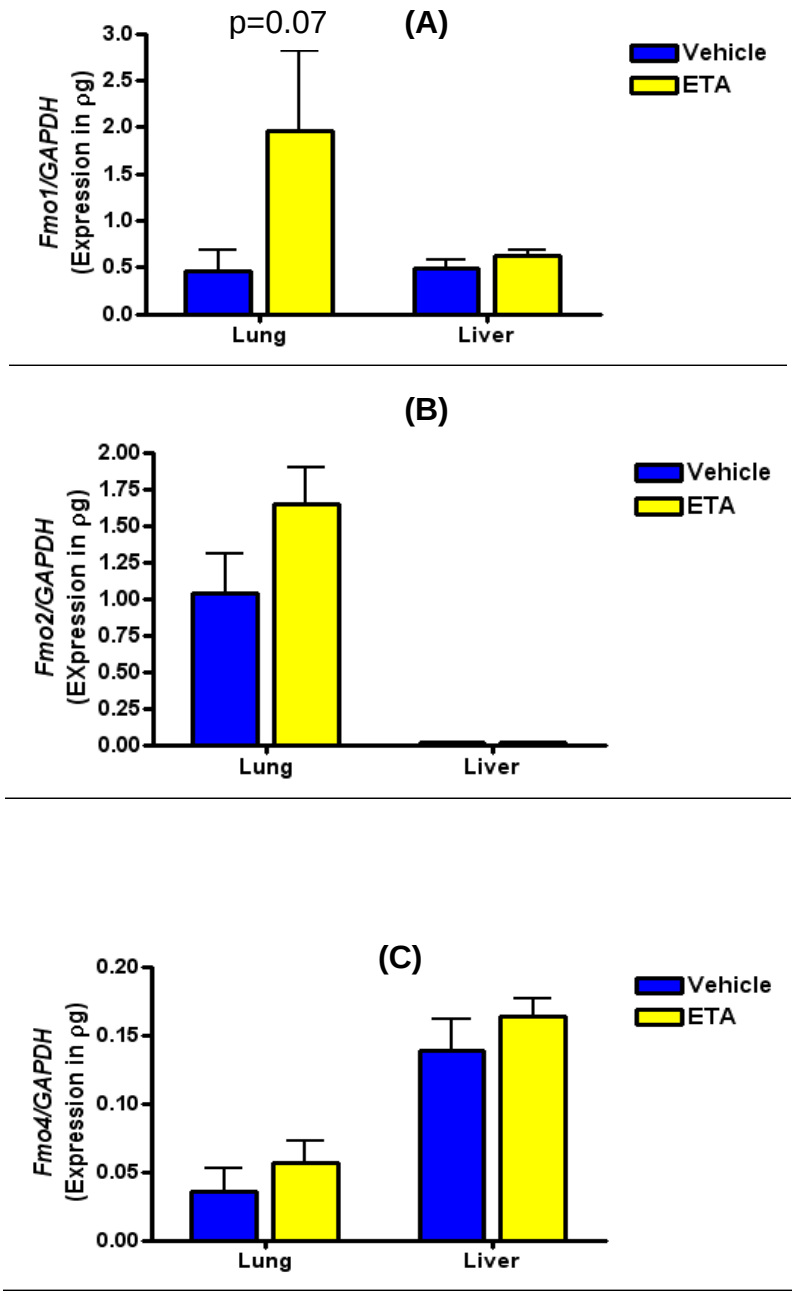

Figure 2.6 ETA treatments effect on *Fmo1, 2* and *4* expressions in wild type female mice.

Fmo1 (A), *Fmo2* (B) and *Fmo4* (C) mRNA levels are shown in lung and liver of wild type female mice after 28-days of ETA treatment in comparison with the corresponding control mice groups. Graphs show mean ± SEM (n= 4 to 5).

FMO3 and FMO5 mRNA levels in Fmo1/2/4 knockout mice and ETA treatment effect

To determine whether the absence of *Fmo1*, *Fmo2* and *Fmo4* in mice have any effect on the expression of other members of the *Fmo* gene family, *Fmo3* and *Fmo5* levels of knockout mice were compared with wild type mice in both lung and liver. ETA- and vehicle-treated mice were grouped together to create a larger sample size (n=10) for *Fmo3* and *Fmo5* expression analysis. *Fmo3* mRNA levels in knockout mice were significantly reduced in lung of both males (p= 0.004) (Fig.2.7 A) and females (p=0.003) (Fig. 2.8 A) compared to wild type mice. Much lower *Fmo3* mRNA expression was observed in male mouse liver (Fig. 2.7 A) compared to females (Fig.2.8 A) which has been reported in previous studies. *Fmo3* expression in female liver was also significantly (p=0.001) reduced compared to wild type mice (Fig. 2.8 A). *Fmo5* mRNA levels in knockout mice were significantly reduced in liver of both males (p= 0.0005) and females (p= 7.94E-10) compared to wild type mice (Fig. 2.7 B and 2.8 B). In lung tissue, there was no significant difference in either sex (Fig.2.7 B and 2.8 B). Thus, genotypic differences were observed for *Fmo3* and *Fmo5* mRNA expression.

Regulation of *Fmo3* mRNA expression with long-term ETA treatment was observed in lung and liver of ETA- and vehicle- treated wildtype and knockout mice. Lung and liver from male and female wildtype and knockout mice did not show any significant difference with respect to *Fmo3* expression (Fig. 2.9 A and 2.10 A). *Fmo5* also did not show any significant expression change in lung and liver from wild type and knockout mice (Fig. 2.9 B and 2.10 B). There were no significant expression differences observed for *Fmo3* or *Fmo5* for wild type and knockout mice with long –term ETA treatment.

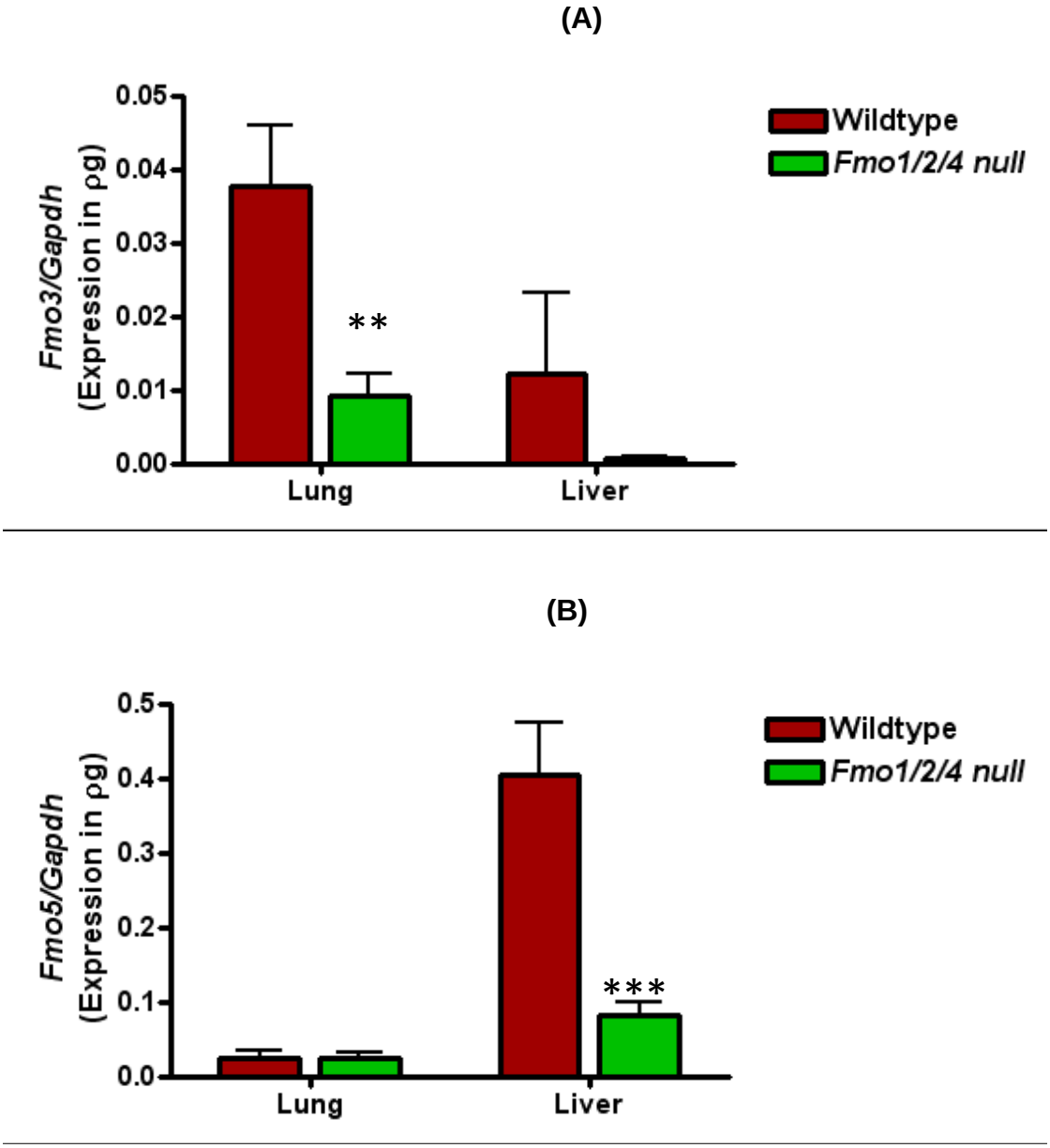

Figure 2.7 *Fmo3* and *Fmo5* message levels in wildtype and knockout male mice.

Graphs show mean ± SEM (n= 9 to 10), lung and liver mRNA levels of *Fmo3* (A) and *Fmo5* (B) of wildtype and knockout male mice. *Fmos* mRNA levels are normalized with *Gapdh* mRNA level. Statistically significance differences between wildtype and Knockout mice are identified by ** $p<0.01$, *** $p<0.001$.

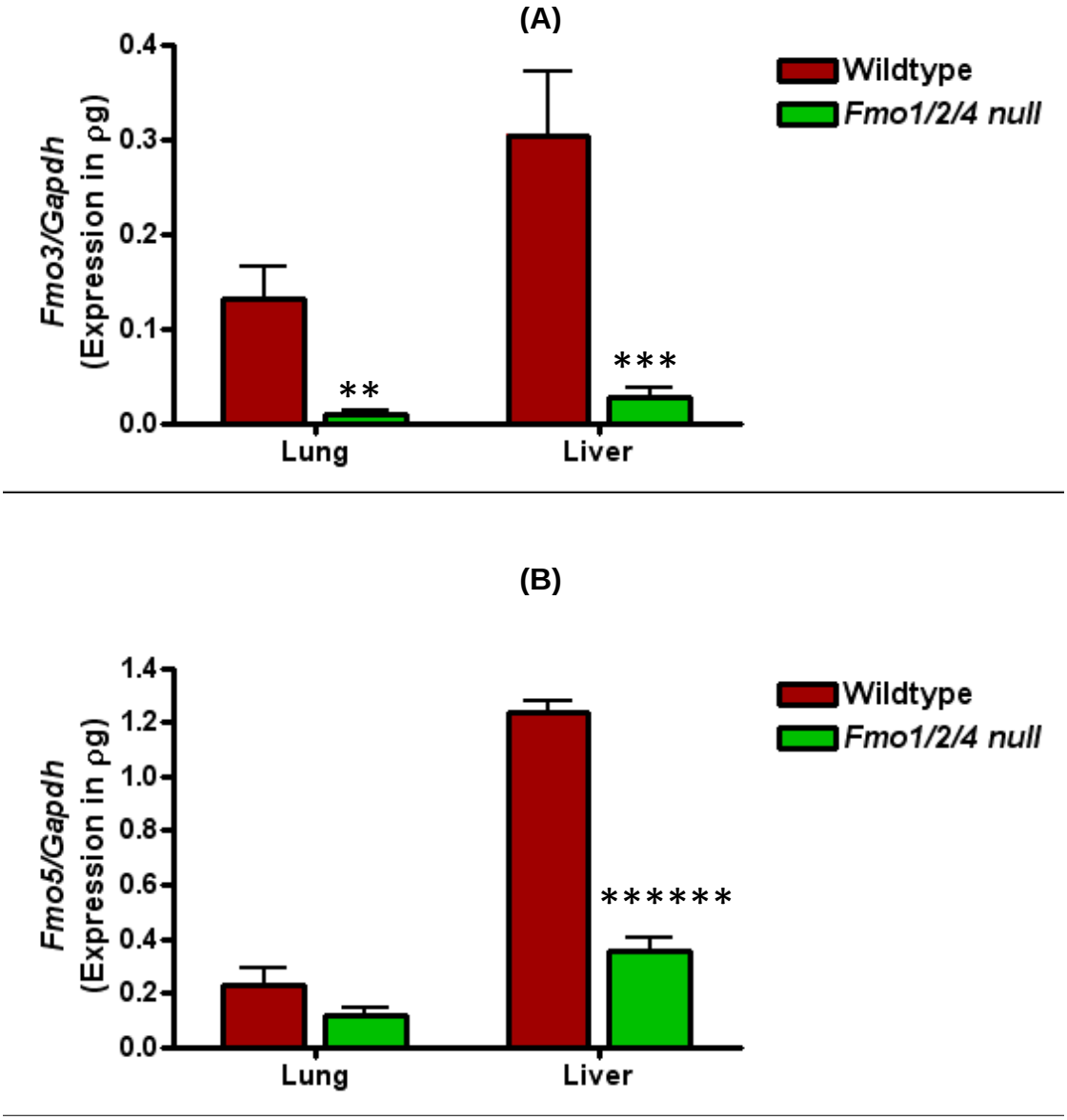

Figure 2.8 *Fmo3* and *Fmo5* message levels in wildtype and knockout female mice.

Graphs show mean ± SEM (n= 9 to 10), lung and liver mRNA levels of *Fmo3* (A) and *Fmo5* (B) of wildtype and knockout female mice. *Fmos* mRNA levels are normalized with *Gapdh* mRNA levels. Statistically significance differences between wildtype and knockout mice are identified by ** p<0.01, ******* p<0.001 and ***** p<0.00001

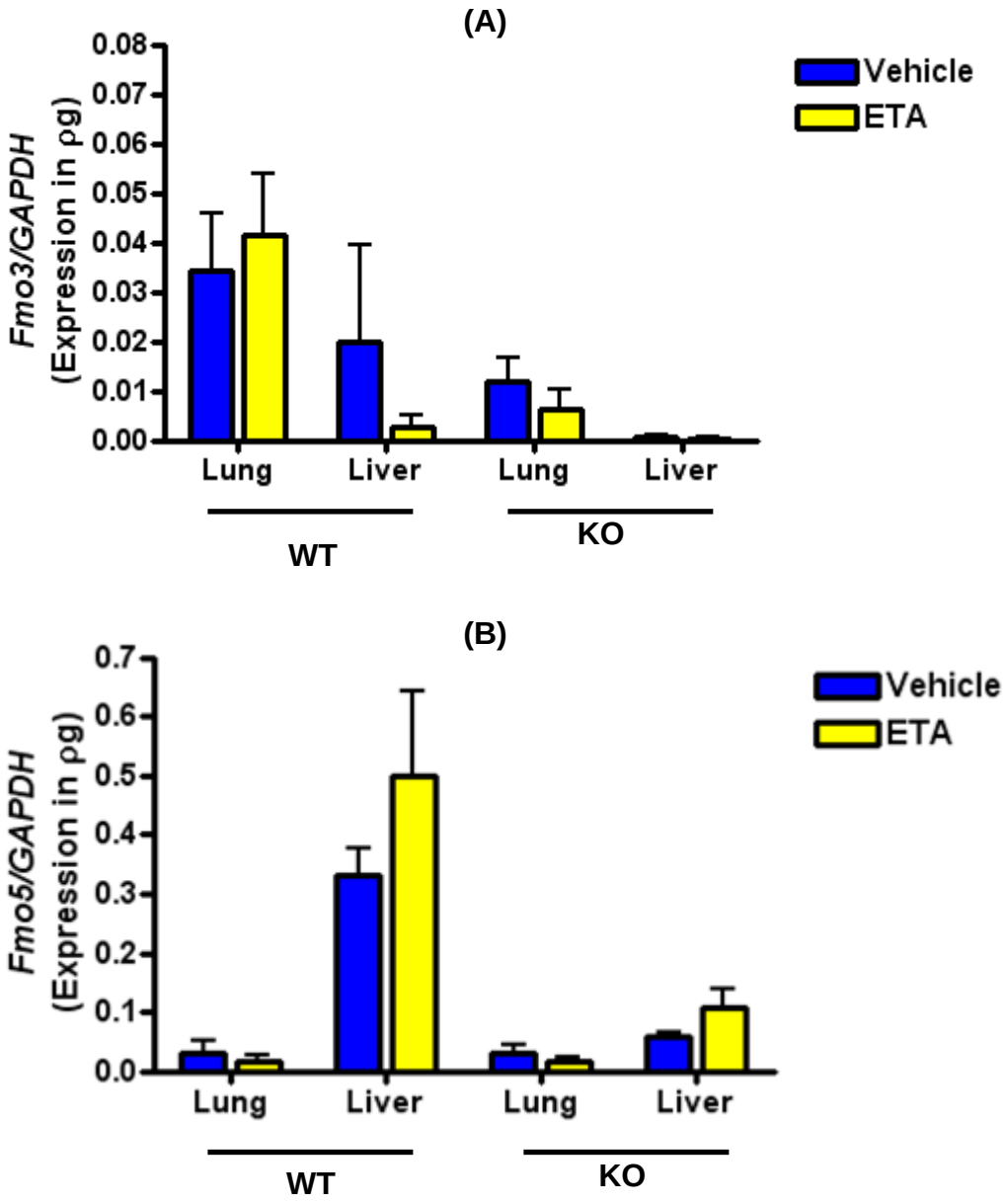

Figure 2.9 Effect of ETA treatments on *Fmo3* and *Fmo5 expressions* in wild type and knockout male mice

Fmo3 (A) and *Fmo5* (B) mRNA levels are shown in lung and liver of wild type and knockout male mice after 28-days of ETA treatment in comparison with the corresponding control mice groups. Graphs show mean ± SEM (n= 4 to 5). Abbreviation; WT-wildtype, KO-knockout.

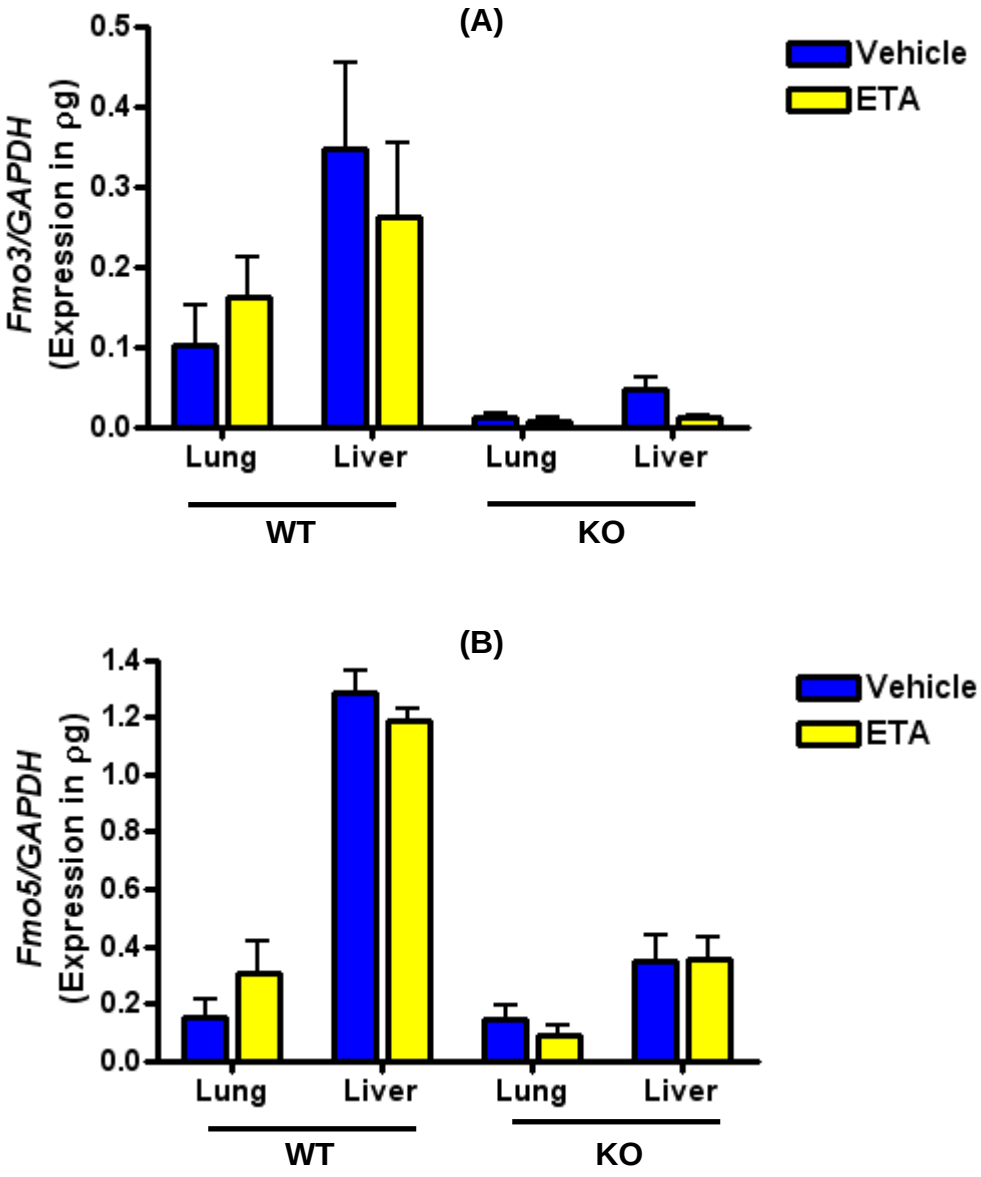

Figure 2.10 Effect of ETA treatments on *Fmo3* and *Fmo5 expressions* in wild type and knockout female mice

Fmo3 (A) and *Fmo5* (B) mRNA levels are shown in lung and liver of wild type and knockout female mice after 28 days of ETA treatment in comparison with the corresponding control mice groups. Graphs show mean ± SEM (n= 4 to 5). Abbreviation; WT-wild type, KO-knockout.

2.5 Discussion

To compare the metabolism of ETA between individuals with a functional FMO2.1 and a truncated, inactive FMO2.2, a novel *Fmo1/2/4* knockout mouse model was utilized. This knockout mouse created by Hernandez et.al, 2006, mimics FMO2 expression in human lung of Caucasians and Asians (only *FMO2*2* alleles). Both the wild type and knockout mice showed FMO-dependent ETA metabolism generating sulfenic acid (ETASO) as shown by HPLC. Minimum inhibitory concentrations (MICs) for sensitive strains of *M. tuberculosis*, tested with the BACTEC method, have been reported to be in the range of 0.25 to 0.5 µg/ml (Rastogi et al. 1996) and 0.3 to 1.2 µg/ml (Heifets et al. 1991). For clinical purposes, the recommended breakpoints for susceptible, moderately susceptible, moderately resistant, and resistant strains are < 1.25, 2.5, 5.0, and >5.0 µg/ml, respectively (Heifets 1988). The ETA plasma and ELF concentrations reached the MIC and above for *M. tuberculosis* in all mice ensuring 125 mg/kg is an appropriate dose to treat infection (Bastian and Colebunders 1999; Schon et al. 2011; Thee et al. 2011).

We have demonstrated that ETA metabolism was affected by FMO genotype. Plasma and ELF drug and metabolite concentrations were significantly different between wild type and knockout mice. In comparison with mice having functional Fmo2, the concentrations of ETA in plasma and ELF of knockout mice were between two to three times and four to five times higher, respectively. The major metabolite, ETASO, followed the same genotypic difference. Plasma ETASO levels in wild type mice were higher at 0.5, 1 and 2 hour post-gavage, whereas ELF ETASO was higher in wild type mice 0.5 and 1 hour post-gavage. The C_{max} for ETASO in wild type mice was up to three times higher than in knockout mice.

ETA concentrations in lung largely exceeded the MIC for *M. tuberculosis* for both genotypes (Heifets et al. 1991; Rastogi et al. 1996). The highest ETA ELF/plasma ratios for wild type and knockout mice were 0.8 ± 0.47 and 1.63 ±1.07, respectively, whereas highest ETASO ELF/plasma ratios for wild type and knockout mice were 0.99 ± 0.64 and 0.50 ± 0.20, respectively. For many reasons, the ELF levels of antibiotics measured in healthy individual may not be an accurate measure of the actual antibiotic concentrations at the site of infection (Kiem and Schentag 2008). In plasma, ETA peaked 1 hour post-gavage in both wild type and knockout mice, whereas ELF ETA concentrations were highest for wild type and knockout mice 2 hour post-gavage. The concentrations of antibiotics in various target organs are the result of a dynamic process of uptake and clearance. If a single dose of antibiotic is given, the peak tissue level will lag behind the peak plasma level. However, after several doses of an antibiotic with a long half-life, steady state kinetics will be achieved both in the plasma and tissue (Schentag 1989). ELF/plasma ratios for ETASO were higher than ETA in wildtype mice while lower in knockout mice, again confirming the FMO genotypic impact on ETA metabolism.

In summary, higher levels of ETASO, compared to ETA were observed at 0.5, 1 and 2 hour in plasma of wild type mice and at 0.5 and 1 hour in ELF. Plasma and ELF levels of ETASO were always significantly less than the prodrug ETA in knockout mice. The relatively higher yield of ETASO in wild type mice may allow for greater depletion of the glutathione pool. Potential generation of more reactive oxygen species gives rise to increased oxidative stress. Reduced conversion of ETA to ETASO in individuals with no functional FMO2 could lower potential oxidative stress. ELF ETASO C_{max} in wild type mice was three to four times higher than in knockout mice, while differences in

ETASO in plasma were not that high. This suggests more glutathione depletion in lung tissue and higher toxicity in wild type mice.

FMO3 and 5 expressions

FMO expression in mammalian species is known to be species-, tissue-, age-, and gender-dependent. The physiological mechanisms controlling and regulating FMO expression are not well understood (Cashman 2003; Motika et al. 2007). Interestingly, this study showed reduced levels of *Fmo3* and *Fmo5* in *Fmo1/2/4* null mice. We had originally hypothesized that, given the overlapping substrate specificity of most *Fmos* that loss of *Fmo1, 2* and *4* would result in up-regulation of *Fmo3* and *Fmo5*. This result suggests that *Fmo3* and *Fmo5* expression could be co-regulated to some degree with *Fmo 1, 2* or *4* isoforms. Little is known about regulation of *FMO* expression and further analysis is required to understand the molecular interactions involved between regulations of various isoforms. The model used in the present study had shortcomings. A mouse in which individual *Fmos* could be knocked out by a tissue- and/or temporally-controlled promoter would be superior to the strain used in this study.

As we observed a degree of ETA metabolism in *Fmo1/2/4* knockout mice, this would imply Fmo3 and/or Fmo5 was responsible for the ETASO produced. As Fmo5 does not S-oxygenate ETA to an appreciable degree (Henderson et al. 2008), Fmo3 is probably responsible for the ETASO formation. Another possibility is that cytochrome P450s (CYPs) may be contributing to the S-oxygenation of ETA. Henderson et al. (2008) demonstrated that ETA metabolism in lung was primarily due to FMO with little or no contribution from CYPs. In this study, metabolism of ETA was inhibited

by FMO the competitive inhibitor thiourea while there was no change in the presence of the general CYP inhibitor SKF-525A.

Fmo1, 2 and 4 regulations

Both *Fmo1* and *Fmo4* mRNA in wild type mice had elevated expression in lung and liver for both males and females. Higher levels of ETASO formation as observed in wild type mice, I hypothesize that higher ETASO might cause glutathione depletion and result in oxidative stress and toxicity indirectly leading to altered *Fmo* expression. To test this hypothesis glutathione depletion and oxidative stress with 4- weeks of ETA treatment should be assessed. *Fmo* expression should also be studying in the *Mycobacterium* infected wild type and knockout mice with and without 4 weeks of ethionamide treatment to understand the mechanism of regulation better in the presence of infection, inflammation and toxicity. Zhang et al, (2009), has shown down-regulation of hepatic *Fmo1, 3* and *5* mRNA in lipopolysaccharide models of inflammation. *FMO* genes are reported to be involved in the oxidative metabolism of various xenobiotics and to catalyze the oxidation of reduced GSH to glutathione disulfide (GSSG) (Cereda et al. 2006). Up-regulation of *Fmo1*, *2* and *4* may disturb GSSG/GSH balance and cause oxidative stress.

Surprisingly, we did measure *Fmo1*, *Fmo2* and *Fmo4* mRNA in some of knockout mice, though the levels of expression were orders of magnitude lower than in wild type mice. *Fmo* expression were seen mostly in lung tissue in comparison to liver tissue of knockout mice. We checked all Fmo primers to ensure we should be amplifying product from a single transcript. *Fmo 1/2/4* knockout mice used in the study have exon 2-9 of *Fmo2*, exon 1-7 of *Fmo4* and the entire *Fmo1* gene deleted on chromasome 1 (Hernandez et al. 2009).

We further investigated *Fmo1* expression in the *Fmo1/2/4* knockout mice. *Fmo1* expression was checked with primers that should be more specific compared to the syber green method. We say essentially the same results with these *Fmo1* primers (data not shown). PCR products from wildtype and Knockout mice were also sequenced to ensure the identity of amplified sequences. We further went ahead and genotyped some of the knockout mice for absence of *Fmo1, 2 and 4 genes*. Lung and liver tissues used for genotyping were same samples which were used for mRNA expression analysis. Genotyping results did not show any *Fmo1,2 and 4* epressions in any of the knockout mice lung or liver sample (Fig. sup. A3.4 & A3.5) confirming that knockout mice did not have *Fmo1*, 2 or 4 expressions. We re-isolated RNA from the same frozen tissue samples. We assumed that *FMO* epressions observed may be coming from the lab contamination of wildtype mice samples. RNA isolation was done in a biosafety level-2 hood which was not usually exposed with mice samples to clear contamination possibility, but again we observed *Fmo1* expressions in lung and liver of knockout mice samples.

Given our findings of altered ETA metabolism, higher ETASO levels in wildtype mice and *FMO* epression changes with long–term ETA treatments, additional studies are warranted to understand better the effects of elevated levels of ETASO on lung toxicty via glutathione depletion in wild type mice with active Fmo2. It would also be interesting to see if the pharmcokinetics of ETA changes with *M. tuberculosis* infection in wild type and knockout mice. This would provide evidence that *Fmo 1, Fmo2* and *Fmo4* expression is likely altered in mouse (and perhaps human) models of chronic infection and inflammation. Ultimately, these data argue for individuals expressing active FMO2.1 (from at least one *FMO2*1* allele), a genotype present at high incidence in regions of Africa. (Phillips and Shephard 2008) which also

coincidentally have highest number of TB reported in lung, with altered ETA metabolism leading to higher production of ETASO, a sulfenic acid, compared to individuals of the *FMO2*2* genotype.

.

Chapter 3 The Anti-Tuberculosis Drug Ethionamide Altered Oxidative Stress Gene Expression in Lung Tissue of Flavin-Containing Monooxygenase 1, 2 and 4 Null Mice

Priti B. Singh[1, 2], Sharon K. Krueger[2], Amy L. Palmer[3], Ian R. Phillips[4], Elizabeth A. Shephard[5], and David E. Williams[1, 2]

[1]Department of Molecular and Environmental Toxicology, Oregon State University, Corvallis OR, USA, [2]The Linus Pauling Institute, Oregon State University, Corvallis, OR, USA , [3]Department of Biomedical Sciences, Oregon State University, Corvallis, OR, USA, [4]School of Biological and Chemical Sciences, Queen Mary, University of London, London, United Kingdom, [5] Departments of Structural and Molecular Biology, University College London, London, United Kingdom

3.1 Abstract

The prodrug ethionamide (ETA), widely used as second-line anti-tuberculosis therapy is activated to ethionamide S-oxide (ETASO) by mycobacterial flavin-containing monooxygenase, EtaA, as well as human enzyme flavin-containing monooxygenase 2.1 (FMO2.1). FMO2.1 is highly expressed in lung tissue and S-oxygenates ETA to ETASO more efficiently than mycobacterial enzyme EtaA *in vitro.* However, most humans do not express active FMO2.1 in lung; rather, they produce only inactive FMO2.2 due to a common polymorphism. ETASO is a sulfenic acid capable of redox-cycling with glutathione producing oxidative stress and toxicity. By utilizing an *Fmo1/2/4* knockout mouse model, we measured higher levels of ETASO in plasma and epithelial lining fluid (ELF) of wild type mice than in knockout mice. We hypothesized that production of higher ETASO may result in glutathione (GSH) depletion causing oxidative stress. ETA dose of 125 mg/kg was given to both wild type and knockout male and female mice orally by gavage for 4-weeks, whereas vet-syrup was given to control mice. This study evaluated the effect of long-term ETA dosing in the presence and absence of FMO 1, 2 and 4 on oxidative stress gene expression profiles in mouse lung. Total RNA was isolated from lung tissue of both wild type and knockout male and female mice and real-time RT-PCR analysis was performed using a commercially available oxidative stress gene array. Array data revealed altered expression of genes in both strains of mice due to ETA treatment, though the number of altered genes was higher in wild type mice, suggesting oxidative stress was higher among ETA-treated wild type mice. Elevated plasma malondialdehyde levels were also observed in both male and female wild type mice, an indication of oxidative damage to membrane lipids. This study suggests that humans undergoing long-term ETA treatment for MDR-TB expressing active FMO2.1 may be at higher risk of ETA toxicity than individuals with inactive FMO2.2.

Key words: Ethionamide, Oxidative stress, Real-time PCR, Flavin-containing monooxygenase

3.2 Introduction

Tuberculosis is an infectious disease caused by the bacillus *Mycobacterium tuberculosis* and approximately one-third of the world's population is infected without exhibiting symptoms of the disease. With increasing emergence of multidrug-resistant (MDR) strains of *M. tuberculosis*, second-line drugs such as ethionamide (ETA) have become increasingly important as replacement for first-line drugs isoniazid (INH) and rifampicin. ETA, can exhibit adverse drug reactions including nausea, vomiting, gastrointestinal distress, and hepatotoxicity (Bastian and Colebunders 1999; Thee et al. 2011).

ETA is a thioamide prodrug that must undergo metabolic activation to exert its cytotoxic effects. The S-oxygenation of the thiourea moiety determines the therapeutic efficacy of ETA. Both mycobacterial flavin-containing monooxygenase, EtaA, and mammalian flavin containing monooxygenase (FMO) metabolize ETA (Baulard et al. 2000; DeBarber et al. 2000). Mammalian and mycobacterial FMOs catalyze thioamide oxygenation in two steps, first to the sulfenic acid and second to the sulfinic acid. The sulfenic acid can react with and deplete nearby nucleophiles, the most likely being glutathione (GSH), or in the case of EtaA, mycothiol (Henderson et al. 2008; Qian and Ortiz de Montellano 2006; Vilcheze et al. 2008). In mammalian tissue, FMO-dependent S-oxygenation of thiocarbamides leads to a futile cycle producing GSH and NADPH depletion, oxidative stress and cell death. FMOs have been demonstrated to produce thiocarbamide-dependent liver toxicity exactly in this fashion (Krieter et al. 1984; Neal and Halpert 1982). It

was also recognized that S-oxygenation of the thiourea moiety of ETA was involved in the bioactivation to a hepatotoxic metabolite (Ruse and Waring 1991). Expression of human FMO3 (but not FMO1) was toxic to mouse C3H/10T1/2 cells upon exposure to some thiocarbamides and GSH appeared to protect the cells from this toxicity (Smith and Crespi 2002). Methamizole, used to treat hyperthyrodism, showed dose-dependent olfactory toxicity via FMO transformed methamizole S-oxide (Genter et al. 1995).

FMO2, the major isoform in lung tissue, exhibits a genetic polymorphism in humans. *FMO2*2* codes for a truncated and nonfunctional FMO2.2 protein present in all Caucasians and Asians genotyped, whereas *FMO2*1* codes for full-length functional FMO2.1, is present in African-American (26%) and Hispanic-American (5%) populations, and up to 50% of Sub-Saharan African populations (Dolphin et al. 1998; Krueger et al. 2002a; Krueger et al. 2002b; Veeramah et al. 2008; Whetstine et al. 2000). We utilized the *Fmo1/2/4* null mouse model developed by Hernandez et al., (2006), and demonstrated significant alterations in ETA metabolism in the presence and absence of Fmo1, 2 and 4. Sulfenic acid, ETASO, was significantly higher in wild type mice than in knockout mice in both plasma and ELF samples (chapter 2). We hypothesized that individuals expressing functional FMO2.1 protein in the lung may be at enhanced risk from ETA-metabolism dependent toxicity. C57BL/6J wild type and *Fmo1/2/4* knockout mice were treated with ETA over a 4-wk dosing interval, commonly used for assessment of long-term drug intervention in *M. tuberculosis*-infected mice, and analyzed indicators of oxidative stress and toxicity. The outcome of this study may provide guidance for physicians seeking to identify and administer the drug most likely to maximize individual drug response and minimize TB drug toxicity.

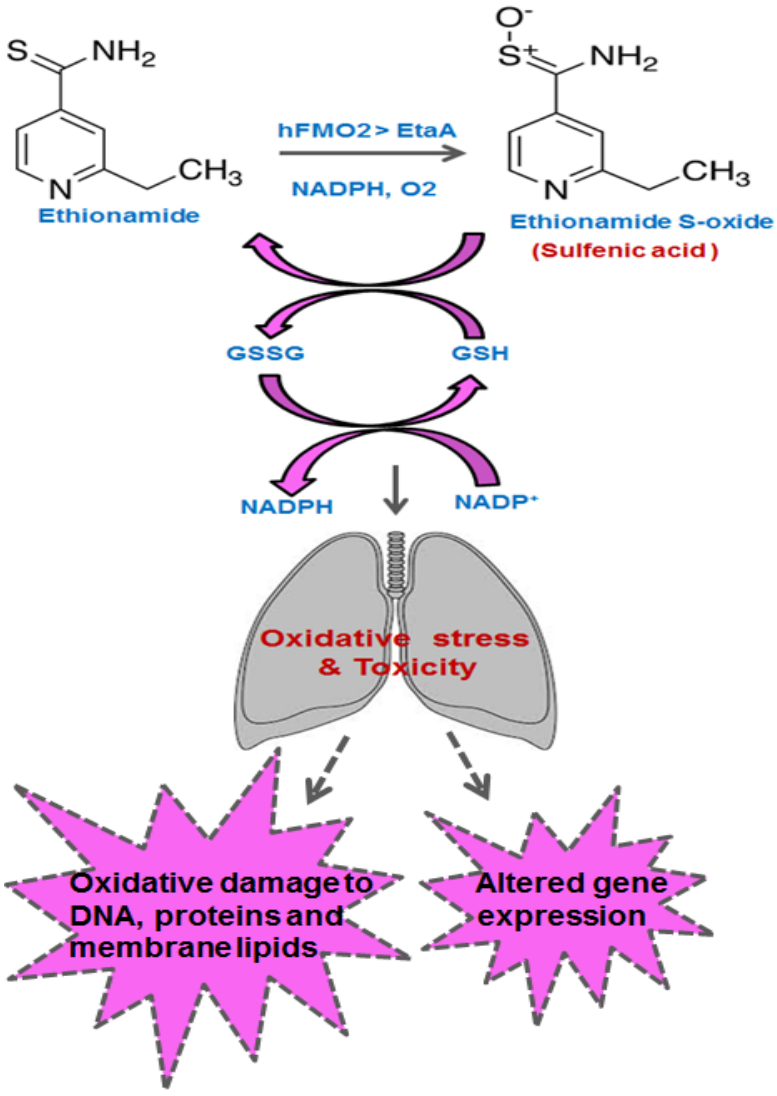

Figure 3.1 Cartoon depicting proposed scheme of ETA S-oxygenation by active FMO2.1 in lung of TB patients

3.3 Materials and methods

Chemicals

High performance liquid chromatography (HPLC) grade ETA was purchased from Sigma-Aldrich (St. Louis, MO). The vehicle for gavage suspension (Vet syrup®) was from FlavoRx (Washington, D.C.)

Animals and Experimental design

All protocols for the handling and treatment of mice were approved by the Oregon State University Institutional Animal Care and Use Committee. Ten to eleven week old male and female C57BL/6J wild type mice were obtained from Jackson Laboratory (Sacramento, CA) and provided one week acclimation before study initiation. *Fmo* $1^{-/-}$, *Fmo2*$^{-/-}$, *Fmo4*$^{-/-}$ eight generation back-crossed knockout mice, on a C57BL/6J background, originated from Elizabeth Shephard and Ian Phillips (University College, London, UK) (Hernandez et al. 2006) and were rederived by Harlan Laboratories (Hillcrest, UK) prior to shipment to Oregon State University (OSU). A breeding colony was established and maintained at OSU. Mice were provided pellet diet (Purina 5053) and water *ad libitum*. Mice were kept on a 12 hour light cycle under a controlled temperature between 22-23^{0}C. Both sexes were included in the study. Four same-sex mice were housed per cage. To eliminate litter effects out of the four mice in the cage, two mice were orally gavaged with ETA (125 mg ETA/ kg body weight) for 4-wks while the remaining two mice were gavaged with vehicle. Vehicle- and ETA-treated mice were distinguished by ear tag color. The gavage volume was 10 µl/g body weights. ETA was ground into fine powder and suspended in Vet syrup® (12.5 µg /µl) with 10 min of sonication and 30 s of vortexing. The drug suspension was vortexed

before each gavage to ensure consistent distribution of the ETA. ETA dosing was done in the late afternoon. Mice were given a one day break from antibiotic dosing after six days of continuous dosing. Body weights of mice were measured every day and mice were dosed accordingly. Animals were monitored twice daily for signs of morbidity, pain or distress.

Sample collection

Isoflurane (3-5%) was used to anesthetize the mice. Mice were *ip* injected with 50 µl of heparin (1000 U/ml) to anti-coagulate for 5 min before isoflurane administration. Once mice were deeply anesthetized and were insensate blood was collected from the posterior vena cava, and mixed with 33 IU of sodium heparin to prevent clotting and stored at room temperature until all samples were collected for the day. Plasma was prepared by centrifugation of whole blood at 2,000 *x g* for 10 min and stored at -80°C. A small amount of plasma aliquot was frozen separately for the urea assay.

Bronchoalveolar lavage fluid collection

After blood collection, the trachea was visualized and a catheter (Terumo, Somerset, NJ) was inserted to a depth of 1 cm after removal of the needle. The chest cavity was quickly opened exposing the heart and providing room for lung expansion. Three 1 ml successive puffs of air were provided by syringe to inflate the lungs. Whole body blood perfusion was performed using cold phosphate buffered saline 1X (PBS) containing 5 U/ml heparin. Perfusion was continued until organs became blanched and fluid exiting the heart was free of color. Lungs were again inflated with three puffs of air and then a 3 ml syringe was used to introduce 1.5 ml of PBS via catheter. After pausing for 10 s, gentle suction was applied to the syringe to recover the BALF. The first

wash was immediately spun for 2 min at 5000 *X g* and supernatant was transferred to a fresh tube. BALF aliquots were dispensed into cryo tubes and were snap frozen. For the glutathione assay, 250 µl of BALF was mixed with 250 µl of 10% perchloric acid (PCA) containing a 10 mM metal chelator diethylenetriamine pentaaceticacid (DTPA), stop solution. Lavage was repeated 4 more times with 1 ml of PBS each time and in the end washes 2-5 were collected in one tube and spun for 2 min at 5000 *X g*. BALF supernatant was aliquoted into cryovials for various assays and snap frozen before storing at -80°C. After lavage, lung and liver tissue were collected and snap frozen and stored at -80°C. Eight to 9 mice per group were used in the BALF collection.

Tissue harvest, RNA extraction and Oxidative Stress RT^2 Profiler PCR Array

Forty mice (5 reps /group) were used for RNA analysis. After blood was collected as described earlier, whole body blood perfusion was performed. A piece of the right liver lobe and the left lung lobe were collected into RNAlater (Quiagen, Valencia, CA), while the rest of the liver and inflation-filled lung lobes were fixed in 10% formalin. Total cellular RNA was extracted from RNAlater-preserved tissue using an RNeasy Mini Kit (Qiagen, Valencia CA) according to manufacturer's protocol. RNA was quantified with a NanoDrop ND 1000 UV-vis spectrophotometer (Wilmington, DE). The relative expression of 84 oxidative stress defense-related genes was evaluated using the mouse oxidative stress and antioxidant defense signaling pathway RT^2 Profiler PCR Array system (catlog number. PAMM-065ZA-12, SABiosciences, Valencia, CA) according to the manufacturer's instructions. DNase-treated total RNA pools of 1 µg from males and 0.7 µg from female, were taken to make cDNAs using the RT^2 First Strand kit (Quiagen, Valencia, CA) and then combined with the RT^2 qPCR Master Mix (Quiagen, Valencia, CA) and added to lyophilized

primer pairs in the 96-well arrays. Thermal cycling was performed on an iQ5 Multicolor Real Time PCR Detection System (Bio-Rad, Hercules, CA). Relative gene expression levels were calculated using the $\Delta\Delta C_T$ method with normalization to glyceraldehyde-3-phosphate dehydrogenase (GAPDH). The quantitative PCR reactions were run at 95°C for 10 min, followed by 40 cycles of 95°C for 15 s and 60°C for 1 min followed with melting curve analysis, according to manufacturer's recommendation. To analyze the PCR-array data, an MS-Excel sheet with macros was downloaded from the manufacturer's website (http://www.sabiosciences.com/pcrarraydataanalysis.php).

Relative gene expression analysis by real time RT-PCR

Total RNA (500 ng) was used for cDNA synthesis using Superscript III First Strand Synthesis kit (Invitrogen, Grand Island, NY). Gene specific primers were designed using Sci Tools provided by Integrated DNA Technology (http://www.idtdna.com/primerquest/Home/Index). Preliminary experiments were done with each primer pair to determine annealing temperature that yielded the greatest amount of specific product with melting temperature (T_m) separable from primer-dimer T_m. PCR products were also run on 2% agarose gels visualized by GelRed (Biotium, Hayward, CA) to confirm a single band with appropriate size. The experimentally determined annealing temperature and primer's concentration for all genes tested are given in Table 3.1. Gene expression was evaluated by iQ5 Multicolor Real Time PCR Detection System (Bio-Rad, Hercules, CA) in duplicate with the RT2 SYBR Green Fluor PCR Master mix (Qiagen, Valencia, CA). Quantitative PCR was performed by above described protocol. A negative control without cDNA template was run with every assay to assess the overall specificity. The oxidative stress PCR array has five housekeeping genes on the plate for expression normalization. Based on that, *Gapdh*, beta-actin (*Actb*) and beta-2-

Table 3.1 Primer sequences and conditions for expression analysis by RT-PCR

Gene name	Forward primer (5'-3')	Reverse primer (5'-3')	Annealing Temperature	Product length	PCR efficiency (%)	Reference
Alb	GCAGACTTGCTGCGATAA	ACACTTCCTGGTCCTCAA	58	122	95	IDT
Actb	ATTGCTGACAGGATGCAGAA	CAGGAGGAGCAATGATCTTGA	60	76	108.2	Xu & Miller 2004
Gapdh	TCTCCCTCACAATTTCCATCCCAG	GGGTGCAGCGAACTTTATTGATGG	64	100	100	Xu & Miller 2004
Gpx3	AAACAGGAGCCAGGCGAGAACT	CCCGTTCACATCTCCTTTCTCAAA	62	111	96.5	Waters et al., 2002
Hspa1a	CATCGAGGAGGTGGATTAGA	GCAGGACAAACTAAGGAGTG	60	121	101	IDT
B2m	TTCTGGTGCTTGTCTCACTGA	CAGTATGTTCGGCTTCCCATTC	60	104	104.4	IDT
Mb	AGTCCTCATCGGTCTGTTTA	TCCTCTGAGCCCTTCATATC	64	98	99	IDT
Nf-kb	TAACTGG AGTTTGACGGTC	ACACACATAGCGGAATCGAA	58	216	90.6	IDT
P53	CTCTCCCCCGCAAAAGAAAA	CTCCTCTGTAGCATGGGCATC	62	133	102	Bitton-worms et al., 2010

IDT- http://www.idtdna.com/primerquest/Home/Index

microglobulin (*B2m*) genes were quantitatively analyzed to find the best housekeeping gene for normalization. Expression levels were determined for all forty mouse samples. PCR reaction efficiencies were also checked for each primer by using cDNA dilution series. Primers with 90 to 110% efficiency were included for further analysis (Table 3.1).

Urea assay

The amount of ELF recovered was calculated by the urea dilution method (Rennard et al. 1986). Urea nitrogen was measured in plasma and BAL supernatant by using a quantitative colorimetric assay (Pointe Scientific, Canton, Mich.) with sensitivity of 0.05 to 150 mg/dL. The dilution of the BAL was calculated from $urea_{plasma}/urea_{BAL}$ (Rennard et al. 1986).

Bradford assay for protein estimation

The protein content of the BAL supernatant was assessed using a Coomassie (Bradford) protein assay (Pierce Biotechnology, Rockford, IL) with a detection limit of 1 µg/mL at an absorbance of 595 nm.

Hydrogen Peroxide (H_2O_2) generation assay

H_2O_2 concentrations were determined spectrophotometrically using a microplate assay kit (Amplex Red; Molecular Probes, Eugene, OR) with an excitation of 560 nm, fluorescence emission detection at 590 nm, and sensitivity of 50 nmol /L.

Malondialdehyde (MDA) estimation

Malondialdehyde (MDA) concentrations were determined in the plasma and BAL supernatant with a spectrophotometric assay (Bioxytech MDA-586; Oxis International, Foster City, CA). This assay is based on the reaction of N-methyl-2-phenylindole with MDA at 25°C. Spectra were recorded from 400-700 nm promptly in 1 nm intervals and 3rd derivatives were calculated using the Northwest Life Science Specialties, LLC derivative application on setting the filter = 29, derivative = 3, polynomial = 3 and scale = 10,00,000. (http://www.nwlifescience.com/sg/worksheet.php). Further calculation was done according to manufacturer's protocol.

Statistical analysis

ETA treated mouse groups (wildtype and knockout) were compared with their corresponding control group via a Student's t-test assuming equal variances. If the overall test differences were below $p \leq 0.05$ then they were considered significant. Protein, MDA, and H_2O_2 concentrations were expressed per liter ELF according to the urea dilution (Rennard et al. 1986).

3.4 Results

In total 108 mice were included for this study. Neither strain of mice showed any adverse effect or behavioral changes during the study course and mice looked healthy. There was no change in body weight due to 4-weeks of vet syrup dosing with or without ETA (Sup. Fig A3.6). ELF protein levels were significantly higher ($p = 0.004$) in knockout male mice than in wild type males regardless of ETA treatment (Fig.3.2). Plasma urea levels of wild type female mice were significantly higher than knockout female mice ($p = 0.017$) (Table 3.2) (Fig. 3.3). The fold dilution of $urea_{1st\ wash}$ ranged from 54 to 171, and the

$urea_{wash\ 2\text{-}5}$ was 114 to 173-fold diluted compared to plasma levels (Table 3.2). Percent ELF recovery from $BAL_{1st\ wash}$ was 1.5± 0.8, whereas from $BAL_{wash\ 2\text{-}5}$, it was 0.9 ± 0.5 which is similar to the 1.0 ± 0.1 ml/100ml (1%) ELF volume recovered from normal human by standard lavage procedure reported in Rennard et al., 1986.

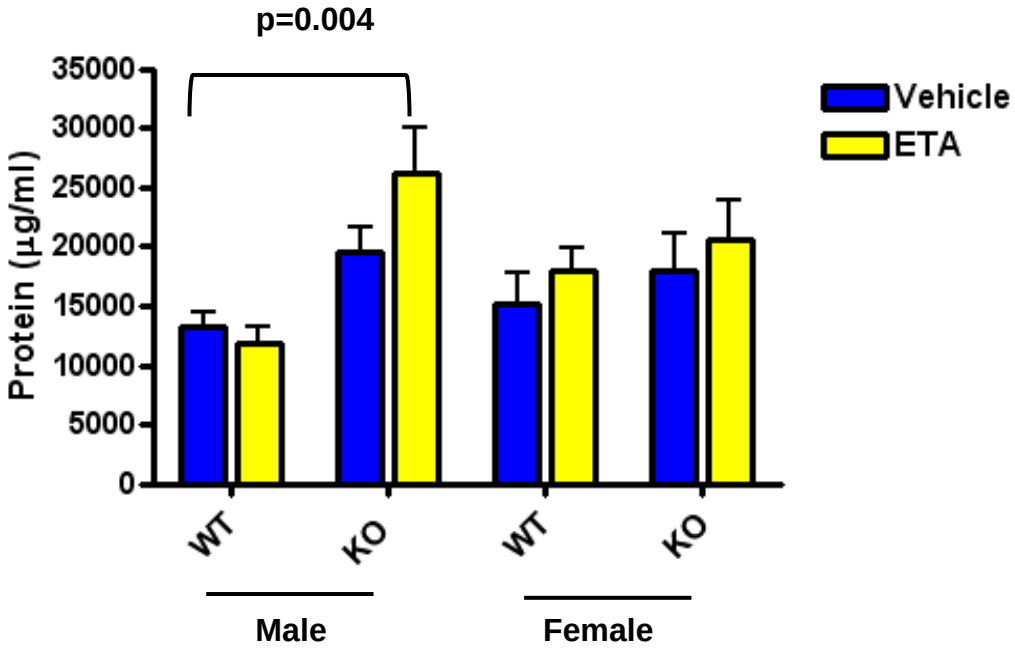

Figure 3.2 ELF protein levels of wild type and knockout mice.
Both male and female mice were treated with 28-days of ETA or vehicle. Graph shows mean± SEM (n= 8-9) per ml of ELF. Knockout male mice ELF protein levels were significantly higher (p=0.004) than wild type male ELF protein levels. Abbreviation WT-wild type; KO-knockout.

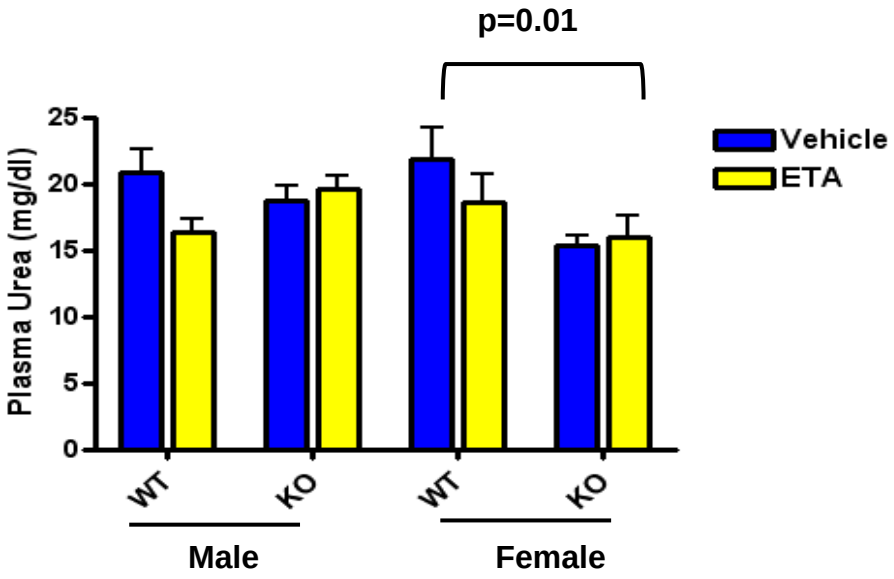

Figure 3.3 Plasma urea concentrations of wild type and knockout mice. Both male and female mice were treated with 28-days of ETA or vehicle. Graph shows mean± SEM (n= 8-9).Wildtype female plasma urea levels were significantly higher (p=0.01) than those of knockout females. Abbreviation WT-wild type; KO-knockout.

Table 3.2. Composition of the BAL in wild type and knockout mice with and without ETA treatment.

	WT (M)		KO (M)		WT (F)		KO (F)	
	Vehicle	ETA	Vehicle	ETA	Vehicle	ETA	Vehicle	ETA
Protein (µg/ml)	161.8±94.8	276.4± 206.1	237.3±74.7	165.3±59.2	156.9±50.2	209.1±95.1	235.3±87.5	308.3±73.7
Plasma urea (mg/dL)	20.8±4.7	16.7±2.5	18.7±3.	19.6±2.7	21.8±6.7	18.5±5.6	15.3±2.2	16±4.5
Urea (mg/dL)- BAL 1st wash	0.37±0.10	0.36±0.16	0.25±0.09	0.17±0.13	0.26±0.07	0.20±0.06	0.22±0.10	0.28±0.14
Urea dilution factor- BAL 1st wash	60±18	54±20	86±29	171±100	89±29	96±37	82±34	65±22
ELF volume recovered (µl)- BAL 1st wash	12±3	12±3	7±2	6±4	7±2	6±2	9±5	10±5
Urea (mg/dL)- BAL 2-5 wash	0.21±0.14	0.18±0.08	0.14±0.08	0.15±0.08	0.19±0.06	0.13±0.04	0.11±0.05	0.16±0.05
Urea dilution factor- BAL 2-5 wash	128±57	119±70	164±63	167±80	144±95	155±62	173±83	114±36
ELF volume recovered (µl)- BAL2-5 wash	21±18	19±10	11±5	13±6	16±11	14±7	9±5	15±5

Data represents the mean ±SEM

Oxidative stress array data

As a discovery tool, we used SuperArray mouse oxidative stress and antioxidant defense pathway arrays, to analyze expression of 84 genes with real-time PCR using total RNA pools from lung of wild type and *Fmo1/2/4* knockout mice with and without 28-days of ETA treatment. Each array has five housekeeping genes, *Actb*, *B2m*, *Gapdh*, β glucoronidase (*Gusb*) and heat shock protein 90 alpha (*Hsp90ab1*). *Gapdh* was choosen for normalization due to most consistent expression among all the samples. An area-proportional Venn diagram made with "BioVenn" a diagram tool for bioinformatics (http://www.cmbi.ru.nl/cdd/biovenn/index.php) illustrates 20 genes that were differentially expressed in ETA treated mice in compared to respective controls (Fig 3.4). The diagram also indicates the number of differentially expressed genes that were common between wild type and knockout male and female mice, such as, *Alb*, *Mb* and *Mpo*. Table 3.3 shows the differentially expressed genes with number of fold-up and -down regulation values. Analysis of the differential expression data takes into account threshold cycle when categorizing data reliability (see Table 3.3 footnotes). Cut-off taken for the fold-up and -down regulation is 1.9 for the genes which have threshold cycle less than 30 in both ETA treated and vehicle treated samples, whereas for other genes expression in which either ETA or vehicle treated sample threshold cycle is more than 30, cut off taken for fold change was more than 2. The threshold cycle cut-off choosen was 35 in both ETA and vehicle treated samples. Differentially expressed genes for which either ETA or vehicle treated samples threshold cycle were 35 or above were not considered.

Long–term ETA treatment altered 12 genes compared to the controls in wildtype male mice. Among these 12 genes, six were up-regulated while 6

Table 3.3 Oxidative stress and antioxidant pathways related genes expression changes in lung of wildtype and knockout mice.

Gene description	Symbol	WT	KO	WT	KO
		M	M	F	F
Albumin	Alb	-3.3[1]	**-25.8**[1]	**158.9**[2]	-1.9[1]
Catalase	Cat			2	
Dual oxidase 1	Duox1	**-9.3**[3]			
Eosinophil peroxidase	Epx	**18.5**[3]		2.4[3]	
Glutathione peroxidase 1	Gpx1	1.9[1]			
Glutathione peroxidase 5	Gpx5			2.3[3]	
Glutathione peroxidase 6	Gpx6	3.8[3]		2.1[3]	
Heat shock protein 1A	Hspa1a			**4.4**[1]	
Keratin 1	Krt1	**-4.9**[3]	-2.3[3]		
Myoglobin	Mb	-3.2[1]	2.8[1]	7[1]	2.2[1]
Myeloperoxidase	Mpo	3.7[3]	-2.2[3]	4.5[3]	3.3[3]
NADPH oxidase activator 1	Noxa1	2[1]			
NADPH oxidase 1	Nox1			2.7[2]	
Peroxiredoxin 4	Prdx4	2.3[1]			
Prostaglandin-endoperoxide synthase 2	Ptgs2			1.9[1]	
Recombination activating gene 2	Rag2		3.7[3]	-3.5[3]	
RecQ protein-like 4	Recql4	-2.3[2]			2[3]
Thyroid peroxidase	Tpo	**-5**[3]	-2.4[3]	2.6[3]	

Thioredoxin interacting protein	Txnip	-2[1]	
Thioredoxin 1	Txn1		2.7[3]

Data presents fold- up and down- regulation of genes related to oxidative stress and anti-oxidant pathways in wildtype and knockout mice lung tissue after 28-days of ETA administration in compare to respective controls.
[1] Genes with a threshold cycle more than 30 in both the ETA treated and control samples, [2]Genes with threshold cycle relatively high (>30) in either the control or the ETA treated sample, and reasonable low in the other sample (<30) [3] Genes threshold cycle relatively low, in both control and test samples (>30). Fold changes higher than 4 are highlighted in bold.
Abbreviation: WT-wild type, KO- knockout, M- male and F-female

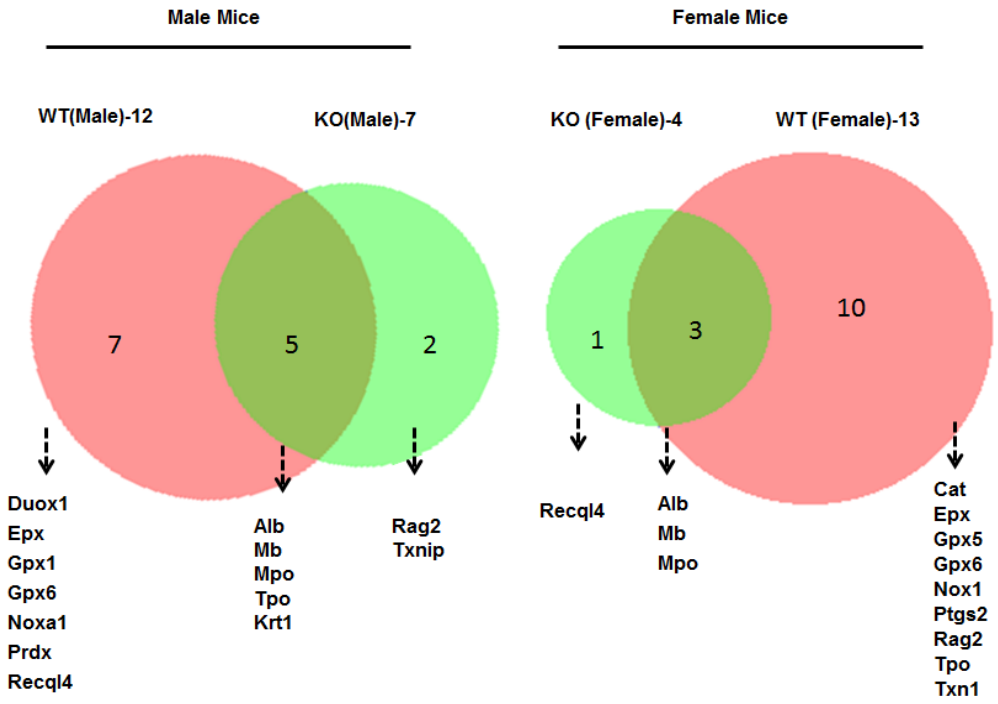

Figure 3.4 Comparative Venn diagram displays the number of differentially expressed genes from the lung tissue.
Differential expressions of genes are shown in the lung of wildtype and knockout mice after 28- days of ETA treatment in comparison with the corresponding control mice groups. Differentially expressed gene IDs are also shown.
Abbreviation: WT-wild type, KO- knockout

other were down regulated. *Epx*, *Duox1*, *Krt1*, *Tpo* were highly affected gene with fold changes of 4 to 18 in comparison to vehicle treated (Table 3.3). Long-term ETA treatment altered fewer genes (7) in knockout male mice in comparison to wild type male mice (12). Five genes with altered expression were common between wild type and knockout mice (Fig.3.4). Long-term ETA treatment in wild type female mice altered 13 genes in compared to controls. Among 13 genes, 11 genes were up-regulated and 2 were down- regulated. *Alb*, *Hspa1a*, *Mb*, and *Mpo* were highly affected genes with fold changes of 4 to 159, in comparison to vehicle treated mice (Table 3.3). In contrast to wild type female mice, fewer genes were altered in knockout mice. Three genes with altered expression were common between wild type and knockout female mice (Fig.3.4). Between both male and female wild type mice, 6 genes were common, while 3 genes were common between male and female knockout mice (Fig. 3.4). In general fold-changes of differentially expressed genes in knockout mice were lower compared to wild type mice (Table 3.3).

Subsets of differentially regulated genes were selected for follow-up validation using cDNA from individual mice. *Alb*, *Mb*, *Mpo* were choosen for further validation in individual samples since they were altered in all the four mice groups wildtype and knockout male and female. *Hsp1a1* was also choosen based on the array data since it is one of the important stress affected genes reported in the literatures. Among all the three housekeeping gene *G*apdh *Actb*, and *B2m* tasted, *Gapdh* was choosen for expression normalization. *GAPDH* expression showed less variability among samples than did *Actb* and *B2m* (Fig 3.5). None to the house keeping genes showed any significant difference between wildtype and knockouts. ETA treatment also did not significantly alter housekeeping gene expression. Assessment of *Alb* expression in individual samples followed the same pattern as shown in PCR array data (Table 3.3, Fig 3.6). It was down-regulated in all the four mice groups, but not significant (Fig 3.6). *Mb* expression was down regulated in

wildtype male, while up-regulated in knockout male in both PCR array as well as in further expression validation (Table 3.3, Fig 3.7). Wildtype female mice also showed *Mb* up-regulation in ETA treatment in comparison to vehicle validating the PCR array, but knockout female mice did not show any expression difference failing to validate PCR array data, though these changes were not significant. (Table 3.3, Fig 3.7). *Hsp1a1* was up-regulated in wild type females also following the trend with PCR array (Table 3.3, Fig 3.8). *Hspa1a* expression with ETA treatment was significantly up-regulated in wildtype female mice (p=0.03) in comparison to vehicle treated mice. *Mpo* expression did not validate PCR array results (data not shown).

P53, *NF-κB*, and *GPx3* were also selected for expression analysis based on a literature search for genes involved in oxidative stress. *P53* was up-regulated in both wild type male and female mice by ETA treatment, whereas it was down- regulated in knockout mice (Fig.3.9). *P53* levels in ETA treated wildtype male and female mice were significantly different than control mice ($p = 0.02$ and $p = 0.03$, respectively). Knockout male mice also had significantly reduced ($p = 0.04$) *p53* expression as a result of ETA treatment. *NF-κB* expression (Fig. 3.10) was similar to that of *p53*; it was up regulated by ETA in wildtype mice, while it was down regulated in knockout mice. *NF-κB* expression was significantly altered ($p = 0.03$) by ETA in female knockout mice. *Gpx3* was also up-regulated in by ETA in wildtype male and female while it was down regulated in knockout male and female mice, (Fig. 3.11). Knockout female mice *Gpx3* expression with ETA treatment was significantly down-regulated ($p = 0.009$) in comparison to control. *GPx3* results from individuals are in contrast with PCR array that did not find expression differences more than 2-fold.

.

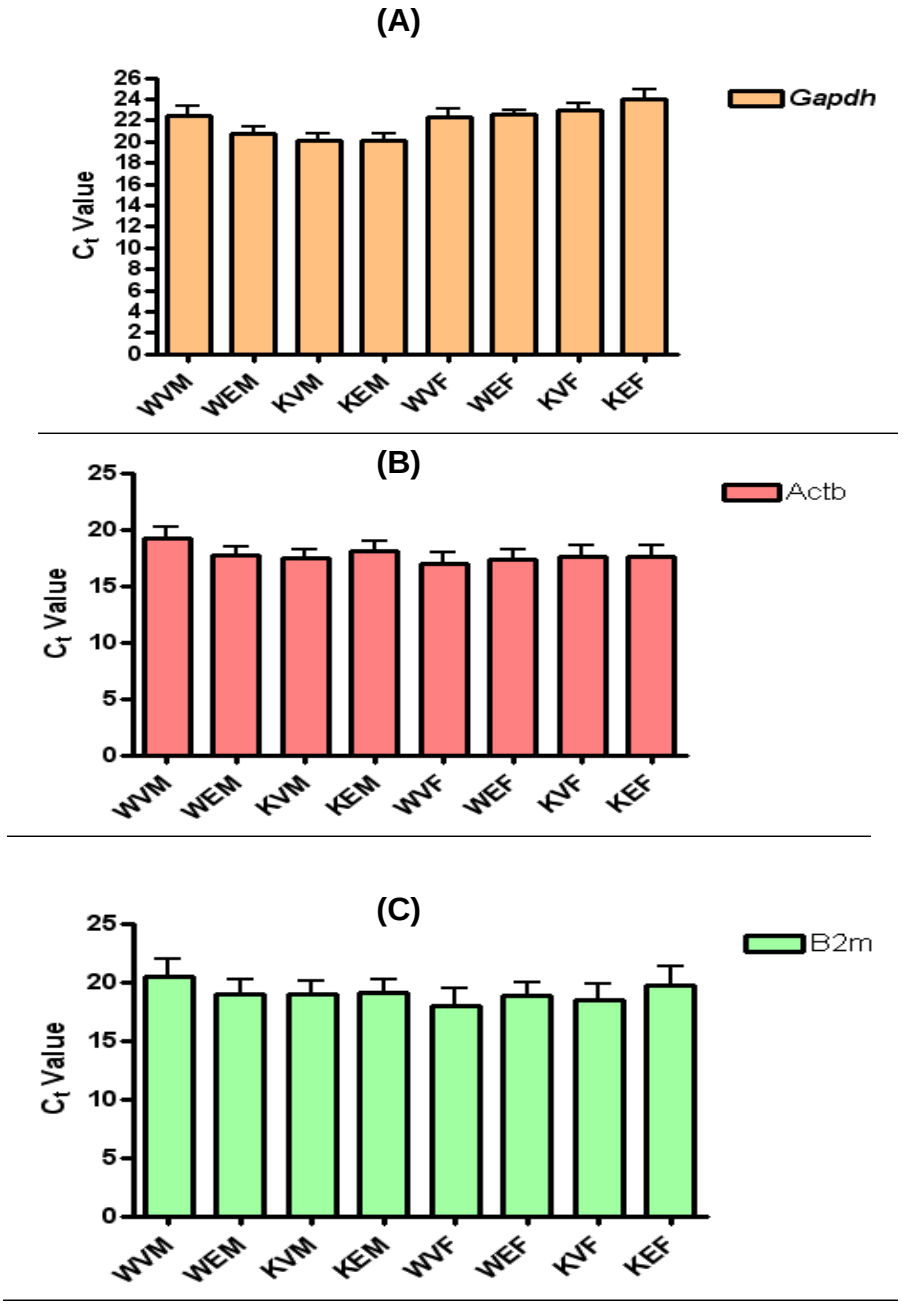

Figure 3.5 Housekeeping gene expression in wildtype and knockout mice.

(A) *Gapdh*, (B) *Actb* and (c) *B2m*. W, K, M, F, E and V represents wild type,knockout, male, female, ethionamide and vehicle , respectively. Graphs shows mean± SEM (n= 4-5).

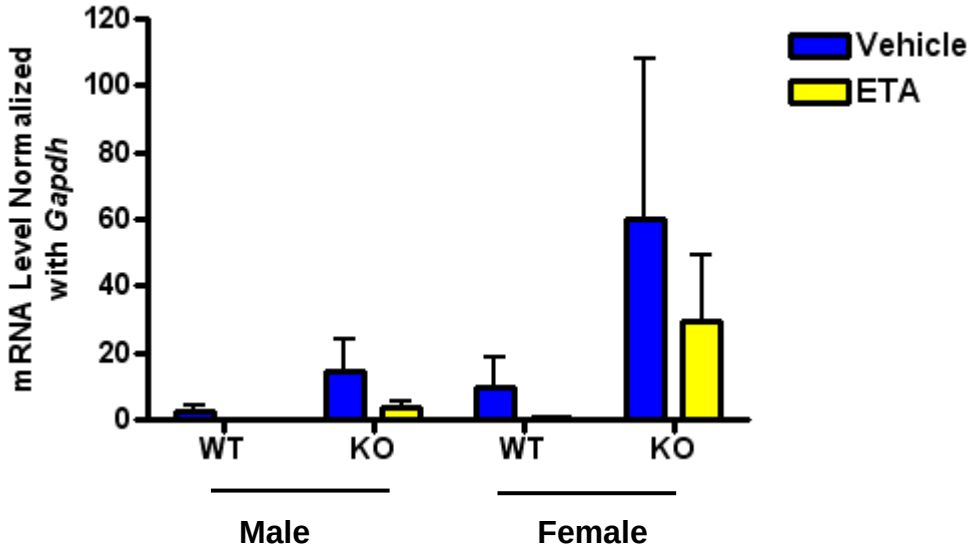

Figure 3.6 *Alb* gene epression in lung of wildtype and knockout mice .
Mice were treated with 28-days of ETA or vehicle. Graph shows mean ± SEM (n= 4 to 5).

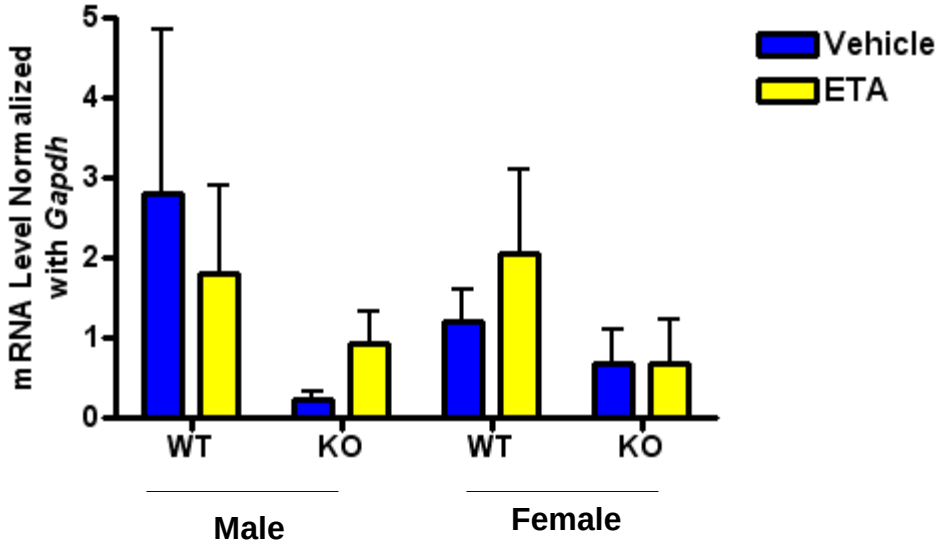

Figure 3.7 *Mb* gene epression in lung of wildtype and knockout mice.
Mice were treated with 28-days of ETA or vehicle. Graphs shows mean± SEM (n= 4 to 5).

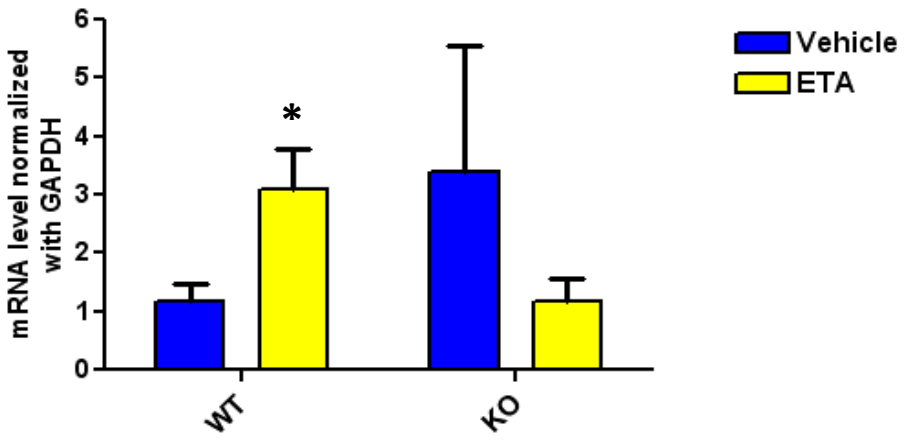

Figure 3.8 *Hspa1a* gene expressions in wildtype and Knockout females.
Mice were treated with 28-days of ETA or vehicle. Graphs shows mean ± SEM (n= 4 to 5). Statistically significant defferences between the ETA treated and corresponding control mice are identified by * p<0.05 .

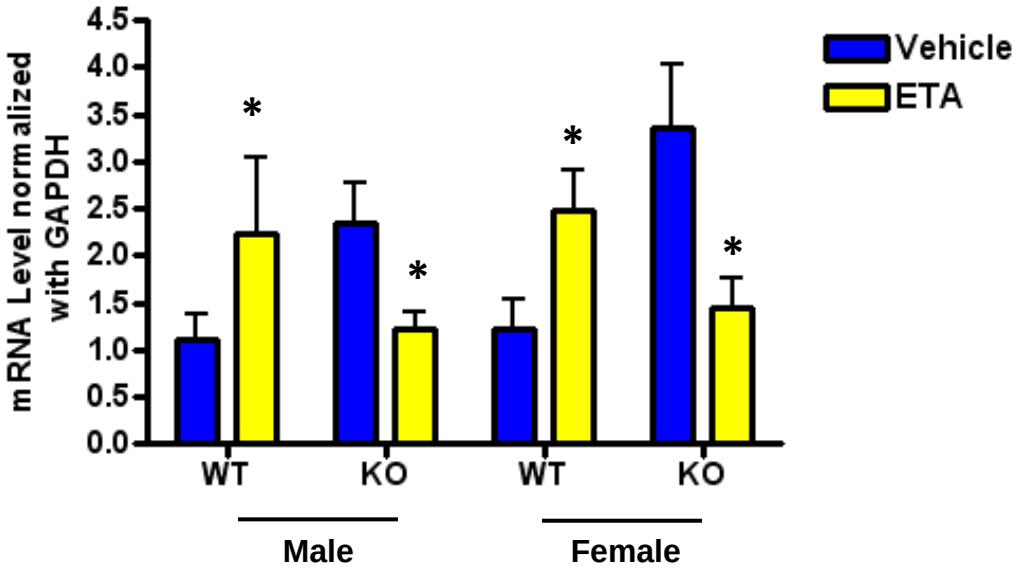

Figure 3.9 *p53* gene expression in wildtype and knockout mice.
Mice were treated with 28-days of ETA or vehicle. Graphs shows mean± SEM (n= 4 to 5). Statistically significant differences between the ETA treated and corresponding control mice are identified by * p<0.05.

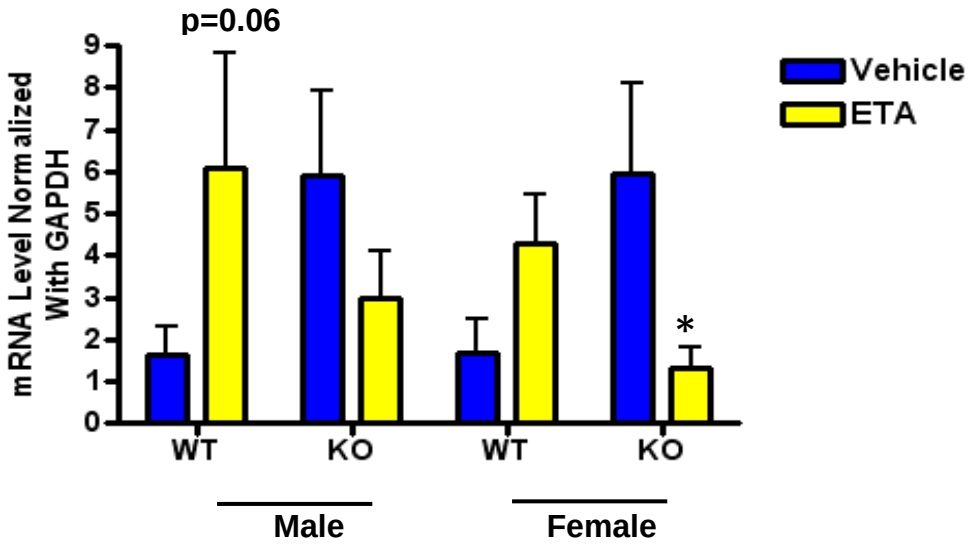

Figure 3.10 *NF-κB* gene expression in wildtype and knockout.
Mice were treated with 28-days of ETA or vehicle .Graphs shows mean± SEM (n= 4 to 5). Statistically significant differences between the ETA treated and corresponding control mice are identified by * p<0.05.

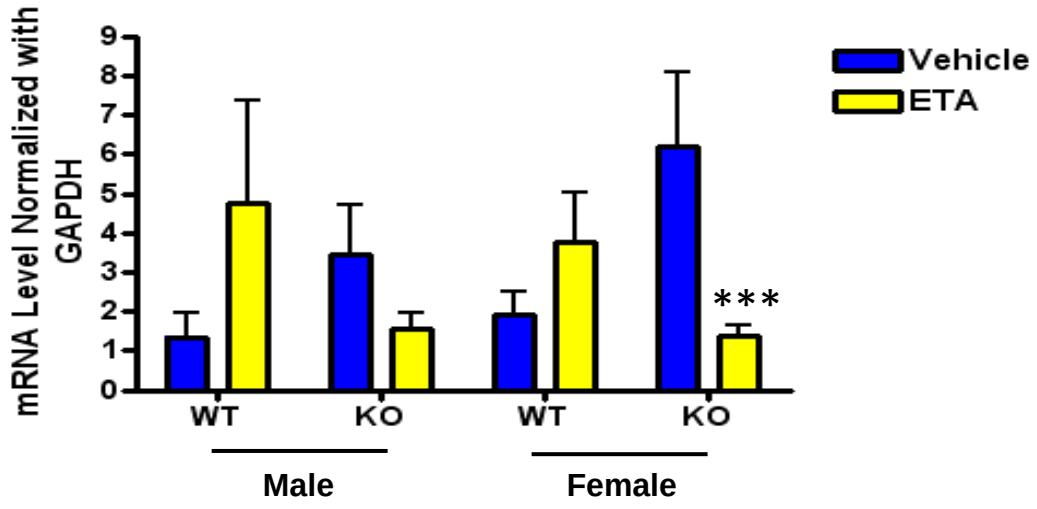

Figure 3.11 *Gpx3* gene expression in wildtype and knockout mice.
Mice were treated with 28-days of ETA or vehicle. Graphs shows mean± SEM (n= 4 to 5). Statistically significant differences between the ETA treated and corresponding control mice are identified by *** p<0.001.

Plasma malondialdehyde (MDA) level

Elevated MDA levels were observed in plasma from wild type male and female mice receiving 28-days of ETA treatment, compared to vehicle treated mice (Fig 3.12). MDA levels in wildtype male mice were significantly elevated ($p = 0.01$) by ETA treatment. There was not much difference noticed in knockout male and female mice with ETA treatment. (Fig 3.12). No significant difference was observed in ELF MDA in wildtype or Knockout mice (Sup. Fig. 3.7). To improve the specificity and sensitivity of the assay, third derivative spectroscopy was used to analyze the MDA data. Derivative spectroscopy helps to eliminate or reduce the effects from drifting baseline and absorption from endogenous substances in biological samples.

ELF hydrogen peroxide level

There was no elevation observed in ELF H_2O_2 due to ETA treatment (Sup. Fig 3.8).

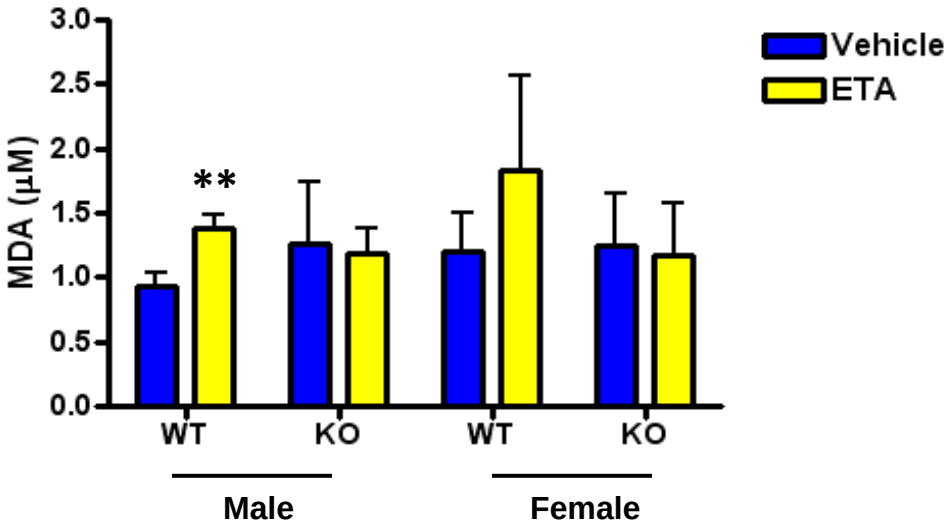

Figure 3.12 Plasma Malondialdehyde (MDA) level in wildtype and knockout mice.
Mice were treated with ETA or vehicle for 28-days.Graphs shows mean± SEM (n= 4 to 5). ETA treated wildtype male mice shows significance denoted by ** p<0.01 versus vehicle treated

3.5 Discussion

The aim of the present investigation was to evaluate the potential oxidative stress and toxicity resulting from long term antibiotic ETA treatment in the presence and absence of FMOs. To date there are few studies investigating flavin containing monooxygenase mediated S-oxygenation and toxicity (Genter et al. 1995; Krieter et al. 1984; Neal and Halpert 1982; Ruse and Waring 1991; Smith and Crespi 2002). Previous lab work with thiourea metabolism via FMO have shown that sulfenic acid was completely eliminated via incubation with 0.5-1.0 mM GSH and resultant production of GSSG (Henderson et al. 2004). This result suggests that individuals producing active FMO2.1 protein may be at enhanced risk of pulmonary toxicity upon exposure

to thiocarbamides. ETA *in vivo* metabolism discussed in chapter 2, showed significantly higher sulfenic acid levels present in plasma and ELF of wild type mice, whereas less sulfenic acid was present in knockout mice with no Fmo2. Because sulfenic acid can undergo glutathione redox cycling, the expectation is that wild type mice may deplete GSH more quickly than knockout mice and will experience higher levels of oxidative stress.

Twenty genes related to oxidative stress and antioxidant pathways were differentially expressed with long-term ETA treatment in wildtype and knockout male and female mice in compare to respective controls. Long-term ETA administration resulted in higher number of genes with altered expression in wild type male and female mice with fewer altered genes among knockouts. In general fold changes of differentially expressed genes in knockouts were smaller compared to wildtype.The reason behind this could be higher sulfenic acid production (observed in both ELF and plasma samples) in wildtype mice with ETA metabolism in the presence of active Fmos. Higher sulfenic acid levels might have depleted more GSH resulting in more oxidative stress and toxicity in wildtype mice.

Out of 12 altered genes in wildtype male and 13 altered genes in wildtype females, 7 genes were shared. Common diffrentially expressed genes confirm that the mechanism of toxicity is likely the same in both genders. There were common altered genes present in wildtype and knockout male and female mice as well which again provides evidence that the same mechanism of action is responsible for differential gene expression. The lower number of altered genes with smaller fold changes observed in knockout mice suggests that these mice experienced a lower level of oxidative insult compared to wild type mice.

PCR array data showed up-regulated *Gpx1,5* and *6* in wildtype males or females. In a separate quantitative PCR analysis, *Gpx3* was also seen upregulated in wildtype male and female mice with ETA treatment . GPX is an antioxidant enzyme family, and up-regulation is a protective mechanism against oxidative stress. Gpx1 protects against cigarette smoke-induced lung inflammation in mice (Duong et al. 2010). Human FMO is known to be "leaky" producing H_2O_2 in the presence of the substrate (Siddens et al, 2014). Antioxidant enzymes like Gpx, can convert H_2O_2 to water by using glutathione, so it is not surprising to see regulation of members of this gene family. The expression of heat shock proteins is well described in both whole lungs and in specific lung cells from a variety of species and in response to a variety of stressors (Hiratsuka et al. 1998; Villar et al. 1993; Wheeler and Wong 2007; Wong and Wispe 1997). Guo et al, (2007) has shown that heat shock protein 70 modulates the activities of Gpx and glutathione reductase (GR) in response to ischemic stress. Wildtype females showed altered expression of *Hspa1a* gene which is a member of the heat shock protein 70 family. *Hspa1a* altered gene expression was validated in individual samples; the significant up-regulation we observed among wildtype females following ETA treatment is again consistent with the notion that wildtype mice experiance higher levels of oxidative stress when FMO is expressed.

The NADPH oxidase pathway is the major means of superoxide generation in neutrophilic leukocytes and macrophages (Babior 1999), and our results implicate a role for this regulation of this pathway in our studies. Based on the literature, *NF-kB* expression is also regulated by oxidative stress (Babior 1999; Koay et al. 2001; O'Reilly et al. 1998; Reuter et al. 2010; Tan et al. 1999), and the NADPH oxidase pathway is important for maximal activation of NF-κB (Koay et al. 2001) which might be the explanation for *NF-kB*, *Noxa1* and *Nox1* co-up-regulation in wildtype mice. Expression of *NF-kB* was up-

regulated in wildtype males and females with the ETA treatment whereas it was reduced in knockout mice with the same treatment. *Noxa1* and *Nox1* were upregulated in wildtype male and female mice respectively which indicates wildtype mice may have experienced higher levels of superoxide production which may result in more toxicity; further validation is required for these genes. Lou et al, 2007 has reported that glutathione depletion induced NF-κB activity in mouse primary hepatocyte cells which has potential implications in relation to the role of NF-kB in liver diseases associated with GSH depletion and oxidative stress. Depletion of reduced GSH and subsequent increases in cytosolic GSSG in response to oxidative stress causes rapid ubiquitination and phosphorylation and thus subsequent degradation of the inhibitory κB (IκB) complex, which is a critical step for NF-κB activation (Ginn-Pease and Whisler 1996; Rahman et al. 1999; Rahman and MacNee 2000). NF-kB regulates the pro-infammatory mediators and protective antioxidant genes in response to oxidative/nitrative stress. Ryan et al.,(2000) has shown that induction of p53 causes an activation of NF-kB that correlates with the ability of p53 to induce apoptosis. ETA treated wildtype male and female mice have elevation of p53 gene expression whereas knockout mice showed significant reduction with ETA treatments compared to vehicle treated mice. In response to high levels of oxidative stresses, p53 exhibits prooxidant activities that may lead to cell death. P53 acts as a activator for Gpx enzymes (Tan et al. 1999). So, higher levels of *p53* expression might be regulating antioxidant activities in wildtype mice.

Wildtype mice have shown higher levels of plasma and epithelial lining fluid (ELF) ETASO, a sulfenic acid, (chapter-2) which can deplete GSH and cause oxidative stress. Long-term ETA treated wildtype mice showed down-regulation of the albumin gene in both males and females. Albumin bound thiol nucleophiles represent a very abundant and important circulating antioxidant

in the physiological system protecting against oxidative damage (Cha and Kim 1996; Roche et al. 2008). Decreased albumin levels resulting from long-term ETA treatment suggests reduced available protein thiols, along with a decrease in glutathione levels which may further enhance oxidative stress; however, changes in expression, while suggestive, did not reach statistical significance. Serum albumin levels in wildtype and knockout mice blood plasma should be examined to shed further light on this possible mechanism.

Mpo expression in mice did not validate the PCR array resuts. It is known that between-platform consistency changes with different primers. Primer sequences of the PCR products for the PCR array are not publically available, so we cannot verify this possible cause of discrepancy (Canales et al. 2006; Dallas et al. 2005; Etienne et al. 2004). Alternatively, as array data was based on pooled RNA, it is not surprising that we were unable to validate all of the array data.

Plasma MDA is a well-known marker of oxidative stress (Nielsen et al. 1997). MDA is the end product of lipid peroxidation, arising from free radical degradation of polyunsaturated fatty acids that can cause cross-linking in lipids, proteins and nucleic acids (Freeman and Crapo 1982). Our finding that MDA levels were increased in plasma of ETA-treated wild type mice suggests that these mice may have elevated levels of free radicals perhaps as the consequence of leaky FMO producing H_2O_2 or GSH depletion.

H_2O_2 level in ELF did not show any significant alteration with ETA treatment in any groups. A lack of difference in H_2O_2 could arise as an artifact due to diffusion of H_2O_2 from samples or from the lag between final dose and lavage sample collection (15-19 hours following the last dose of ETA). The

reported ETA half-life is 3-4 hours in mice, so it is possible that H_2O_2 estimation in lavage fluid must fall within this same range.

In conclusion, long-term ETA treatment affected wild type mice and *Fmo1/2/4* knockout mice differently. Oxidative stress and anti-oxidant pathway associated gene expression analysis revealed more altered gene expression in wildtype male and female mice in comparison to knockout mice. The observed changes are consistent with the idea that individuals expressing active FMO have an elevated increased risk of ETA toxicity with TB treatment. Altered redox state due to oxidative stress can increase inflammatory responses in TB patients and cause more complications.

Further analysis of ETA therapeutic efficacy and toxicity in the presence and absence of FMOs need to be addressed in future studies by using wildtype and knockout mice infected with *Mycobacterium tuberculosis.* The data confirms the possibility that individuals expressing active FMO2.1 protein will be at greater risk of experience elevated levels of oxidative stress if they take ETA to treat TB, than those individuals encoding non-functional FMO2.2. Whether or not elevated oxidative stress would pose a noticeable problem for these individuals can't be determined at this time. Though it is advisable that clinicians should always incorporate exogenous antioxidant in the regimen of TB-infected patients in Sub-Saharan Africa and educate them about possible risk factors of ETA treatments.

Chapter 4 General discussion

Tuberculosis (TB) continues to be the most common infectious disease in the world with approximately one-third of the world's population infected with *Mycobacterium tuberculosis.* In 2012, 8.6 million people fell ill with TB and 1.3 million died (Eurosurveillance editorial 2013). In 2012, sub-Saharan Africa carried the greatest proportion of new TB cases per population (Eurosurveillance editorial 2013). The increased incidence of resistance to first-line antibiotics, including isoniazid and rifampicin, causes health organizations to recommend second-line antibiotics as first-line intervention; one of the most important is ETA (Bastian and Colebunders 1999; Thee et al. 2011).

ETA is a substrate for phase 1 drug metabolizing flavin-containing monooxygenases (FMOs) (Henderson et al. 2008; Qian and Ortiz de Montellano 2006). FMOs metabolize numerous foreign chemicals, including drugs, pesticides and dietary components and, thus, mediate interactions between humans and their chemical environment (Cashman 2003; Krueger and Williams 2005; Ziegler 2002). Not much is known about FMOs and their genetic variants in disease and drug response. Loss-of function mutations of FMO3 cause the disorder trimethylaminuria (Akerman et al. 1999a; Akerman et al. 1999b) (Hernandez et al. 2003). More common variants that decrease enzyme activity are associated with increased drug efficacy (Lattard et al. 2003). FMO2 is a major isoform in lung, though unlike nonhuman primates and other mammals, FMO2 is not a prominent functionally active enzyme in humans (Yueh et al. 1997). Most humans are homozygous for a nonsense mutation that inactivates FMO2 (Dolphin et al. 1998), but a substantial proportion of sub-Saharan Africans express functional FMO2.1 (Veeramah et al. 2008) and, are predicted to respond differently to drugs and other foreign

chemicals. The highest incidence of individuals with active FMO2.1 and highest incidences of TB co-incidentally occur in Sub-Saharan Africa where increasing number of resistance to front-line TB drugs every year is of great importance.

The distribution of *FMO2*1* and *FMO2*2* alleles among world populations has implications for inter-ethnic and, in African and Hispanic populations, inter-individual variation in response to drugs and in susceptibility to toxic chemicals that are substrates of FMO2, particularly those for which lung is the target organ or route of entry. Our central hypothesis is that individuals producing active FMO2.1 will exhibit differences in the plasma and target tissue concentrations of ETA and ETASO (specific aim 1) resulting in enhanced oxidative stress and toxicity with long-term ETA treatment (specific aim 2) and will experience reduced therapeutic efficacy in inhibition and killing of mycobacteria (specific aim 3).

To study our hypothesis we used *Fmo1/2/4* knockout mice developed by deleting exons 2-9 of *Fmo2*, 1-7 of *Fmo4* and the entire *Fmo1* gene by chromosomal engineering (Hernandez et al. 2006). In our study *Fmo1/2/4* knockout mice, mimic the human lung environment of Caucasians and Asians where there is no active FMO2 present. Whereas wild type mice model the individuals with active Fmo2.1, such as those of African and Hispanic descent. The use of *Fmo*-knockout mouse strain in our studies demonstrated an important role of FMOs in ETA metabolism and toxicity, although this mouse has shortcomings. This mouse line is null *for Fmo1, 2 and 4*, not only *Fmo2*. Our mouse model is *Fmo1* null which is beneficiary for our studies since as opposed to humans; mice have significant expression of *Fmo1* in lung and liver. The mouse Fmo1 enzymatic specificity constant (K_{cat}/K_m) for ETA is 2.62 while for human FMO1 it is 0.86 which is much lower than mice (Henderson et

al. 2008), so the simultaneous absence of both Fmo1 and 2 in our mouse model is a better mimic for human lung with very low FMO1 and *FMO2*2* genotype, than a simple *Fmo2* null mouse would be. Unlike humans, male mice do not express hepatic Fmo3 (Cashman 2003; Hernandez et al. 2004; Hines et al. 1994), so wild type female mice are a better model of humans with the *FMO2*1* genotype than are male mice. On the other hand, *Fmo1/2/4* knockout female mice are expected to be a better model of FMO expression with human of the *FMO2*2* genotype. The enzymatic specificity constants for human and mouse FMO2 for ETA is 0.19 and 0.2, respectively (Henderson et al. 2008).

The first study with a single 125 mg/kg oral dose of ETA in wildtype and knockout mice demonstrated that FMOs play an important role in ETA metabolism. HPLC analysis of plasma and epithelial lining fluid (ELF) samples showed FMO-dependent ETA S-oxygenation resulting in ETA S-oxide (ETASO) a sulfenic acid, and to a lesser degree, 2-ethyl-4-amidopyridine (ETAA) in both wild type and knockout mice. The ETA plasma and ELF concentrations exceeded the minimum inhibitory concentration (MIC) for *M. tuberculosis* and above ensuring that 125 mg/kg is an appropriate dose to treat infection (Heifets et al. 1991; Rastogi et al. 1996). In comparison, concentrations of ETA in plasma and ELF of knockout mice had higher ETA levels than ETASO while wild type mice had higher level of ETASO than ETA. The ETASO, a sulfenic acid, was significantly higher in wild type mice than knockouts in both plasma and ELF samples. We still see ETA metabolism in knockout mice, this suggests that Fmo3, Fmo5 and/or another mouse Fmo might be responsible for ETASO generation. In mice 9 isoforms of FMOs have been documented (Hernandez et al. 2004; Hines et al. 2002) though not much is known about FMOs other than 1-5. Fmo5 does not S-oxygenate ETA to an appreciable degree (Henderson et al. 2008). The possibility of cytochrome P450s (CYPs) being involved in ETA metabolism is not likely as Henderson et

al. (2008), demonstrated that ETA metabolism in lung was inhibited by the competitive inhibitor of FMO, thiourea, whereas there was no change in activity due to the presence of the general CYP inhibitor SKF-525A.

The second, 28-day ETA exposure scenario in mice resulted in a higher number of differentially expressed genes related to oxidative stress and antioxidant pathways in wild type mice of both sexes. Higher levels of malondialdehyde were also detected in plasma from wildtype mice. These data all suggests that oxidative stress was higher in ETA-treated wild type mice than in knockouts. Higher levels of ETASO, detected in wildtype mice plasma and ELF, may have mediated glutathione depletion causing the observed oxidative stress. Long-term ETA treated wild type mice also showed altered hepatic and pulmonary *Fmo 1, 2* and *4* expression patterns. *Fmo 1, 2* and *4* expression changes in wild type mice suggest a probable association with ETA metabolism and oxidative stress/ toxicity. Other studies have shown altered *FMO* expression under oxidative stress, inflammation and disease conditions (Malaspina et al. 2001; Rahman et al. 2009; Zhang et al. 2009).

Lastly with respect to ETA therapeutic efficacy for *M. avium* inhibition and killing in the presence and absence of FMOs, we determined that oral 50 mg/kg dosing of ETA was not capable of efficient reduction of the bacterial load in either wild type or knockout mice. ETA dose of 50 mg/kg has shown effective bactericidal activity towards *M. tuberculosis* in some models (Cynamon & Sklaney 2003) but not others (klemens et al. 1993). The 50 mg/kg of ETA dose did not reach the MIC for *M. avium* infected wild type mice in our study protocol. Interestingly, ETA treated wildtype mice showed significant higher bacterial load than knockout mice in both lung and spleen which does suggest the FMO role in the mice vulnerability to bacterial infection in the presence of substrate ETA.

In-vitro ETA toxicity analysis utilizing the *FMO2.1* and *2.2* stably transfected human bronchial epithelial cell line BEAS-2B, showed that ETA toxicity was independent of FMO expression. We propose that primary alveolar type 1 cells naturally expressing FMO2 in C57BL/6 wild type mice and primary alveolar type 1 cells from *Fmo1/2/4* knockout mice (Hernandez et al. 2006), which do not express *Fmo2,* might be a better model to study FMO metabolism mediated ETA cytotoxicity in host cells.

Taking into account the variations in enzymatic activity between ethnic groups can lead to the development of better drug regimes ("personalized medicine"). Decreased adverse side effects lead to more successful therapeutic compliance and bacterial clearance for long-term TB treatment. *Fmo 1/2/4* knockout mice model are suitable for the study of ETA pharmacokinetics and for examination the impact of the human FMO2 genetic polymorphism in lung on the efficacy and toxicity associated with long-term ETA for TB therapy. Oral administration of ETA suggests that intestinal (primarily FMO1) and liver FMO (FMO3) may play an role in the pharmacokinetics of this prodrug and in its demonstrated hepatotoxicity (Bastian and Colebunders 1999). It is possible that ETA side effects could be avoided by changing the route of administration. Since TB occurs primarily in the lungs, a delivery system of this drug could be devised through inhalation. A smaller dose of drug delivered by inhalation would avoid the GI tract by initially targeting the lung, decreasing overall toxicity.

Drug metabolizing enzymes genetic variants and the consequences of these for disease and drug response, has increased awareness of the pharmacological and toxicological significance of these enzymes. This is a first *in vivo* study highlighting *FMO2* genetic variants effects on drug metabolism and toxicity. This work highlights the possible importance of the FMO2

polymorphism on ETA selection for TB treatment to maximize treatment efficacy and minimize toxicity. These studies suggest that humans expressing active FMO2.1 may be at higher risk of ETA toxicity than individuals with inactive FMO2.2 that are undergoing long-term ETA treatment for MDR-TB. Future study of *M. tuberculosis* infected mice with a 125 mg/kg dose of ETA is warranted to reveal FMO2 genotypic effects on ETA therapeutic efficacy.

BIBLIOGRAPHY

Akerman, B. R., S. Forrest, L. Chow, R. Youil, M. Knight & E. P. Treacy (1999a) Two novel mutations of the FMO3 gene in a proband with trimethylaminuria. *Hum Mutat,* 13**,** 376-9.

Akerman, B. R., H. Lemass, L. M. Chow, D. M. Lambert, C. Greenberg, C. Bibeau, O. A. Mamer & E. P. Treacy (1999b) Trimethylaminuria is caused by mutations of the FMO3 gene in a North American cohort. *Mol Genet Metab,* 68**,** 24-31.

Atta-Asafo-Adjei, E., M. P. Lawton & R. M. Philpot (1993) Cloning, sequencing, distribution, and expression in Escherichia coli of flavin-containing monooxygenase 1C1. Evidence for a third gene subfamily in rabbits. *J Biol Chem,* 268**,** 9681-9.

Babior, B. M. (1999) NADPH oxidase: an update. *Blood,* 93**,** 1464-76.

Banerjee, A., E. Dubnau, A. Quemard, V. Balasubramanian, K. S. Um, T. Wilson, D. Collins, G. de Lisle & W. R. Jacobs, Jr. (1994) inhA, a gene encoding a target for isoniazid and ethionamide in Mycobacterium tuberculosis. *Science,* 263**,** 227-30.

Bastian, I. & R. Colebunders (1999) Treatment and prevention of multidrug-resistant tuberculosis. *Drugs,* 58**,** 633-61.

Baulard, A. R., J. C. Betts, J. Engohang-Ndong, S. Quan, R. A. McAdam, P. J. Brennan, C. Locht & G. S. Besra (2000) Activation of the pro-drug ethionamide is regulated in mycobacteria. *J Biol Chem,* 275**,** 28326-31.

Bermudez, L. E., P. Kolonoski, M. Petrofsky, M. Wu, C. B. Inderlied & L. S. Young (2003) Mefloquine, moxifloxacin, and ethambutol are a triple-drug alternative to macrolide-containing regimens for treatment of Mycobacterium avium disease. *J Infect Dis,* 187**,** 1977-80.

Bermudez, L. E., P. Kolonoski, M. Wu, P. A. Aralar, C. B. Inderlied & L. S. Young (1999) Mefloquine is active in vitro and in vivo against Mycobacterium avium complex. *Antimicrob Agents Chemother,* 43**,** 1870-4.

Bitton-Worms, K., E. Pikarsky, A. Aronheim (2010) The AP-1 repressor protein, JDP2, potentiates hepatocellular carcinoma in mice. *Mol Cancer*, 9, 54.

Canales, R. D., Y. Luo, J. C. Willey, B. Austermiller, C. C. Barbacioru, C. Boysen, K. Hunkapiller, R. V. Jensen, C. R. Knight, K. Y. Lee, Y. Ma, B. Maqsodi, A. Papallo, E. H. Peters, K. Poulter, P. L. Ruppel, R. R. Samaha, L. Shi, W. Yang, L. Zhang & F. M. Goodsaid (2006) Evaluation of DNA microarray results with quantitative gene expression platforms. *Nat Biotechnol,* 24**,** 1115-22.

Cashman, J. R. (1995) Structural and catalytic properties of the mammalian flavin-containing monooxygenase. *Chem Res Toxicol,* 8**,** 166-81.

Cashman, J.R. (2003) The role of flavin-containing monooxygenases in drug metabolism and development. *Curr Opin Drug Discov Devel,* 6**,** 486-93.

Cashman, J. R. (2004) The implications of polymorphisms in mammalian flavin-containing monooxygenases in drug discovery and development. *Drug Discov Today,* 9**,** 574-81.

Cashman, J. R. & J. Zhang (2002) Interindividual differences of human flavin-containing monooxygenase 3: genetic polymorphisms and functional variation. *Drug Metab Dispos,* 30**,** 1043-52.

Centers for Disease, C. & Prevention (2013) Trends in tuberculosis--United States, 2012. *MMWR Morb Mortal Wkly Rep,* 62**,** 201-5.

Cereda, C., E. Gabanti, M. Corato, A. de Silvestri, D. Alimonti, E. Cova, A. Malaspina & M. Ceroni (2006) Increased incidence of FMO1 gene single nucleotide polymorphisms in sporadic amyotrophic lateral sclerosis. *Amyotroph Lateral Scler,* 7**,** 227-34.

Cha, M. K. & I. H. Kim (1996) Glutathione-linked thiol peroxidase activity of human serum albumin: a possible antioxidant role of serum albumin in blood plasma. *Biochem Biophys Res Commun,* 222**,** 619-25.

Conte, J. E., Jr., G. Wang, E. T. Lin & E. Zurlinden (2001) High-performance liquid chromatographic-tandem mass spectrometric method for the determination of ethionamide in human plasma, bronchoalveolar lavage fluid and alveolar cells. *J Chromatogr B Biomed Sci Appl,* 753**,** 343-53.

Cohen, Y., Perronne, C., Lazard, T., Truffot-Pernot, C., Grosset, J., Vilde, J. L., & Pocidalo, J. J. (1995). Use of normal C57BL/6 mice with established Mycobacterium avium infections as an alternative model for evaluation of antibiotic activity. *Antimicrobial Agents and Chemotherapy*, *39*(3), 735–738.

Cynamon, M. H. & M. Sklaney (2003) Gatifloxacin and ethionamide as the foundation for therapy of tuberculosis. *Antimicrob Agents Chemother,* 47**,** 2442-4.

Dallas, P. B., N. G. Gottardo, M. J. Firth, A. H. Beesley, K. Hoffmann, P. A. Terry, J. R. Freitas, J. M. Boag, A. J. Cummings & U. R. Kees (2005) Gene expression levels assessed by oligonucleotide microarray analysis and quantitative real-time RT-PCR -- how well do they correlate? *BMC Genomics,* 6**,** 59.

DeBarber, A. E., K. Mdluli, M. Bosman, L. G. Bekker & C. E. Barry, 3rd (2000) Ethionamide activation and sensitivity in multidrug-resistant Mycobacterium tuberculosis. *Proc Natl Acad Sci U S A,* 97**,** 9677-82.

Dolphin, C. T., D. J. Beckett, A. Janmohamed, T. E. Cullingford, R. L. Smith, E. A. Shephard & I. R. Phillips (1998) The flavin-containing monooxygenase 2 gene (FMO2) of humans, but not of other primates, encodes a truncated, nonfunctional protein. *J Biol Chem,* 273**,** 30599-607.

Dover, L. G., A. Alahari, P. Gratraud, J. M. Gomes, V. Bhowruth, R. C. Reynolds, G. S. Besra & L. Kremer (2007) EthA, a common activator of thiocarbamide-containing drugs acting on different mycobacterial targets. *Antimicrob Agents Chemother,* 51**,** 1055-63.

Duong, C., H. J. Seow, S. Bozinovski, P. J. Crack, G. P. Anderson & R. Vlahos (2010) Glutathione peroxidase-1 protects against cigarette smoke-induced lung inflammation in mice. *Am J Physiol Lung Cell Mol Physiol,* 299**,** L425-33.

Eom, H. J., J. M. Ahn, Y. Kim & J. Choi (2013) Hypoxia inducible factor-1 (HIF-1)-flavin containing monooxygenase-2 (FMO-2) signaling acts in silver nanoparticles and silver ion toxicity in the nematode, Caenorhabditis elegans. *Toxicol Appl Pharmacol,* 270**,** 106-13.

Etienne, W., M. H. Meyer, J. Peppers & R. A. Meyer, Jr. (2004) Comparison of mRNA gene expression by RT-PCR and DNA microarray. *Biotechniques,* 36**,** 618-20, 622, 624-6.

Eurosurveillance editorial, t. (2013) WHO publishes Global tuberculosis report 2013. *Euro Surveill,* 18.

Fraaije, M. W., N. M. Kamerbeek, A. J. Heidekamp, R. Fortin & D. B. Janssen (2004) The prodrug activator EtaA from Mycobacterium tuberculosis is a Baeyer-Villiger monooxygenase. *J Biol Chem,* 279**,** 3354-60.

Francois, A. A., C. R. Nishida, P. R. de Montellano, I. R. Phillips & E. A. Shephard (2009) Human flavin-containing monooxygenase 2.1 catalyzes oxygenation of the antitubercular drugs thiacetazone and ethionamide. *Drug Metab Dispos,* 37**,** 178-86.

Freeman, B. A. & J. D. Crapo (1982) Biology of disease: free radicals and tissue injury. *Lab Invest,* 47**,** 412-26.

Furnes, B., J. Feng, S. S. Sommer & D. Schlenk (2003) Identification of novel variants of the flavin-containing monooxygenase gene family in African Americans. *Drug Metab Dispos,* 31**,** 187-93.

Gandhi, N. R., A. Moll, A. W. Sturm, R. Pawinski, T. Govender, U. Lalloo, K. Zeller, J. Andrews & G. Friedland (2006) Extensively drug-resistant tuberculosis as a cause of death in patients co-infected with tuberculosis and HIV in a rural area of South Africa. *Lancet,* 368**,** 1575-80.

Genter, M. B., N. J. Deamer, B. L. Blake, D. S. Wesley & P. E. Levi (1995) Olfactory toxicity of methimazole: dose-response and structure-activity studies and characterization of flavin-containing monooxygenase activity in the Long-Evans rat olfactory mucosa. *Toxicol Pathol,* 23**,** 477-86.

Ginn-Pease, M. E. & R. L. Whisler (1996) Optimal NF kappa B mediated transcriptional responses in Jurkat T cells exposed to oxidative stress are dependent on intracellular glutathione and costimulatory signals. *Biochem Biophys Res Commun,* 226**,** 695-702.

Guo, S., W. Wharton, P. Moseley, H. Shi (2007) Heat shock protein 70 regulates cellular redox status by modulating glutathione-related enzyme activities. *Cell Stress Chaperones*, 12, 245-254

Guo, W. X., L. L. Poulsen & D. M. Ziegler (1992) Use of thiocarbamides as selective substrate probes for isoforms of flavin-containing monooxygenases. *Biochem Pharmacol,* 44**,** 2029-37.

Hanoulle, X., Wieruszeski, J. M., Rousselot-Pailley, P., Landrieu, I., Locht, C., Lippens, G., & Baulard, A. R. (2006). Selective intracellular accumulation of the major metabolite issued from the activation of the

prodrug ethionamide in mycobacteria. *J Antimicrob Chemother, 58*, 768-772

Heifets, L. (1988) Qualitative and quantitative drug-susceptibility tests in mycobacteriology. *Am Rev Respir Dis,* 137**,** 1217-22.

Heifets, L. B., P. J. Lindholm-Levy & M. Flory (1991) Comparison of bacteriostatic and bactericidal activity of isoniazid and ethionamide against Mycobacterium avium and Mycobacterium tuberculosis. *Am Rev Respir Dis,* 143**,** 268-70.

Henderson, M. C., S. K. Krueger, J. F. Stevens & D. E. Williams (2004) Human flavin-containing monooxygenase form 2 S-oxygenation: sulfenic acid formation from thioureas and oxidation of glutathione. *Chem Res Toxicol,* 17**,** 633-40.

Henderson, M. C., L. K. Siddens, J. T. Morre, S. K. Krueger & D. E. Williams (2008) Metabolism of the anti-tuberculosis drug ethionamide by mouse and human FMO1, FMO2 and FMO3 and mouse and human lung microsomes. *Toxicol Appl Pharmacol,* 233**,** 420-7.

Heng, B. C., X. Zhao, S. Xiong, K. W. Ng, F. Y. Boey & J. S. Loo (2010) Toxicity of zinc oxide (ZnO) nanoparticles on human bronchial epithelial cells (BEAS-2B) is accentuated by oxidative stress. *Food Chem Toxicol,* 48**,** 1762-6.

Hernandez, D., S. Addou, D. Lee, C. Orengo, E. A. Shephard & I. R. Phillips (2003) Trimethylaminuria and a human FMO3 mutation database. *Hum Mutat,* 22**,** 209-13.

Hernandez, D., P. Chandan, A. Janmohamed, R. Phillips l & E. A. Shephard (2006) Deletion of genes from the mouse genome using Cre/loxP technology. *Methods Mol Biol,* 320**,** 307-19.

Hernandez, D., A. Janmohamed, P. Chandan, B. A. Omar, I. R. Phillips & E. A. Shephard (2009) Deletion of the mouse Fmo1 gene results in enhanced pharmacological behavioural responses to imipramine. *Pharmacogenet Genomics,* 19**,** 289-99.

Hernandez, D., A. Janmohamed, P. Chandan, I. R. Phillips & E. A. Shephard (2004) Organization and evolution of the flavin-containing monooxygenase genes of human and mouse: identification of novel gene and pseudogene clusters. *Pharmacogenetics,* 14**,** 117-30.

Hines, R. N., J. R. Cashman, R. M. Philpot, D. E. Williams & D. M. Ziegler (1994) The mammalian flavin-containing monooxygenases: molecular characterization and regulation of expression. *Toxicol Appl Pharmacol,* 125**,** 1-6.

Hines, R. N., K. A. Hopp, J. Franco, K. Saeian & F. P. Begun (2002) Alternative processing of the human FMO6 gene renders transcripts incapable of encoding a functional flavin-containing monooxygenase. *Mol Pharmacol,* 62**,** 320-5.

Hiratsuka, M., M. Yano, B. N. Mora, I. Nagahiro, J. D. Cooper & G. A. Patterson (1998) Heat shock pretreatment protects pulmonary isografts from subsequent ischemia-reperfusion injury. *J Heart Lung Transplant,* 17**,** 1238-46.

Hukkanen, J., O. Pelkonen, J. Hakkola & H. Raunio (2002) Expression and regulation of xenobiotic-metabolizing cytochrome P450 (CYP) enzymes in human lung. *Crit Rev Toxicol,* 32**,** 391-411.

Iber, H., M. B. Sewer, T. B. Barclay, S. R. Mitchell, T. Li & E. T. Morgan (1999) Modulation of drug metabolism in infectious and inflammatory diseases. *Drug Metab Rev,* 31**,** 29-41.

Inderlied, C. B., C. A. Kemper & L. E. Bermudez (1993) The Mycobacterium avium complex. *Clin Microbiol Rev,* 6**,** 266-310.

Janmohamed, A., D. Hernandez, I. R. Phillips & E. A. Shephard (2004) Cell-, tissue-, sex- and developmental stage-specific expression of mouse flavin-containing monooxygenases (Fmos). *Biochem Pharmacol,* 68**,** 73-83.

Johnston, J. P., P. O. Kane & M. R. Kibby (1967) The metabolism of ethionamide and its sulphoxide. *J Pharm Pharmacol,* 19**,** 1-9.

Klemens, S. P., M. S. DeStefano & M. H. Cynamon(1993). Therapy of multidrug-resistant tuberculosis: lessons from studies with mice. Antimicrob Agents Chemother, 37(11), 2344-2347

Kiem, S. & J. J. Schentag (2008) Interpretation of antibiotic concentration ratios measured in epithelial lining fluid. *Antimicrob Agents Chemother,* 52**,** 24-36.

Kim, Y. M. & D. M. Ziegler (2000) Size limits of thiocarbamides accepted as substrates by human flavin-containing monooxygenase 1. *Drug Metab Dispos,* 28**,** 1003-6.

Koay, M. A., J. W. Christman, B. H. Segal, A. Venkatakrishnan, T. R. Blackwell, S. M. Holland & T. S. Blackwell (2001) Impaired pulmonary NF-kappaB activation in response to lipopolysaccharide in NADPH oxidase-deficient mice. *Infect Immun,* 69**,** 5991-6.

Krieter, P. A., D. M. Ziegler, K. E. Hill & R. F. Burk (1984) Increased biliary GSSG efflux from rat livers perfused with thiocarbamide substrates for the flavin-containing monooxygenase. *Mol Pharmacol,* 26**,** 122-7.

Krueger, S. K., M. C. Henderson, L. K. Siddens, J. E. VanDyke, A. D. Benninghoff, P. A. Karplus, B. Furnes, D. Schlenk & D. E. Williams (2009) Characterization of sulfoxygenation and structural implications of human flavin-containing monooxygenase isoform 2 (FMO2.1) variants S195L and N413K. *Drug Metab Dispos,* 37**,** 1785-91.

Krueger, S. K., S. R. Martin, M. F. Yueh, C. B. Pereira & D. E. Williams (2002a) Identification of active flavin-containing monooxygenase isoform 2 in human lung and characterization of expressed protein. *Drug Metab Dispos,* 30**,** 34-41.

Krueger, S. K., L. K. Siddens, M. C. Henderson, E. A. Andreasen, R. L. Tanguay, C. B. Pereira, E. T. Cabacungan, R. N. Hines, K. G. Ardlie & D. E. Williams (2005) Haplotype and functional analysis of four flavin-containing monooxygenase isoform 2 (FMO2) polymorphisms in Hispanics. *Pharmacogenet Genomics,* 15**,** 245-56.

Krueger, S. K., L. K. Siddens, S. R. Martin, Z. Yu, C. B. Pereira, E. T. Cabacungan, R. N. Hines, K. G. Ardlie, J. L. Raucy & D. E. Williams (2004) Differences in FMO2*1 allelic frequency between Hispanics of Puerto Rican and Mexican descent. *Drug Metab Dispos,* 32**,** 1337-40.

Krueger, S. K. & D. E. Williams (2005) Mammalian flavin-containing monooxygenases: structure/function, genetic polymorphisms and role in drug metabolism. *Pharmacol Ther,* 106**,** 357-87.

Krueger, S. K., D. E. Williams, M. F. Yueh, S. R. Martin, R. N. Hines, J. L. Raucy, C. T. Dolphin, E. A. Shephard & I. R. Phillips (2002b) Genetic polymorphisms of flavin-containing monooxygenase (FMO). *Drug Metab Rev,* 34**,** 523-32.

Lattard, V., J. Zhang, Q. Tran, B. Furnes, D. Schlenk & J. R. Cashman (2003) Two new polymorphisms of the FMO3 gene in Caucasian and African-American populations: comparative genetic and functional studies. *Drug Metab Dispos,* 31**,** 854-60.

Lawton, M. P. & R. M. Philpot (1993) Functional characterization of flavin-containing monooxygenase 1B1 expressed in Saccharomyces cerevisiae and Escherichia coli and analysis of proposed FAD- and membrane-binding domains. *J Biol Chem,* 268**,** 5728-34.

Lou, H., & N. Kaplowitz (2007). Glutathione depletion down-regulates tumor necrosis factor alpha-induced NF-kappaB activity via IkappaB kinase-dependent and -independent mechanisms. *J Biol Chem*, 282(40), 29470-29481.

Lounis, N., N. Veziris, A. Chauffour, C. Truffot-Pernot, K. Andries, & V. Jarlier (2006). Combinations of R207910 with drugs used to treat multidrug-resistant tuberculosis have the potential to shorten treatment duration. *Antimicrob Agents Chemother*, 50(11), 3543-3547.

Malaspina, A., N. Kaushik & J. de Belleroche (2001) Differential expression of 14 genes in amyotrophic lateral sclerosis spinal cord detected using gridded cDNA arrays. *J Neurochem,* 77**,** 132-45.

McCombie, R. R., C. T. Dolphin, S. Povey, I. R. Phillips & E. A. Shephard (1996) Localization of human flavin-containing monooxygenase genes FMO2 and FMO5 to chromosome 1q. *Genomics,* 34**,** 426-9.

Morgan, E. T. (2009) Impact of infectious and inflammatory disease on cytochrome P450-mediated drug metabolism and pharmacokinetics. *Clin Pharmacol Ther,* 85**,** 434-8.

Motika, M. S., J. Zhang & J. R. Cashman (2007) Flavin-containing monooxygenase 3 and human disease. *Expert Opin Drug Metab Toxicol,* 3**,** 831-45.

Neal, R. A. & J. Halpert (1982) Toxicology of thiono-sulfur compounds. *Annu Rev Pharmacol Toxicol,* 22**,** 321-39.

Nichols, W. K., R. Mehta, K. Skordos, K. Mace, A. M. Pfeifer, B. A. Carr, T. Minko, S. W. Burchiel & G. S. Yost (2003) 3-methylindole-induced toxicity to human bronchial epithelial cell lines. *Toxicol Sci,* 71**,** 229-36.

Nielsen, F., B. B. Mikkelsen, J. B. Nielsen, H. R. Andersen & P. Grandjean (1997) Plasma malondialdehyde as biomarker for oxidative stress: reference interval and effects of life-style factors. *Clin Chem,* 43**,** 1209-14.

O'Reilly, M. A., R. J. Staversky, B. R. Stripp & J. N. Finkelstein (1998) Exposure to hyperoxia induces p53 expression in mouse lung epithelium. *Am J Respir Cell Mol Biol,* 18**,** 43-50.

Palmer, A. L., V. L. Leykam, A. Larkin, S. K., Krueger, I. R. Phillips, E. A. Shephard, & D. E. Williams (2012). Metabolism and pharmacokinetics of the anti-tuberculosis drug ethionamide in a flavin-containing monooxygenase null mouse. *Pharmaceuticals (Basel)*, 5(11), 1147-1159.

Park, E. J., J. Choi, Y. K. Park & K. Park (2008) Oxidative stress induced by cerium oxide nanoparticles in cultured BEAS-2B cells. *Toxicology,* 245**,** 90-100.

Park, S. K., P. M. Tedesco & T. E. Johnson (2009) Oxidative stress and longevity in Caenorhabditis elegans as mediated by SKN-1. *Aging Cell,* 8**,** 258-69.

Phillips, I. R. & E. A. Shephard (2008) Flavin-containing monooxygenases: mutations, disease and drug response. *Trends Pharmacol Sci,* 29**,** 294-301.

Poulsen, L. L., R. M. Hyslop & D. M. Ziegler (1979) S-Oxygenation of N-substituted thioureas catalyzed by the pig liver microsomal FAD-containing monooxygenase. *Arch Biochem Biophys,* 198**,** 78-88.

Poulsen, L. L., K. Taylor, D. E. Williams, B. S. Masters & D. M. Ziegler (1986) Substrate specificity of the rabbit lung flavin-containing monooxygenase for amines: oxidation products of primary alkylamines. *Mol Pharmacol,* 30**,** 680-5.

Prema, K. & K. P. Gopinthan (1976) Metabolism of ethionamide, a second-line antituberculosis drug. *J. Indian Inst. Sci.* 58, 16–27.

Qian, L. & P. R. Ortiz de Montellano (2006) Oxidative activation of thiacetazone by the Mycobacterium tuberculosis flavin monooxygenase EtaA and human FMO1 and FMO3. *Chem Res Toxicol,* 19**,** 443-9.

Quemard, A., G. Laneelle & C. Lacave (1992) Mycolic acid synthesis: a target for ethionamide in mycobacteria? *Antimicrob Agents Chemother,* 36**,** 1316-21.

Rae, J. M., M. D. Johnson, M. E. Lippman & D. A. Flockhart (2001) Rifampin is a selective, pleiotropic inducer of drug metabolism genes in human hepatocytes: studies with cDNA and oligonucleotide expression arrays. *J Pharmacol Exp Ther,* 299**,** 849-57.

Rahman, I., F. Antonicelli & W. MacNee (1999) Molecular mechanism of the regulation of glutathione synthesis by tumor necrosis factor-alpha and dexamethasone in human alveolar epithelial cells. *J Biol Chem,* 274**,** 5088-96.

Rahman, I. & W. MacNee (2000) Regulation of redox glutathione levels and gene transcription in lung inflammation: therapeutic approaches. *Free Radic Biol Med,* 28**,** 1405-20.

Rahman, M. F., J. Wang, T. A. Patterson, U. T. Saini, B. L. Robinson, G. D. Newport, R. C. Murdock, J. J. Schlager, S. M. Hussain & S. F. Ali (2009) Expression of genes related to oxidative stress in the mouse brain after exposure to silver-25 nanoparticles. *Toxicol Lett,* 187**,** 15-21.

Rastogi, N., V. Labrousse & K. S. Goh (1996) In vitro activities of fourteen antimicrobial agents against drug susceptible and resistant clinical isolates of Mycobacterium tuberculosis and comparative intracellular activities against the virulent H37Rv strain in human macrophages. *Curr Microbiol,* 33**,** 167-75.

Raviglione, M. C. (2006) The Global Plan to Stop TB, 2006-2015. *Int J Tuberc Lung Dis,* 10**,** 238-9.

Rennard, S. I., G. Basset, D. Lecossier, K. M. O'Donnell, P. Pinkston, P. G. Martin & R. G. Crystal (1986) Estimation of volume of epithelial lining fluid recovered by lavage using urea as marker of dilution. *J Appl Physiol (1985),* 60**,** 532-8.

Reuter, S., S. C. Gupta, M. M. Chaturvedi & B. B. Aggarwal (2010) Oxidative stress, inflammation, and cancer: how are they linked? *Free Radic Biol Med,* 49**,** 1603-16.

Roche, M., P. Rondeau, N. R. Singh, E. Tarnus & E. Bourdon (2008) The antioxidant properties of serum albumin. *FEBS Lett,* 582**,** 1783-7.

Rothschild, B. M., L. D. Martin, G. Lev, H. Bercovier, G. K. Bar-Gal, C. Greenblatt, H. Donoghue, M. Spigelman & D. Brittain (2001) Mycobacterium tuberculosis complex DNA from an extinct bison dated 17,000 years before the present. *Clin Infect Dis,* 33**,** 305-11.

Ruse, M. J. & R. H. Waring (1991) The effect of methimazole on thioamide bioactivation and toxicity. *Toxicol Lett,* 58**,** 37-41.

Sahbazian, B. & S. E. Weis (2005) Treatment of active tuberculosis: challenges and prospects. *Clin Chest Med,* 26**,** 273-82, vi.

Saunders, B. M., A. A. Frank & I. M. Orme (1999) Granuloma formation is required to contain bacillus growth and delay mortality in mice chronically infected with Mycobacterium tuberculosis. *Immunology,* 98**,** 324-8.

Schentag, J. J. (1989) Clinical significance of antibiotic tissue penetration. *Clin Pharmacokinet,* 16 Suppl 1**,** 25-31.

Schmith, V. D. & J. F. Foss (2008) Effects of inflammation on pharmacokinetics/pharmacodynamics: increasing recognition of its contribution to variability in response. *Clin Pharmacol Ther,* 83**,** 809-11.

Schon, T., P. Jureen, E. Chryssanthou, C. G. Giske, E. Sturegard, G. Kahlmeter, S. Hoffner & K. A. Angeby (2011) Wild-type distributions of seven oral second-line drugs against Mycobacterium tuberculosis. *Int J Tuberc Lung Dis,* 15**,** 502-9.

Shephard, E. A., C. T. Dolphin, M. F. Fox, S. Povey, R. Smith & I. R. Phillips (1993) Localization of genes encoding three distinct flavin-containing monooxygenases to human chromosome 1q. *Genomics,* 16**,** 85-9.

Siddens, L. K., S. K. Krueger, M. C. Henderson and D. E. Williams (2014) Mammalian flavin-containing monooygenase as a source of hydrogen peroxide. Submitted to *Biochem. pharmacol*.

Siddens, L. K., M. C. Henderson, J. E. Vandyke, D. E. Williams & S. K. Krueger (2008) Characterization of mouse flavin-containing monooxygenase transcript levels in lung and liver, and activity of expressed isoforms. *Biochem Pharmacol,* 75**,** 570-9.

Smith, P. B. & C. Crespi (2002) Thiourea toxicity in mouse C3H/10T1/2 cells expressing human flavin-dependent monooxygenase 3. *Biochem Pharmacol,* 63**,** 1941-8.

Stop, T. B. P. (2006) The Global Plan to Stop TB, 2006-2015. actions for life: towards a world free of tuberculosis. *Int J Tuberc Lung Dis,* 10**,** 240-1.

Tan, M., S. Li, M. Swaroop, K. Guan, L. W. Oberley & Y. Sun (1999) Transcriptional activation of the human glutathione peroxidase promoter by p53. *J Biol Chem,* 274**,** 12061-6.

Thee, S., H. I. Seifart, B. Rosenkranz, A. C. Hesseling, K. Magdorf, P. R. Donald & H. S. Schaaf (2011) Pharmacokinetics of ethionamide in children. *Antimicrob Agents Chemother,* 55**,** 4594-600.

Tsukamura, M. & S. Yamori (1990) [In-vitro susceptibility of Mycobacterium avium complex to isoniazid and ethionamide]. *Kekkaku,* 65**,** 243-7.

Vannelli, T. A., A. Dykman & P. R. Ortiz de Montellano (2002) The antituberculosis drug ethionamide is activated by a flavoprotein monooxygenase. *J Biol Chem,* 277**,** 12824-9.

Veeramah, K. R., M. G. Thomas, M. E. Weale, D. Zeitlyn, A. Tarekegn, E. Bekele, N. R. Mendell, E. A. Shephard, N. Bradman & I. R. Phillips (2008) The potentially deleterious functional variant flavin-containing monooxygenase 2*1 is at high frequency throughout sub-Saharan Africa. *Pharmacogenet Genomics,* 18**,** 877-86.

Vilcheze, C., Y. Av-Gay, R. Attarian, Z. Liu, M. H. Hazbon, R. Colangeli, B. Chen, W. Liu, D. Alland, J. C. Sacchettini & W. R. Jacobs, Jr. (2008) Mycothiol biosynthesis is essential for ethionamide susceptibility in Mycobacterium tuberculosis. *Mol Microbiol,* 69**,** 1316-29.

Vilcheze, C., T. R. Weisbrod, B. Chen, L. Kremer, M. H. Hazbon, F. Wang, D. Alland, J. C. Sacchettini & W. R. Jacobs, Jr. (2005) Altered NADH/NAD+ ratio mediates coresistance to isoniazid and ethionamide in mycobacteria. *Antimicrob Agents Chemother,* 49**,** 708-20.

Villar, J., J. D. Edelson, M. Post, J. B. Mullen & A. S. Slutsky (1993) Induction of heat stress proteins is associated with decreased mortality in an animal model of acute lung injury. *Am Rev Respir Dis,* 147**,** 177-81.

Walker, M. K., J. R. Boberg, M. T. Walsh, V. Wolf, A.Trujillo, M. S. Duke, L. A. Felton (2012). A less stressful alternative to oral gavage for pharmacological and toxicological studies in mice. *Toxicology and Applied Pharmacology*, *260*, 65–69.

Waters, K.M., S. Safe, K.W. Gaido (2002) Differential gene expression in response to methoxychlor and estradiol through ERalpha, ERbeta, and AR in reproductive tissues of female mice. *Toxicol Sci*, 63, 47-56.

Wheeler, C. W. & T. M. Guenthner (1990) Spectroscopic quantitation of cytochrome P-450 in human lung microsomes. *J Biochem Toxicol,* 5**,** 269-72.

Wheeler, D. S. & H. R. Wong (2007) Heat shock response and acute lung injury. *Free Radic Biol Med,* 42**,** 1-14.

Whetstine, J. R., M. F. Yueh, D. G. McCarver, D. E. Williams, C. S. Park, J. H. Kang, Y. N. Cha, C. T. Dolphin, E. A. Shephard, I. R. Phillips & R. N. Hines (2000) Ethnic differences in human flavin-containing monooxygenase 2 (FMO2) polymorphisms: detection of expressed protein in African-Americans. *Toxicol Appl Pharmacol,* 168**,** 216-24.

Wong, H. R. & J. R. Wispe (1997) The stress response and the lung. *Am J Physiol,* 273**,** L1-9.

Xu, M. & M. S. Miller (2004) Determination of murine fetal Cyp1a1 and 1b1 expression by real-time fluorescence reverse transcription-polymerase chain reaction. *Toxicol Appl Pharmacol,* 201**,** 295-302.

Yueh, M. F., S. K. Krueger & D. E. Williams (1997) Pulmonary flavin-containing monooxygenase (FMO) in rhesus macaque: expression of FMO2 protein, mRNA and analysis of the cDNA. *Biochim Biophys Acta,* 1350**,** 267-71.

Zhang, J. & J. R. Cashman (2006) Quantitative analysis of FMO gene mRNA levels in human tissues. *Drug Metab Dispos,* 34**,** 19-26.

Zhang, J., M. R. Chaluvadi, R. Reddy, M. S. Motika, T. A. Richardson, J. R. Cashman & E. T. Morgan (2009) Hepatic flavin-containing monooxygenase gene regulation in different mouse inflammation models. *Drug Metab Dispos,* 37**,** 462-8.

Zhu, M., R. Namdar, J. J. Stambaugh, J. R. Starke, A. E. Bulpitt, S. E. Berning & C. A. Peloquin (2002) Population pharmacokinetics of ethionamide in patients with tuberculosis. *Tuberculosis (Edinb),* 82**,** 91-6.

Ziegler, D. M. (1993) Recent studies on the structure and function of multisubstrate flavin-containing monooxygenases. *Annu Rev Pharmacol Toxicol,* 33**,** 179-99.

Ziegler, D.M. (2002) An overview of the mechanism, substrate specificities, and structure of FMOs. *Drug Metab Rev,* 34**,** 503-11.

Zurita, E, Chagoyen, M., Cantero, M., Alonso, R., González-Neira, A., López-Jiménez, A., Montoliu, L. (2011). Genetic polymorphisms among C57BL/6 mouse inbred strains. *Transgenic Research*, *20*(3), 481–489.

APPENDICES

A1

Therapeutic Efficacy of Ethionamide against *Mycobacterium avium* Infection in Flavin Containing Monooxygenase 1/2/4 null mice

A1.1 Abstract

The prodrug ethionamide (ETA) is metabolized by bacterial flavin monooxygenase, EtaA, and mammalian flavin containing monooxygenase (FMO). FMO2 is a major isoform in lung expressed in most mammals, but humans have differing polymorphism. Active FMO 2.1, is present in up to 50% of Sub-Saharan African population, approximately 26% of African-American, and 2-7 % of Hispanic population, whereas all the Caucasians and Asians genotyped till date are homozygous for the allele *FMO2*2* encoding inactive protein FMO2.2. We hypothesized that the presence of active FMO2.1 in lung would reduce the ETA efficacy in bacterial killing. *Mycobacterium avium* infected C57BL/6 wild type and *Fmo 1/2/4* knockout mice were utilized to evaluate ETA therapeutic efficacy by using dose of 50 mg/kg of body weight compared to vehicle for 28-days. An ETA dose of 50 mg/kg did not show a significant toxic effect against mycobacterium infection compared to vehicle treated, though wildtype treated with ETA had significant higher bacterial load compared to knockouts with ETA treated. This study left the fundamental question of the role of FMO2 polymorphism on ETA therapeutic efficacy unresolved but the presence of higher bacterial load in ETA treated wildtype does suggest the FMO role in the mice vulnerability to bacterial infection in the presence of substrate ETA.

A1.2 Introduction

ETA is one of the most widely used drugs for the treatment of multidrug-resistant tuberculosis (MDR-TB). Like isoniazid, and pyrazinamide,

ETA is a prodrug that needs to be activated. ETA is sulfoxygenated by mycobacterial flavin monooxygenase, EtaA, as well as FMO1, FMO2.1, and FMO3 present in humans and other mammals (Francois et al. 2009; Henderson et al. 2004; Henderson et al. 2008; Qian and Ortiz de Montellano 2006; Vannelli et al. 2002). Both EtaA and FMO can catalyze ETA oxygenation in two steps, first to the ETA sulfoxide (ETASO), a sulfenic acid, and second to the sulfinic acid. The third product detectable, 2-ethyl-4-amidopyridine (ETAA) is thought to be a spontaneous breakdown product of the sulfinic acid (DeBarber et al. 2000; Fraaije et al. 2004; Vannelli et al. 2002). Formation of the sulfinic acid is required for bacterial killing (Baulard et al. 2000). Henderson et al. (2008), has shown that both human and mouse lung and liver microsomes effectively carried out the first oxygenation of ETA to the sulfenic acid but the second oxygenation yielding ETAA was slow. Thus mammalian FMOs may not be as effective in the second oxygenation to the sulfinic acid as bacterial EtaA. We hypothesized that the presence of active FMO2.1 in lung might affect ETA therapeutic efficacy in mycobacterium killing. All mouse and human FMOs had catalytic efficiencies for ETA much higher than reported for bacterial EtaA (Vannelli et al. 2002), so in human lung, FMO2.1 may effectively compete with EtaA, lowering the drug bioavailability to bacteria result in reduced ETA therapeutic efficacy. To date the exact ETA metabolite responsible for bacterial killing has not been characterized. ETAA is not-toxic to mycobacteria, and ETASO is seen present outside the bacterial cell wall and accumulated over time by following ETA activation directly within living mycobacterial cell by high resolution magic angle spinning-NMR (HRMAS-NMR) (Hanoulle et al. 2006), so it has been proposed that a sulfinic acid intermediate is the putative active compound. ETASO is toxic to mycobacteria and its minimum inhibitory concentration (MIC) varies according to the level of EtaA in bacterial cells (DeBarber et al. 2000). The second possible mechanism involves active FMO2.1 in lung enhancing bacterial killing

rather than decreasing ETA bioavailability. ETASO formed by FMO2.1 oxygenation might be directly available for mycobacterium to further metabolize to the sulfinic acid intermediate responsible for bacterial killing and expedite the process. The highest incidence (up to 50%) of individuals with the allele encoding *FMO2*1* is in Sub-Saharan Africa where co-incidentally higher numbers of MDR-TB cases occur so determining whether the human FMO polymorphism affects ETA efficacy is of great importance.

In this study, the efficacy of ETA in wild type mice model the human population with genotype *FMO2*1* and *Fmo1/2/4* knockout mice model Caucasians and Asians with the *FMO 2*2/2*2* genotype. Both the wild type and knockout mice were infected with *M. avium. M. avium* is the most prevalent opportunistic infection along with tuberculosis in patients with acquired immune deficiency syndrome (AIDS), but also infects immunocompetent individuals, in particular children and patients suffering from pulmonary disorders (Inderlied et al. 1993). ETA is one of the effective antibiotics against the M. avium complex (MAC) (Tsukamura and Yamori 1990), although the ETA minimum inhibitory concentration (MIC) for *M. avium* strains are in a broad range from 0.3 to >15 µg/ml in 7H12 broth, and from 2.5 to > 15 µg/ml in 7H10 agar (Heifets et al. 1991). ETA has high bactericidal activity against *M. tuberculosis* and less bactericidal activity to *M. avium* (Heifets et al. 1991).

Oral gavage dosing protocol of 28- days is commonly used to assess antibiotics therapeutic efficacy against *M. avium* infection (Bermudez et al. 2003; Bermudez et al. 1999). As gavaging can induce stress and potentially confounding experimental measurements, we used an oral dosing formulation to incorporate ETA into a pill or cookie that mice would voluntarily consume when it was placed into their cage as a less stressful drug administration

method for the treatment (Walker et al. 2012). The purpose of the present study was to evaluate the comparative bactericidal efficacy of ETA in the presence and absence of FMO, by utilizing a wild type and *Fmo1/2/4* knockout mouse model of infection.

A1.3 Materials and Method

Cookie formulation

A bacon flavored transgenic dough (Bio-Serve, Frenchtown, NJ) was used to formulate cookies containing ETA. The cookies containing the ETA drug were made after mixing the cookie dough and ETA with the help of a mortar and pestle until the yellow color of the drug ETA became visually uniform (Fig. A 1.1 a). The die cavities of a pill mold base plate were then filled with dough containing ETA and small dough cookies of about 60 mg each were obtained (Fig. A 1.1 b). The pills were left to dry for about 1 hour before being transferred to a glass container and stored at 4°C.

Cookie versus gavage dosing of ETA

To compare the efficiency of ETA dosing by cookie versus gavage, plasma ETA levels, 1 hour post-gavage or cookie feeding was measured in wild type and knockout mice. The 50 mg /kg dose of ETA was with approximate 60 mg of beacon flavored cookie dough (Bio-Serve, Frenchtown, NJ) were given to wild type and knockout mice. Both wild type and knockout mice finished eating the cookie within one minute. Mice for gavage method of ETA administration received 50 mg/kg of ETA dose in vet syrup suspension (FlavoRx, Washington, D.C). Blood samples were collected after 1 hour from

the posterior vena-cava. ETA concentrations were measured in plasma by the extraction method described earlier in chapter 2 (Palmer et al. 2012).

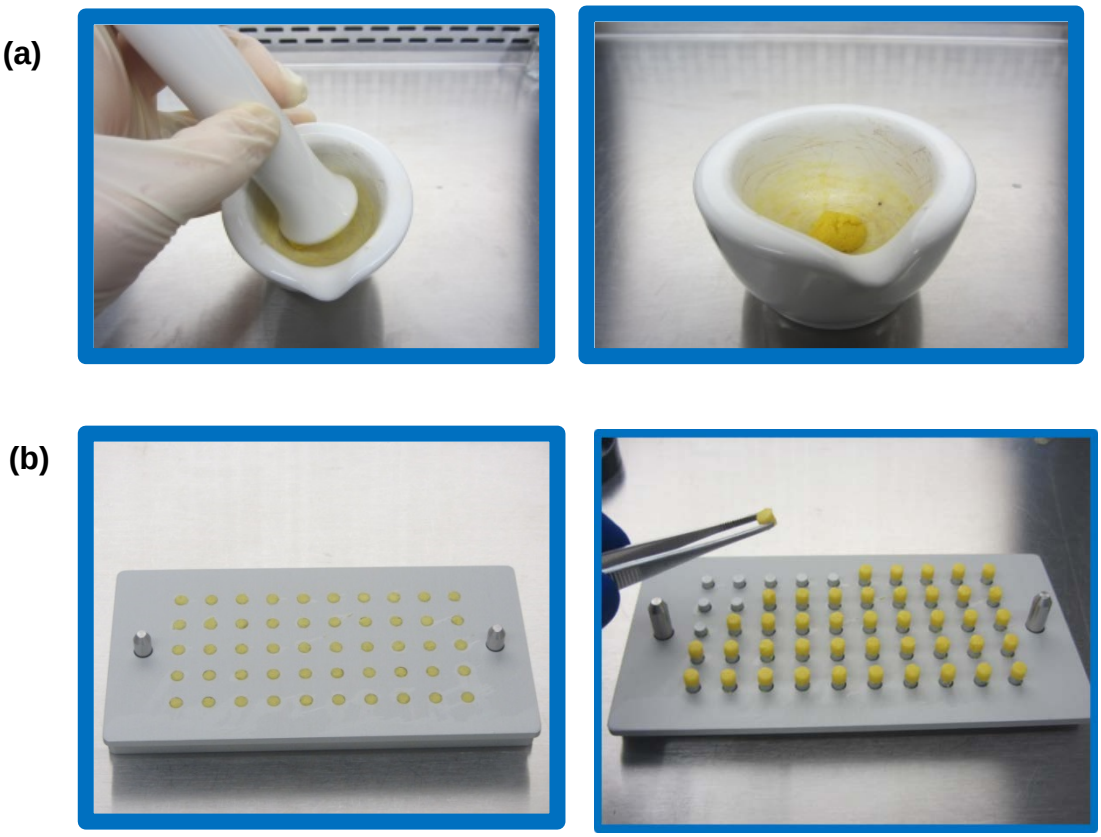

Figure A1.1 Cookie preparation
(a) ETA is added to the transgenic dough diet and mixed by pestle and mortar until the ETA yellow color appears uniform. (b) The die cavities of the pill mold are filled with the dough and cookies ejected out of the die by placing the mold base plate on top of the mold punch pins.

Mycobacterium

MAC 101 (serotype 1), originally isolated from the blood of an AIDS patient, was used for the study (Bermudez et al. 2003; Bermudez et al. 1999). *M. avium* organisms were cultured on Middlebrook 7H10 agar (Difco, Detroit, MI) supplemented with oleic acid, albumin, dextrose, and catalase (OADC) for 10 days at 37°C. For infection of mice, transparent colony morphotypes were harvested and resuspended in Hank's buffered salt solution (HBSS) and adjusted to a concentration of $2X10^7$ CFU/ml.

Mice and experimental design

Experiments were carried out with 12-week old C57BL/6 wild type mice (Jackson Laboratories, Sacramento, CA) and *Fmo1/2/4* knockout male mice originated from Elizabeth Shephard and Ian Phillips (University College, London, UK) (Hernandez et el., 2006). Briefly, mice were infected with approximately 2 X 10^7 CFU of *M. avium* in HBSS solution by intranasal administration. After 7 days, ETA treatment (50mg/kg in 60 mg of bacon flavored cookie) was initiated and continued for next 28- days, 6 day / week. A control group of mice was infected but received only cookie without ETA. An additional group of mice were euthanized at day 7 after infection to establish the initial level of infection before the initiation of therapy.

CFU analysis lung and spleen

At the termination of treatment, the lung and spleen tissue of control and treated mice were aseptically removed, the organs were weighed and homogenized in 500 µl of sterile HBSS in a Bullet Blender (Next-advance, Averill Park, NY) set for 5 min. Serial 10-fold dilutions were plated onto 7H10 agar (Difco, Detroit, MI) with OADC enrichment. After 14 days at 37^0C,

colonies were counted and the number of CFU per gram of tissue was calculated.

Histopathology

Lung and liver were collected upon necropsy and fixed in 10% formalin. Fixed tissues were processed to paraffin blocks, and hematoxylin and eosin-(H&E) stained sections were analyzed for granulomas. For liver tissue, granuloma data is reported as average number of granulomas in five different microscopic fields, while for lung tissue, data is reported as average percentage area covered with granulomas in six different microscopic fields.

Susceptibility assay

Bacteria from ETA treated wild type and knockout mice lung were tested for ETA resistance. Laboratory maintained *M. avium* MAC 101 was tested as a non-tissue control. To set-up the base level of ETA resistance, MIC was performed by a broth macrodilution method with laboratory maintained *M. avium* MAC 101. In brief, bacteria from tissues were resuspended in HBSS until visually turbid (approximate 10^8 CFU/ml). All tubes were equilibrated using visually turbidity. Bacteria were diluted 1:1000 into 7H9 broth (approximate 10^5 CFU/ml) and ETA concentration of 128 µg /ml to 4µg/ml was added in bacterial tube by 1:1 serial dilution. Tubes were incubated at 37^0C in a shaking incubator at 200 rpm for six days, and then scored. CFU of original equilibrated inoculum tubes was confirmed with diluting and plating.

Statistical analysis

The ETA dosing efficacy comparison of gavage versus cookie in wild type and knockout mice was done by a two way of analysis of variance (ANOVA). CFU counts followed an exponential distribution so a likelihood ratio (LR) test was applied for the statistical significance of the differences between the number of viable organisms recovered from the lung and spleen. The bacterial load comparison between wildtype ETA treated and knockout ETA treated were examined via a Student's t-test analysis assuming equal variances. Differences between experimental groups were considered significant at p values of ≤0.05.

1.4 Results

ETA plasma level, cookie versus gavage dosing

Both wild type and knockout mice metabolized ETA, administered by gavage or cookie. The average ETA plasma level was higher in knockout than wildtype mice (Fig. A1.2) as previously reported in chapter 2. Two-way ANOVA analysis showed a significant genotypic difference (p=0.01) of ETA in plasma level from wild type versus knockout mice, though there was no significant difference observed due to mode of ETA administration (p=0.42) (Fig. A1.2). The average ETA concentration achieved 1 hour post-gavage in wild type and knockout mice with cookie dosing was 4.9 ±1.77µg /ml and 7.95 ±1.65 µg /ml, respectively.

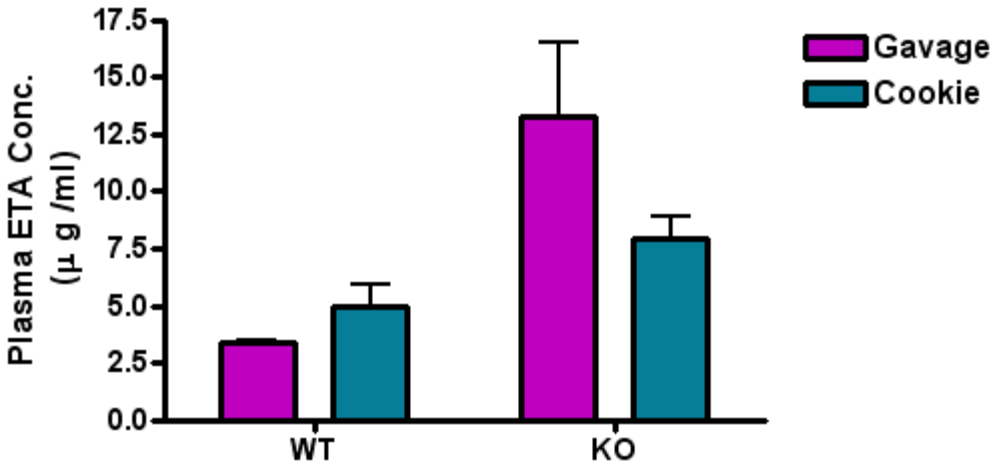

Figure A1.2 Plasma ETA levels of following dosing by gavage or cookie in wild type and knockout mice.
Graphs show mean± SEM (n= 3 to 6). Plasma ETA concentrations were measured 1 hour post-gavage or post-cookie consumption.

CFU analysis lung and spleen

A sixty mg bacon-flavored cookie with ETA (50 mg/kg body weight) was given six days per week for four-weeks to wild type and knockout mice infected with *M. avium.* Treatment with ETA reduced the mycobacterial cell count in knockout mice lung and spleen compare to vehicle treated but it did not reach statistical significance (lung, p=0.1 and spleen, p=0.16) (Fig.A1.3a & b). The number of bacterial cells was higher in wild type mice with ETA treatment compared to controls treated in both lung and spleen, though it was not statistically significant (lung, p=0.18, spleen, p=0.28) (Fig. A1.3a & b). A significant genotypic difference (wild type versus knockout) was observed in the number of viable bacterial cells recovered in lung (p=.0.001) and spleen (p=0.04) (Fig.A1.3a & b) regardless of any treatment. Bacterial load in wildtype treated with ETA was significantly higher compared to knockout in both lung (p=0.0001) and spleen (p=0.01) (Fig.A1.3a & b).

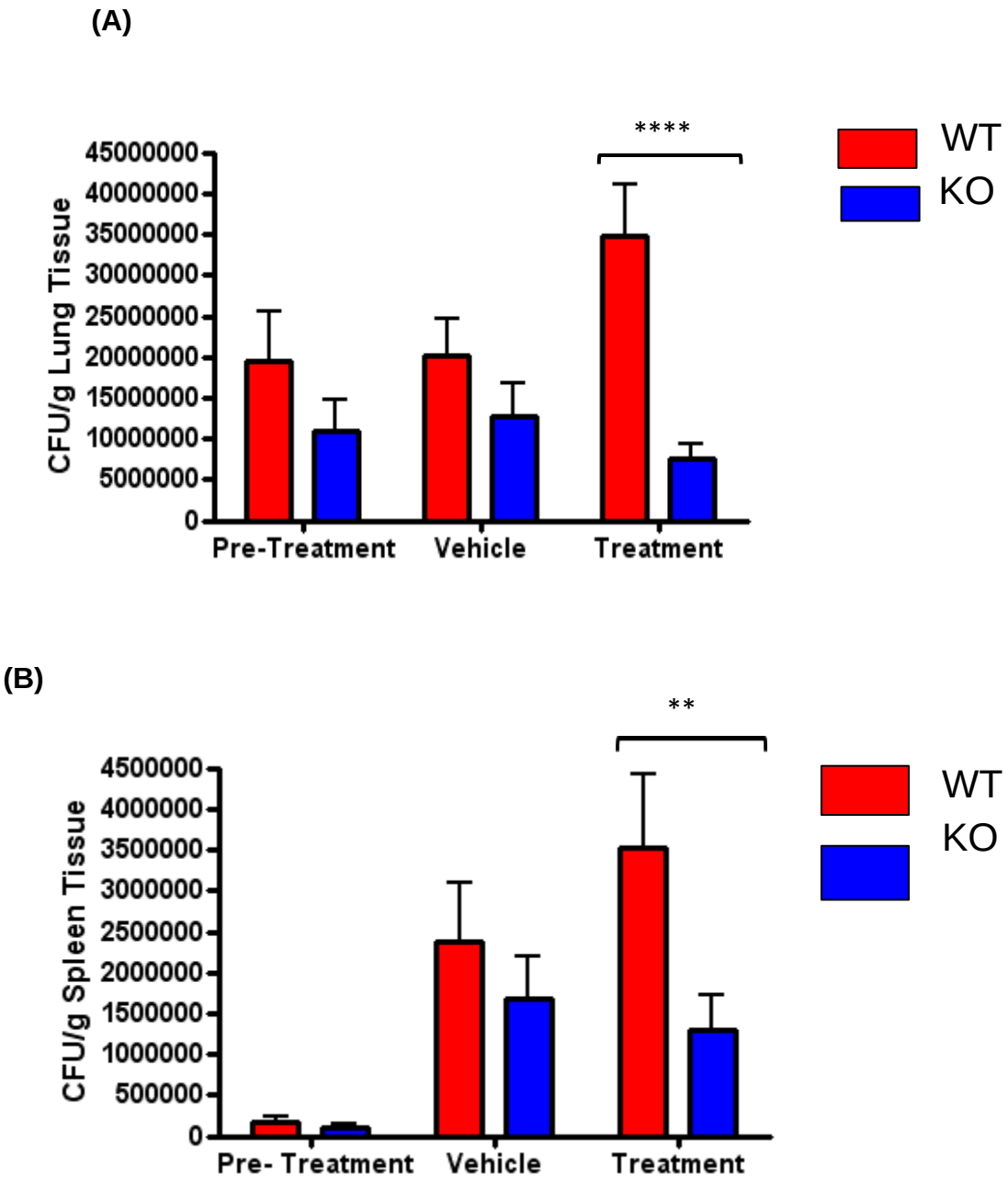

Figure A1.3 Activity of ETA against *M. avium* in wild type and knockout mice (A) Lung, (B) Spleen.

Graphs show mean ± SEM (n= 5-15). Pre-treatment mice were euthanized after seven days after infection (before treatment initiation) to establish the base level of infection. ETA treated wildtype shows a by significant higher bacterial load denoted by **** $p<0.0001$ and ** $p<0.01$ versus ETA treated knockout

Susceptibility assay

A MIC of 90% was determined for *M. avium* MAC (101) maintained in the lab. An ETA concentration at 1-2 µg/ml showed some inhibition, while 8µg/ml resulted in full inhibition. ETA susceptibility assay was performed with bacteria recovered from ETA-treated wild type and knockout mice to compare drug resistance. The results showed similar ETA resistance profiles for bacteria recovered from wild type and knockout mice (Table A1.1). In general wild type mice had a little higher resistance compared to knockouts but this was not significant.

Granulomas analysis

Granulomas which are, a hallmark of host defense against mycobacterial infection, were analyzed in lung and liver sections stained by H&E. Both vehicle and ETA treated *M. avium* infected wild type and knockout mice showed granuloma formation in both lung and liver. There was not much difference in the number of granulomas present in ETA treated wild type and knockout mice compared to control (Fig.A1.4a and A1.5a). Granulomas structures and sizes were similar in wild type and knockout mice. The genotypic difference in the amount of lung granulomas between wild type and knockout mice was not quite significant (p= 0.053) (Fig.A1.4a).

Table A1.1 ETA susceptibility profile for *M. avium* from ETA- treated wild type and knockout mouse lung samples

	Tube ID (µg/ml) ETA						
	1(128)	2(64)	3(32)	4(16)	5(8)	6(4)	7(0)
Wild type	-	-	-	+	++	++++	++++
Wild type	-	-	-	+	++	++++	++++
Wild type	-	-	-	++	+++	++++	++++
Knockout	-	-	-	++	+++	++++	++++
Knockout	-	-	-	++	+++	++++	++++
Knockout	-	-	-	++	+++	++++	++++
MAH(101)	-	-	-	+	++	++++	++++
MAH(101)	-	-	-	+	++	++++	++++

Turbidity Key:

- None; full inhibition
+ Small particles, but clear;
++ More particles, but clear; intermediate inhibition
+++ Partially turbid; intermediate inhibition
++++ Full turbid; no inhibition

Two lab- grown MAH (101) samples were included in the assay as non-tissue controls. ETA concentrations from 128 µg /ml to 4 µg /ml were observed.

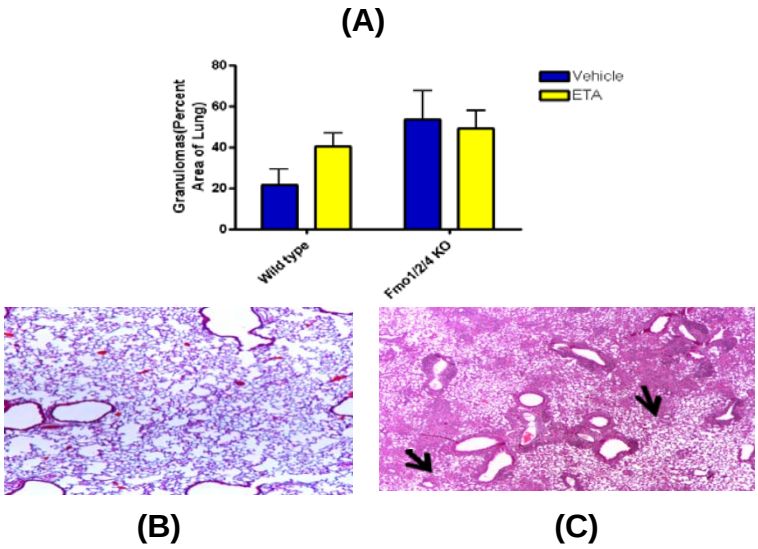

Figure A1.4 Granulomas in lung of wild type and knockout mice.
Graphs show mean percent area ± SEM (n= 4) (A). Un-infected lung section (B) and *M. avium* infected lung section of granulomas (C). Arrows are pointing to granulomas

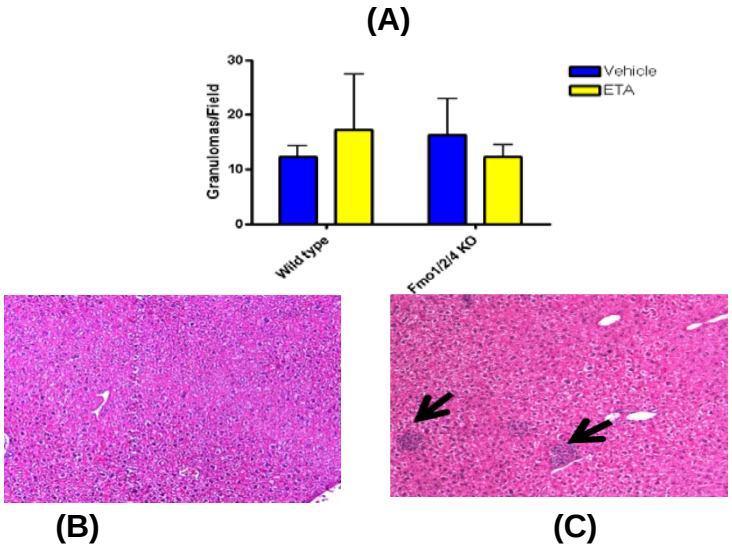

Figure A1.5 Number of granulomas present in liver sections of wild type and knockout mice.
Graphs show mean ± SEM (n= 4) (A). Un-infected liver section (B) and *M. avium* infected liver section showing granulomas (C). Arrows are pointing to granulomas

1.4 Discussion

Wild type mice to model the human population with the *FMO2*1* allele and *Fmo1/2/4* knockout mice modeling Caucasians and Asians with the FMO2*2/ 2*2 genotype were utilized to compare the therapeutic efficacy of ETA. We hypothesized that active FMO2.1 would reduce the ETA therapeutic efficacy. Both wild type and knockout mice infected with *M. avium* were treated with ETA (50 mg/kg) for 28-days and then lung and spleen samples were analyzed for bacterial load and granuloma formation. Fifty mg/kg of ETA dose has been shown to be an effective treatment in mice infected with *M. tuberculosis* (Cynamon and Sklaney 2003) , though no studies were located with mice infected with *M. avium* at this dose. The ETA plasma level comparisons suggested that ETA administration by cookie was as efficient as gavage. The *in vivo* mycobacterium infection model drug administration by the non-stressful oral cookie dosing might be a better option than 28-days of stressful gavage.

ETA bactericidal effect was defined as the bacterial load at the end of the experiment being smaller in ETA treated mice than the bacterial load in vehicle treated mice. Neither wildtype nor Knockout mice showed any significant difference in the bacterial load following ETA treatment in either lung or spleen. The presence or absence of FMOs also does not seem to affect granuloma formation or structure in wild type and knockout mice. No significant treatment effect was seen in number of granulomas in wild type and knockout mice compared to control. Average plasma ETA level one hour post consumption in wildtype mice did not reach to MIC for *M. avium* MAC 101 strain with 50 mg/kg of ETA dose with cookie whereas in knockout mice average plasma ETA level was almost equal to MIC concentration. Heifets, (1988) have reported that bactericidal activity of ETA towards *M. avium* is very

poor, by broth determined MIC method, approximate 32% of *M. avium* strains were classified under very resistant category whereas approximate 20% strain came under moderate resistant category for ETA from a total 31 *M. avium* strains tested. Besides correlation between MIC and concentration attainable *in vivo*, the clinical outcome of antibiotics treatments may also depend on other properties like bactericidal potency, post antibiotic effect or any other additional pharmacokinetics parameters. Our CFU results suggest that the *M. avium* 101 strain used in the study was not susceptible to the ETA treatment.

Bacterial load in lung and spleen of knockouts treated with ETA was significantly less than in the wild types treated with ETA. This data suggest that wildtype treated with ETA were more susceptible to mycobacterium infection compared to knockout treated with ETA. Since the 50 mg/kg dose was not effective for the *M. avium* infection treatment, we cannot directly compare ETA therapeutic efficacy in wildtype and knockouts, but the significantly higher number of bacterial cells present in wildtype ETA treated mice compared to knockout ETA treated suggest a link to FMOs role susceptibility to bacterial infection in the presence of substrate ETA. Presence of FMO might be competing with mycobacterium enzyme EtaA in ETA metabolism, reducing bioavailability of the drug and resulting in a higher bacterial load in wildtype compared to knockout. To check that the observed higher load of bacteria in ETA treated wildtype was not due to a developed resistance, an ETA susceptibility test was performed using bacteria recovered from treated wild type and bacteria recovered from ETA treated knockout. Wild type mice showed a small difference in resistance but not significant enough to prove acquired resistance.

Cohen et al, (1995) have demonstrated that C57BL/6 mice are relevant to *M. avium* infection and evaluation of antibiotic activity. The bacterial load

had not changed much after 28-days in lung tissue of both vehicle, wild type and knockout mice compared to the pre-treatment group which was euthanized after 7 days of infection to set up the base level of infection, this suggest the control mechanism of the host in the chronic phase of infection (Saunders et al. 1999), which confirms that wildtype and knockout mice used in the study were suitable for bacterial infection analysis. Both knockout and wildtype mice used in the study are C57BL/6 background though from different sources, knockout mice were generated in London whereas wildtype mice were from the Jackson laboratory, USA. There was significant genotypic difference in the number of bacteria in wild type mice compared to knockouts regardless of any treatment. Genotypic effect was also observed in the lung section area covered with granulomas between wild type and knockout mice. The area covered with granulomas was higher in knockout mice than wild type mice suggesting more protection from chronic infection in knockout mice since granuloma formation is required to control chronic infection, by surrounding and walling off sites of infection to prevent bacterial dissemination and maintain a state of chronic infection (Saunders et al. 1999). Observed genotypic differences between strains might be due to different provider's sources and separated breeding stocks for a long time, which might have allowed some genetic differences to accumulate over time (Zurita et.al.2010) or may be due entirely to FMO differences. These results suggest that growing wildtype and knockout mice of the same background together in the same conditions and appropriate handling are important to avoid any kind of confounding results due to accumulated genetic differences over time.

In conclusion, 50 mg/kg of ETA was not clinically effective against *M. avium* and that is why this study could not answer ETA therapeutic efficacy in the presence and absence of FMOs in this mouse model. The significantly higher bacterial load present in ETA treated wildtype compared to ETA treated

knockout mice is very interesting and suggests that presence of FMO in wildtype mice is making these mice more susceptible to bacterial infection when ETA is dosed at suboptimal levels. Another study with a higher dose of ETA and susceptible *M. avium* strain is needed to answer ETA therapeutic efficacy in the presence and absence of FMO in the present mouse.

A2

Real-time cytotoxicity analysis of the anti-tuberculosis drug Ethionamide (ETA) on a human bronchial epithelial cell-line (BEAS-2B), stably expressing human flavin-containing monooxygenase 2

A2.1 Abstract

Stably transfected human bronchial epithelial (BEAS-2B) cells which express human flavin containing monooxygenase 2.1 (hFMO2.1) were used to analyze if the anti-tuberculosis prodrug ethionamide (ETA) is toxic to cells. Cells transfected with inactive hFMO2.2 were used as a control. Fluorescence- activated cell sorter (FACS) analysis was used to select cells expressing FMO2 isoforms. The first oxygenation of ETA via FMO produces ethionamide sulfoxide (ETASO), a sulfinic acid which can redox cycling with glutathione (GSH) and cause oxidative stress. The real-time cell analyzer (RTCA) xCELLigence platform was used to monitor ETA induced cell-viability and toxicity in BEAS-2B cells expressing FMO2 isoforms. Real-time analysis did show ETA toxicity at 500 and 1000 μM of ETA concentration but it was independent of FMO2.1 expression.

A2.2 Introduction

Tuberculosis (TB) continues to be the most common infectious disease in the world with approximately one-third of the world population infected with *Mycobacterium tuberculosis*. Approximately 2% of new TB cases in the world are attributed to multidrug-resistant strains which are resistance to frontline therapeutics, results in treatment of patients with “second-line” drugs. Among these second- line drugs for the treatment of multidrug-resistance tuberculosis (MDR-TB), one of the most effective is ethionamide (ETA). ETA and other similar second-line drugs such as thiacetazone (TAZ), and thiourea (TU), are prodrugs and get metabolized by the bacterial flavin monooxygenase (EtaA)

(Qian and Ortiz de Montellano 2006; Vannelli et al. 2002). EtaA catalyzes S-oxygenation of these drugs to metabolites toxic to the bacteria. ETA is also a substrate for human flavin-containing monooxygenase 2 (FMO2). However, most human do not express active FMO2.1 in lung (Yueh et al. 1997) and produce only inactive FMO2.2. The highest incidence of individuals with active FMO2.1 and the highest incidences of TB co-occur in Sub-Saharan Africa (Veeramah et al. 2008) where resistance to front-line TB drugs is of great concern. It has been shown that FMO2.1 is more efficient in the first S-oxygenation of ETA to sulfenic acid than EtaA (Henderson et al. 2008). The sulfenic acid is capable of redox-cycling with glutathione (Henderson et al. 2004) producing oxidative stress and toxicity. We hypothesize that; individuals expressing active FMO2.1 will have enhanced oxidative stress, pulmonary toxicity and cell death with ETA treatment.

We selected human BEAS-2B cell utilized in many studies examining oxidative stress and toxicity (Heng et al. 2010; Nichols et al. 2003; Park et al. 2008). The xCELLigence System of real-time cell analyzers (RTCA) was used to study the effect of ETA metabolism on cell viability and toxicity. RTCA allows for label-free and dynamic monitoring of cellular phenotypic changes continuously by measuring electrical impedance.

A2.3 Materials and methods

BEAS-2B cell culture and stable transfection

A BEAS-2B cell line, derived from human bronchial epithelial cells, was purchased from the American Type Culture Collection (ATCC) (Manassas, VA). BEAS-2B cells were maintained in bronchial epithelial cell growth medium (BEGM) (Lonza, Allendale, NJ) containing penicillin-streptomycin at

100 unit /ml (Corning-Cellgro, Manassas, VA.). Cells were grown and maintained in 25 cm^2 cell culture flasks at 37^0C in a 5% CO_2 humidified incubator. Culture flask were coated with fibronectin (0.01 mg/ml) (Sigma-Aldrich, St. Louis, MO), collagen (0.03 mg/ml) (Sigma-Aldrich, St. Louis, MO) and bovine serum albumin (BSA) (0.01 mg/ml) (Sigma-Aldrich, St. Louis, MO) mixed in basal media without growth factor. One set of cells were transfected with pIRES vector having $AcGFP_1$-CpG-hFMO2.1 (Fig. A 2.1) and another set of cells (controls) were transfected with pIRES vector with $AcGFP_1$-CpG-hFMO2.2 with the help of lipofectamine^{TM} 2000 transfection reagent (Invitrogen, Hercules, CA). Transfection was confirmed by western blot and flow cytometric analysis (BD Bioscience, San Jose, California) for GFP fluorescence. Transfected cells were maintained with the antibiotic gentamycin (G-418) (Sigma-Aldrich, St. Louis, MO) selection for stable incorporation of FMO2.1 and FMO2.2 up to 5 passages.

Fluorescence activated cell sorter (FACS) analysis

FACS analysis was done to select GFP positive cells with high amount of fluorescence on MoFlow^{TM} Astrios, flow cytometer cell sorter (Beckman Coulter, Brea CA). FACS analysis was done to effectively remove non-fluorescing cells from the transfected cell-line. Sorted cells were regrown and re-checked by flow cytometer to confirm the maintained level of fluorescence after 2-3 passages. Cells were always maintained on gentamycin selection.

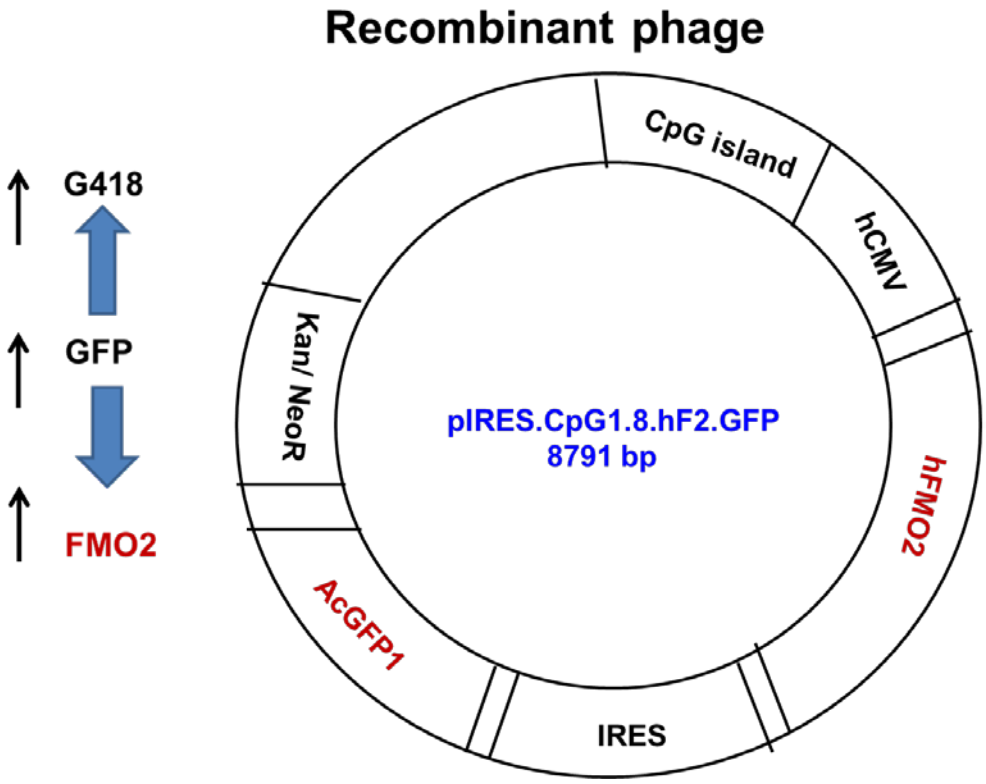

Figure A2.1 pIRES vector having $AcGFP_1$-CpG-hFMO2
Vector was designed in a way to translate GFP and FMO2 as unfused protein, higher GFP production implies higher FMO2 synthesis.

Real-time xCELLigence impedance analysis

BEAS-2B cell attachment, spreading and proliferation were optimized in E-plate 16 (ACEA Biosc., San Diego, CA) by continuously monitoring using the xCELLigence System, RTCA DP Analyzer (ACEA Biosc., San Diego, CA). Seeding number of BEAS-2B cells was also optimized for the best growth curve by xCELLigence System. Five thousand cells were seeded in each well of the E-Plate 16 coated with fibronectin, collage and BSA in BEBM media as mentioned before and maintained in BEGM media (Lonza, Allendale, NJ).

Approximately 24 hours later, ETA at concentrations of 100, 500 and 1000 µM were added to the wells containing the cells. Vehicle, 0.1% of ethanol, was also included in the treatment. Cell-electrode impedance was monitored using the RTCA DP Analyzer every 15–30 minutes to produce time-dependent cell response dynamic curves up to 70 hours. The electronic readout of cell-sensor detected impedance is displayed as arbitrary units called Cell Index (CI) values. The CI value at each time point is defined as (Rt-Rb)/15 where Rt is defined as the cell-electrode impedance of the well with the cells at different time points, and Rb is defined as the background impedance of the well with the media alone. The normalized Cell Index is calculated by dividing the Cell Index value at particular time point by the Cell Index value at the time of interest.

A 2.4 Result

Stable cell transfection and FACS analysis

Both FMO2.1 and 2.2 transfected BEAS-2B cells maintained on gentamycin for selection showed GFP fluorescence in FACS analysis after 4-5 generation (Fig. A 2.2 A & C) confirming the successful transfection. The best highest 5% GFP fluorescing cells, co-expressing FMO2.1 and 2.2, were successfully sorted by FACS analysis (Fig. A 2.2 B & D). Since GFP and FMO2 were cloned as a fused protein, higher levels of GFP fluorescence suggested higher levels of FMO2 expression. Re-grown sorted cells, re-analyzed by FACS analysis after 2-3 passages showed little reduced level of GFP fluorescence than before but whole cell population was maintaining GFP fluorescence suggesting all the cells expressing FMO2.1 and 2.2 (data not shown). After selection both the cell lines had similar fluorescence levels (Fig. A 2.2 B & D).

Cytotoxicity analysis by Real-time xCELLigence

The kinetic profiles for ETA with different concentration for cells expressing FMO2.1 and 2.2 are shown in Figure A 2.3. The cell index number for cells treated with 100 µM of ETA and vehicle were almost same in FMO2.1 or 2.2 expressing cells. The cell index number of cells treated with 500 µM and 1000 µM of ETA has reduced in compare to vehicle treated FMO2.1 and 2.2 expressing cells (Fig. A 2.3). ETA treatment with 500 µM concentration was found to induce lesser decrease in cell index value in compare to cells treated with 1000 µM.

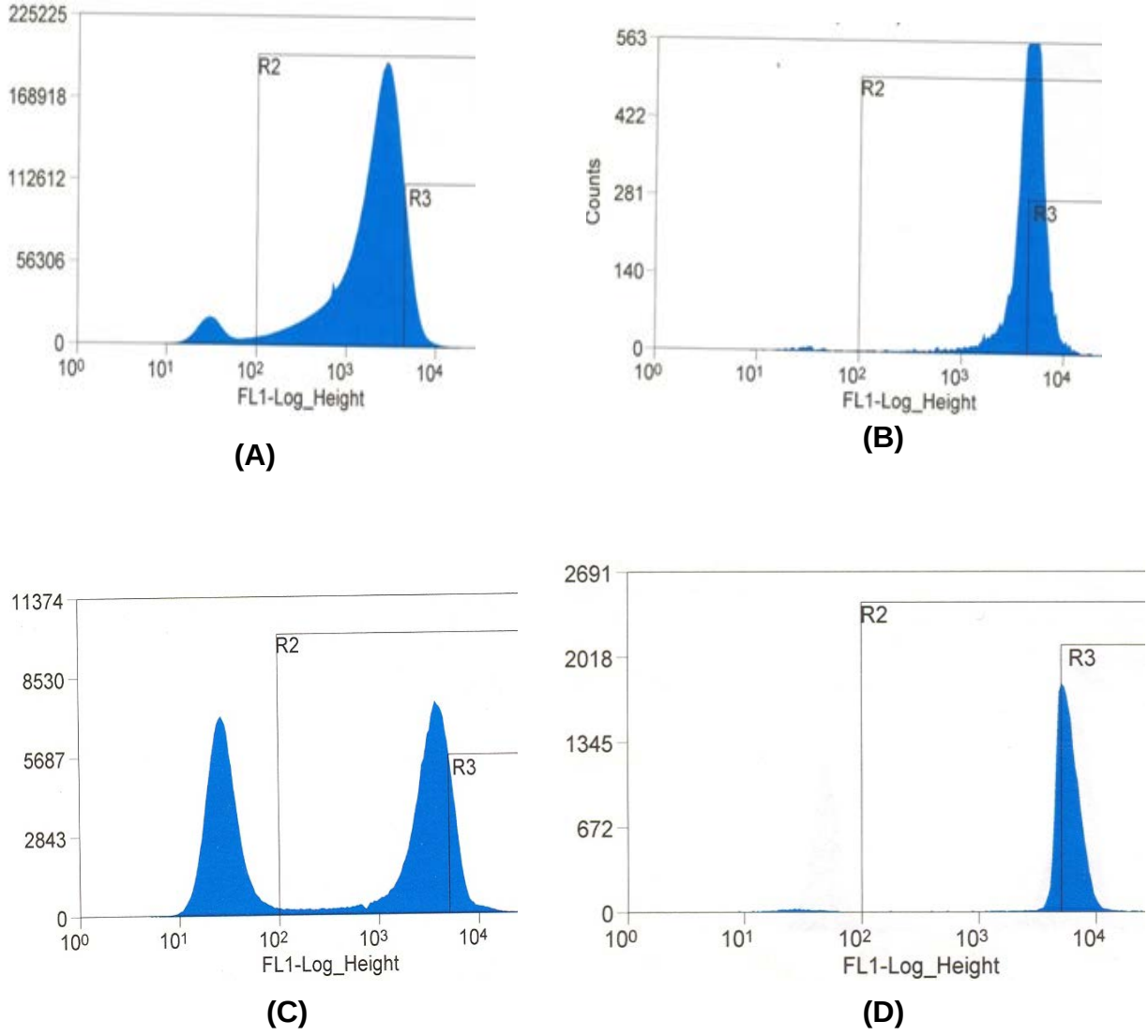

Figure A2.2. Pre- and post-sort BEAS-2B cells selected for GFP levels. FMO and GFP are co-expressed. (A) hFMO2.1-GFP, pre-sort, (B) hFMO2.1-GFP post-sort, (C) hFMO2.2-GFP, pre-sort, (D) hFMO2.2-GFP, post-sort

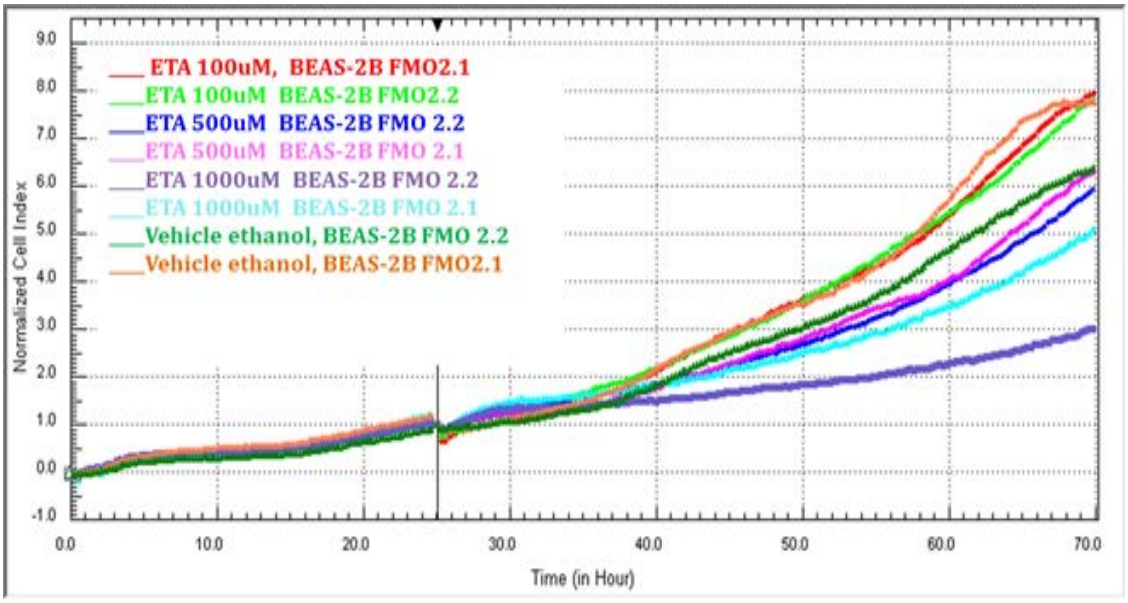

Figure A2.3 Real-time proliferation of FMO-transfected BEAS-2B cells. Different color codes shows different ETA concentration and cell types.

A2.5 Discussion

FMO2 has been firmly established as an efficient catalyst of ETA S-oxygenation (Francois et al. 2009; Henderson et al. 2008), but the role of this bioactivation process in a human bronchial epithelial cell line overexpressing FMO2.1 and 2.2 has not been established prior. We hypothesized that BEAS-2B cells expressing FMO2.1 would show oxidative stress and toxicity with ETA treatment compared to cells expressing inactive FMO2.2. Cytotoxicity associated with ETA metabolism was determined by the xCELLigence RTCA platform which allows cell viability to be measured continuously and in real-time. The Cell index number of cells treated with 100 µM of ETA and vehicle were almost the same suggesting no toxicity associated with ETA at this concentration in either of the cells expressing FMO2.1 or 2.2. The cell index number of cells treated with 500 µM and 1000 µM of ETA has reduced in

compare to vehicle treated FMO2.1 and 2.2 expressing cells. Kinetic profiles provided by the xCELLigence System indicated that the rate and dynamics of cytotoxicity varied with 500 and 1000 µM of ETA concentration treatment. ETA treatment with 500 µm concentration was found to induce a lesser decrease in cell index value after ETA treatment, while 1000 µM has shown higher decrease in cell index compared to vehicle treated cells. This data suggest cells killing kinetics to be ETA concentration-dependent such that higher concentration induced cytotoxicity much faster compared to lower concentration, as indicated by the rate of decline in cell index value (Fig. A 2.3).

We have hypothesized that ETA mediated cytotoxicity in cells would depend on expressing hFMO2.1 and not hFMO2.2, but interestingly, xCELLigence kinetic profile did not follow that. It showed ETA toxicity at 500 and 1000 µM concentration in cells expressing FMO2.1 as well as FMO2.2 suggesting that cytotoxicity at these concentrations was independent of FMO levels present in the cells. It also suggests that in general ETA concentration of 500 and 1000 µm is toxic for BEAS-2B cells. Another set of cells in T-25 flask growing together of xCELLigence analysis were checked for GFP fluorescence on flow cytometer and this time it showed much reduced level of GFP fluorescence. So, we thought that the reason of FMO independent toxicity in both the cells type could be that FMO2.1 was not being produced at levels that would have functional consequence. We have hypothesized that ETA major metabolite ETASO a sulfenic acid can deplete glutathione level and result in oxidative stress. BEAS-2B cells have very high level of glutathione, may be sulfenic acid produced was not enough to deplete sufficient amount of GSH to show any metabolism dependent toxicity. Nicholes et.al. (2002) has shown that 3-methylindole (3MI) increased the cell death of BEAS-2B cells expressing cytochrome p450 when glutathione level was depleted with

diethylmaleate. In present BEAS-2B transfected cell model, FMO expression was not maintained due to unknown reason.

In conclusion ETA cytoxicity shown in FMO2.1 and 2.2 expressing cells via real-time xCELLigence analysis was independent of FMO expression level. We think primary alveolar type 1 cells naturally expressing FMO2 from C57BL/6 wild type mice and primary alveolar type 1 cells from *Fmo1/2/4* knockout mice (Hernandez et al. 2006) which do not express *Fmo2* might be a better model to study FMO metabolism mediated ETA cytotoxicity in host cells.

A3 Supplemental materials

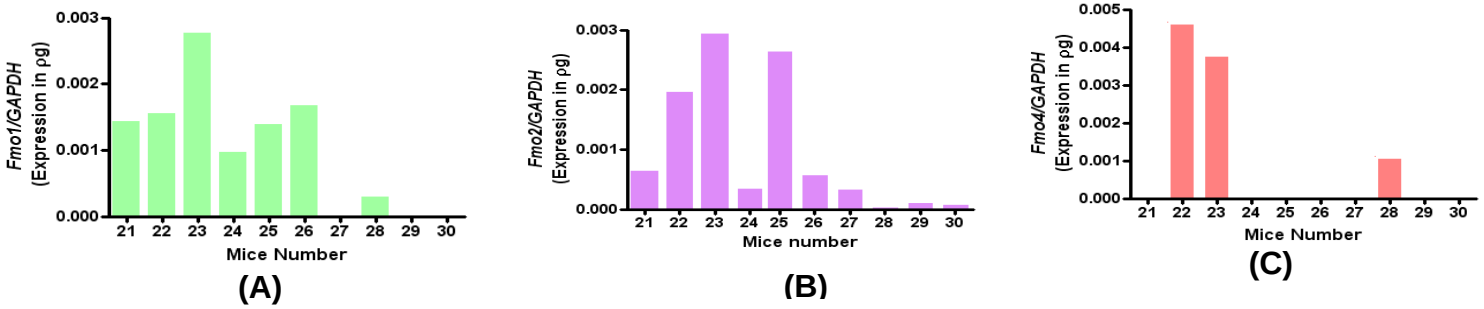

Figure A 3.1 *Fmo1* (A), *Fmo2* (B) and *Fmo4* (C) mRNA expression in lung of knockout male mice.
Mice have received ETA or vehicle for 28-days. Mice number from 21 to 25 are vehicle treated while from 26 to 30 are ETA treated**.** Mice which are not showing any expression either they did not give Ct value or Ct values were more than cut off 35, so included as no expression.

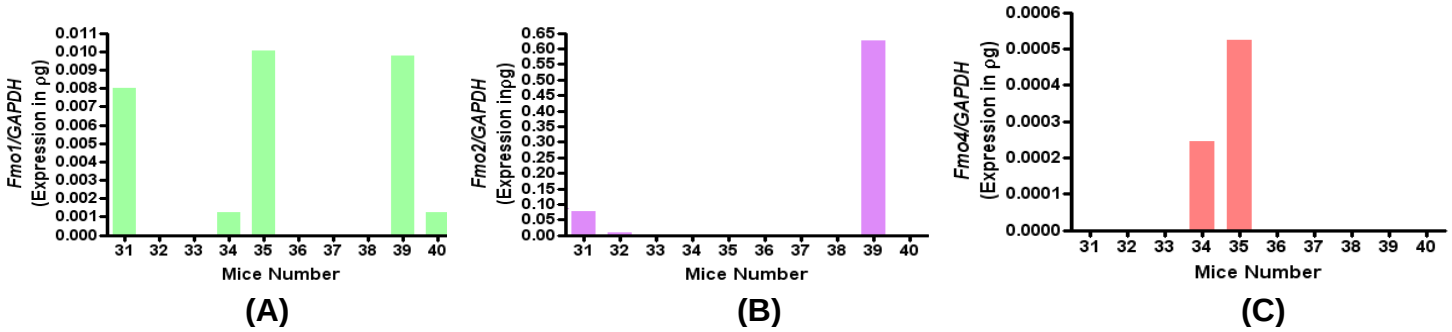

Figure A 3.2 *Fmo1* (A), *Fmo2* (B) and *Fmo4* (C) mRNA expression in knockout female mice lung.
Mice have received ETA or vehicle for 28-days. Mice number from 31 to 35 are vehicle treated while from 36 to 40 are ETA treated**.** Mice which are not showing any expression either they did not give Ct value or Ct values were more than cut off 35, so included as no expression.

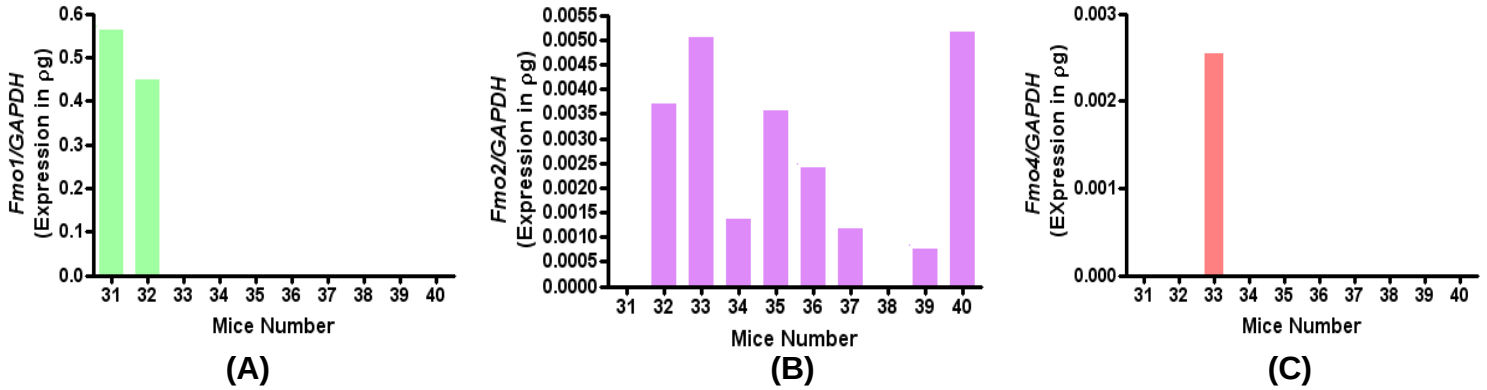

Figure A3.3 *Fmo1* (A), *Fmo2* (B) and *Fmo4* (C) mRNA expression in knockout female mice liver.
Mice have received ETA or vehicle for 28-days. Mice number from 31 to 35 are vehicle treated while from 36 to 40 are ETA treated**.** Mice which are not showing any expression either they did not give Ct value or Ct values were more than cut off 35, so included as no expression.

Mice genotyping

Tested genes included *Fmo1*, *Fmo2*, *Fmo3* and *Fmo4*, using primers and PCR conditions described in Hernandez et al. (2009). Both lung and liver tissue of wildtype and knockout mice preserved in RNA later at -80^{0}C were used in genotyping.

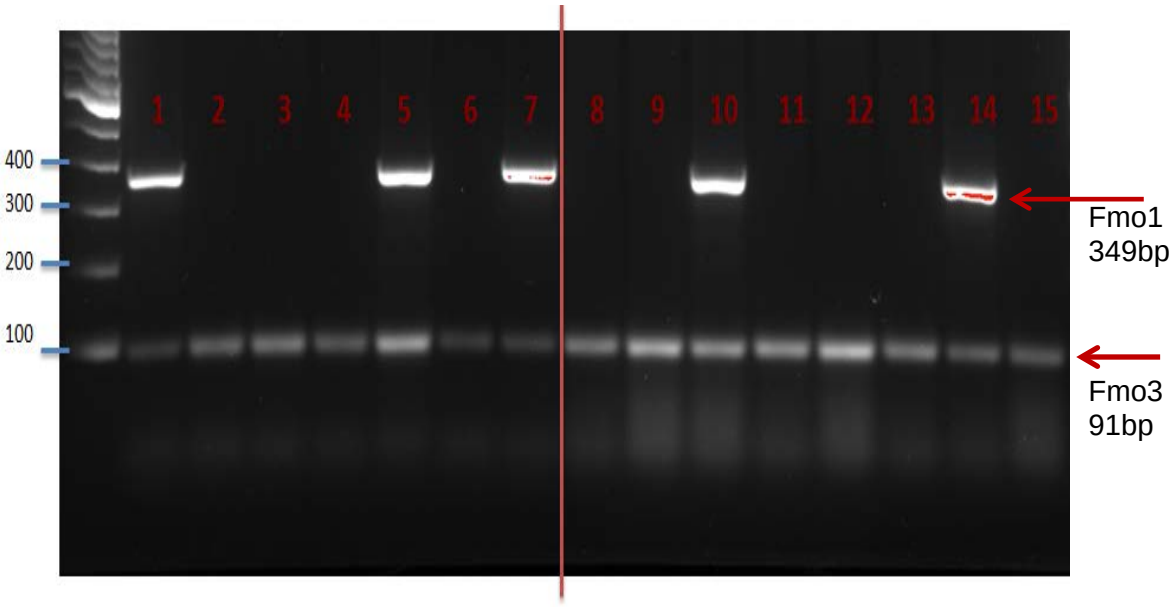

Figure A3.4 Mouse genotyping with *Fmo1* and *Fmo3* genes.
DNA was isolated from mouse lung and liver and amplified by PCR using primers specific for the mouse *Fmo1* and *Fmo3.* WT, KO, M and F represent wild type, knockout, male and female, respectively. Number mentioned after male (M) or female (F) are actual mice number.

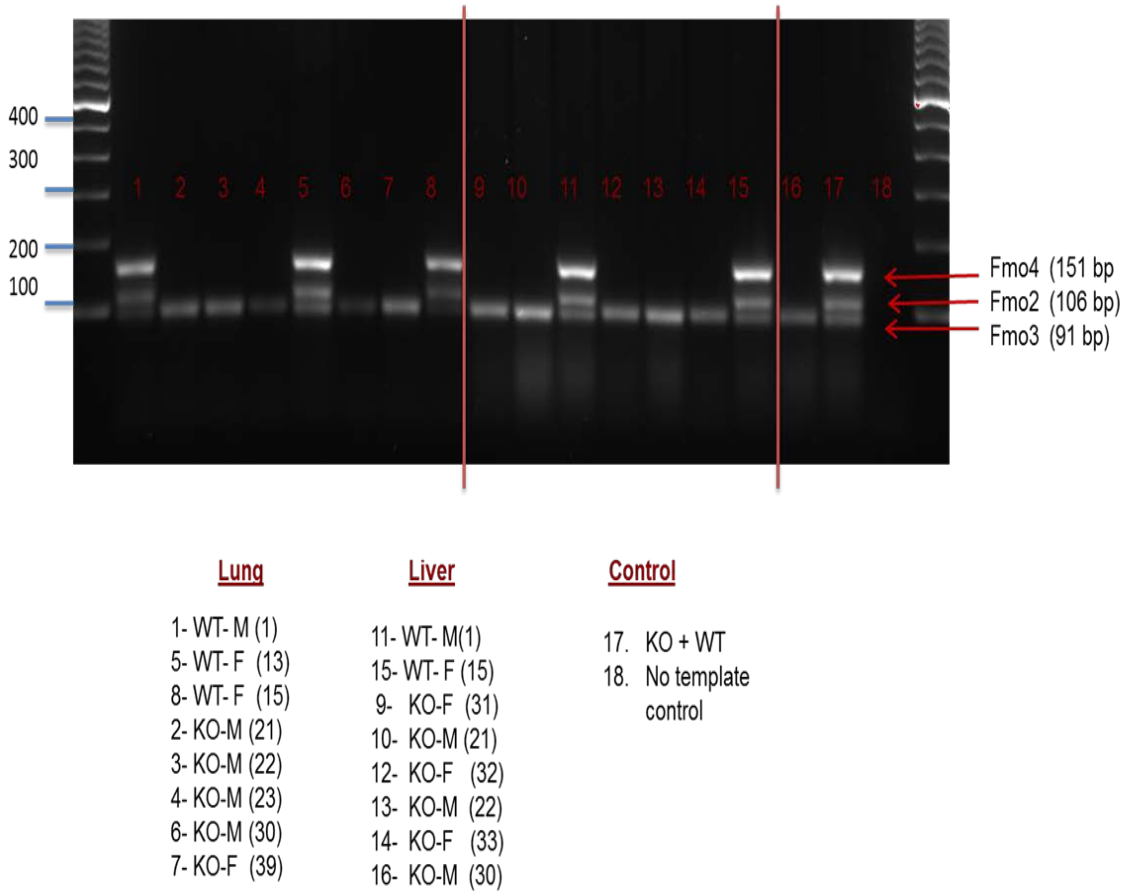

Figure A3.5 Mouse genotyping with *Fmo2*, *3*, 4 genes.
DNA was isolated from mouse lung and liver and amplified by PCR using primers specific for the mouse *Fmo2, 4* and *3.* WT, KO, M and F represent wild type, knockout, male and female, respectively. Number mentioned after male (M) or female (F) are actual mice number.

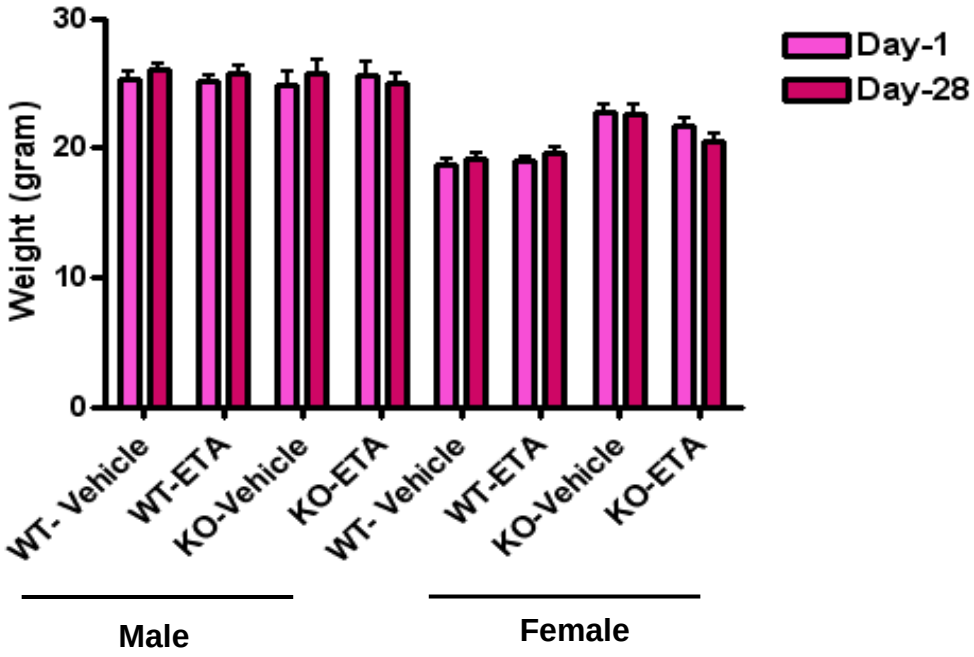

Figure A3.6 Mice body weight change in 28-days of ETA treatment.
Mice body weight at beginning (day 1) and end (day 28) of the ETA and vehicle dosing. Graphs show mean ± SEM.
Abbreviation: WT-wild type, KO-knockout, M-male and F-female.

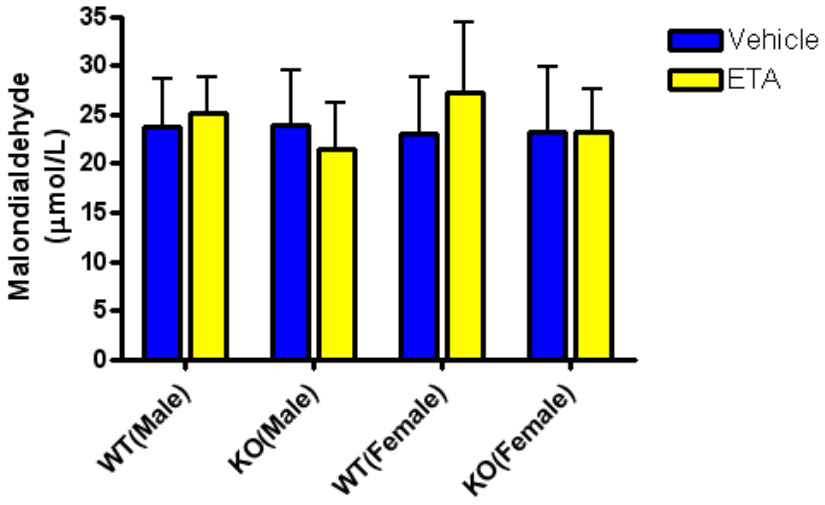

Figure A3.7 ELF MDA concentrations in wildtype and knockout mice.
Bars show mean ± SEM (n= 4). Both wildtype and knockout mice were treated with ETA or vehicle for 28-days. Abbreviation WT-wildtype, KO-knockout.

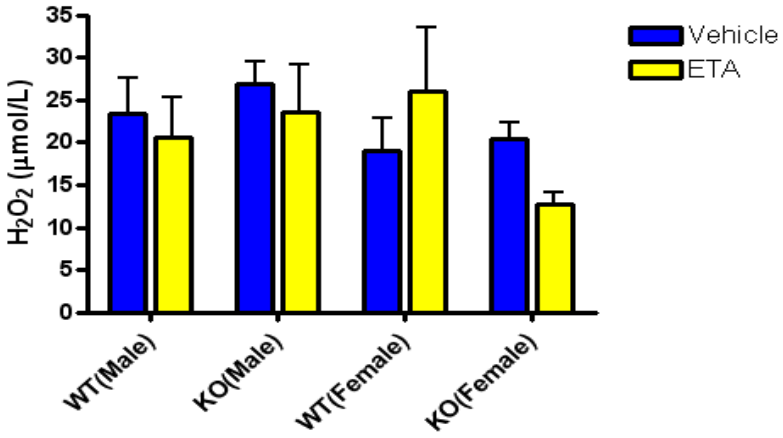

Figure A3.8 H_2O_2 concentrations in ELF from wildtype and knockout mice.
Bars show mean ± SEM (n= 8-9). Both wildtype and knockout mice were treated with ETA or vehicle for 28-days. Abbreviation WT-wildtype, KO-knockout.